JOHANNES GUTENBERG UNIVERSITÄT MAINZ

Influence of vitamin D on the hepatitis B virus life cycle in different genotypes

Dissertation

zur Erlangung des Grades

"Doktor der Naturwissenschaften"

am Fachbereich Biologie
der Johannes Gutenberg-Universität
in Mainz

vorgelegt von

Malin Finkernagel

geboren am 20. April 1988 in Gießen

Mainz, August 2016

Diese Dissertation wurde im Fachbereich Biologie der Johannes Gutenberg-Universität in Mainz angenommen.

Dekan:

Interner Gutachter:

Externer Gutachter:

Tag der mündlichen Prüfung: 16. Dezember 2016

Zusammenfassung

Trotz eines sehr effektiven Impfstoffes seit den 1980er Jahren leiden über 240 Millionen Menschen weltweit an einer chronischen HBV (Hepatitis-B-Virus)-Infektion. HBV, das zur Familie der *Hepadnaviridae* gehört, wird über Körperflüssigkeiten und Bluttransfusionen übertragen und infiziert nahezu ausschließlich die menschliche Leber. Das Virus wird in acht Genotypen unterteilt, deren Genom-Varietät > 8% beträgt. Die Genotypen sind weltweit unterschiedlich verteilt und unterscheiden sich in ihrem Krankheitsverlauf im Hinblick auf das Ansprechen auf Behandlungen mit antiviralen Medikamenten und der Entwicklung des HCC (hepatozellulären Karzinoms), das durch das Virus auftritt (Tian und Jia, 2016). Klinische Analysen zeigen auf, dass in chronisch infizierten HBV-Patienten die Virus-Last saisonal variiert. Dies wird durch das Hormon Vitamin D induziert, das durch Sonneneinstrahlung auf der Haut produziert wird. Niedrige Vitamin-D-Konzentrationen sind mit hohen Virus-Replikationsraten assoziiert (Farnik et al., 2013). Infizierte Hepatozyten sezernieren neben dem Virus selbst große Mengen an SVPs (subviralen Partikeln), die ausschließlich aus den viralen Oberflächen-Proteinen (HBsAg) bestehen und nicht-infektiöse Sphären und Filamente bilden. Während VPs (Virionen) und Filamente ESCRT- (*endosomal sorting complexes required for transport*-) abhängig durch sogenannte multivesikuläre *bodies* (MVBs) freigesetzt werden, verläuft die Freisetzung von Sphären über den ER-/Golgi-Sekretionsweg (Jiang et al., 2015). Ziel dieser Arbeit war es, den Effekt von Vitamin D auf den HBV-Lebenszyklus in verschiedenen Genotypen in Zellkulturmodellen zu untersuchen und einen potentiellen Mechanismus der Inhibition aufzuzeigen.

Zur Untersuchung des Einflusses wurden sechs verschiedene Vitamin-D-Analoga in stabil und transient HBV-exprimierenden Hepatomzelllinien sowie infizierte PHHs (primäre humane Hepatozyten) getestet. Analysen des Zellkultur-Überstandes und der Zelllysate zeigen eine Veränderung des Verhältnisses viraler Komponenten sowohl intra- als auch extrazellulär, die auf eine verminderte Freisetzung des Virus durch Vitamin D schließen lassen. Die Virus-Transkripte werden hierbei jedoch nicht beeinflusst. Zudem führt Vitamin D zu einer verringerten Expression des viralen Faktors α-Taxilin. Die Ergebnisse deuten darauf hin, dass α-Taxilin, das essentiell für die MVB-vermittelte Freisetzung von HBV ist (Hoffmann et al., 2013), für den beobachteten Effekt von Vitamin D verantwortlich ist. Vergleichende Analysen der Genotypen lassen eine unterschiedlich starke Reduktion der HBV-Freisetzung durch Vitamin-D-Behandlung beobachten. Genotyp C reagierte hierbei nahezu gar nicht auf die Behandlung mit Vitamin D. Es wird geschlussfolgert, dass sich die Behandlung mit Vitamin D zur weiteren Charakterisierung der HBV-Genotypen eignet, über die bisher wenig vergleichende *in vitro*-Analysen durchgeführt wurden. Die vorgestellte Arbeit verdeutlicht die Bedeutung der Untersuchungen des Einflusses von Vitamin D auf den HBV-Lebenszyklus und der vergleichenden Betrachtung der HBV-Genotypen.

Summary

In spite of a very effective vaccine being available since the 1980s, over 240 million people worldwide suffer from chronic HBV (Hepatitis B virus) infection. HBV, belonging to the family *Hepadnaviridae*, is transmitted via body fluids and blood transfusions and infects the human liver. HBV is classified into eight different genotypes with a genome-variety of > 8%. The genotypes are regionally distributed and differ in their progression of disease with regard to the response to antivirals and the development of HCC (hepatocellular carcinoma) (Tian and Jia, 2016). Some clinical observations indicate that in chronic HBV-infected patients the virus load varies seasonally due to the triggering factor vitamin D, which is produced in the skin by the exposure of sun (Farnik et al., 2013). Infected hepatocytes release, in addition to the virus itself, huge amounts of SVPs (subviral particles), which consist of the viral surface proteins (HBsAg) and form spheres and filaments. While the VPs (virions) and filaments are released ESCRT (endosomal sorting complexes required for transport) -dependently via MVBs (multi vesicular bodies), the secretion of the spheres occurs via the ER-/Golgi-pathway (Jiang et al., 2015). The aim of this project was to analyze whether vitamin D has a direct effect on the HBV life cycle in the different genotypes and to determine a potential mechanism of the inhibition in cell culture systems.

For analyzing the influence, six different vitamin D analogs were tested in stably and transiently HBV expressing hepatoma cell lines and PHHs (primary human hepatocytes). The investigation of the cell culture supernatant and cell lysates reveals an altered ratio of viral components intra- and extracellularly, presenting evidence for a reduced release of the virus upon vitamin D treatment. Hereby, the viral transcripts were not influenced. Furthermore, vitamin D leads to a diminished expression of the viral factor α-Taxilin. The results indicate that α-Taxilin, which is crucial for the MVB-dependent release of HBV (Hoffmann et al., 2013), is causative for the observed effect of vitamin D. The comparative analysis of the HBV genotypes showed differences in the reduction on release of HBV upon vitamin D treatment. Here, the HBV genotype C did not react at all on vitamin D treatment. It is assumed that the treatment with vitamin D is a suitable tool for the further characterization of the HBV genotypes, as hitherto only limited *in vitro* analyses were performed.

The presented work reveals the impact on the analysis of the influence of vitamin D on the HBV life cycle and the comparative characterization of the HBV genotypes.

Preface

The experimental research leading to the presented data was conducted from 15th May 2013 until 14th May 2016 at the *Paul-Ehrlich-Institut* (PEI) in Langen in the Division of Virology. The work resulted in four coauthor publications. The data of the main project are illustrated in the thesis and protected by copyright of the Division of Virology of the PEI, Langen.

Intracellular accumulation of subviral HBsAg particles and diminished Nrf2 activation in HBV genotype G expressing cells lead to an increased ROI level

Kai-Henrik Peiffer, Sami Akhras, Kiyoshi Himmelsbach, Matthias Hassemer, **Malin Finkernagel**, Gert Carra, Michael Nübling, Michael Chudy, Hauke Niekamp, Dieter Glebe, Christoph Sarrazin, Stefan Zeuzem, Eberhard Hildt, Journal of Hepatology, Apr, 2015, 62 (4) 791–798, impact factor: 11.34.

Characterization of TXLNA as a novel factor controlling the release of hepatitis C virus

Fabian Elgner, Christian Donnerhak, Huimei Ren, Regina Medvedev, André Schreiber, Lorenz Weber, Markus Heilmann, Daniela Ploen, Kiyoshi Himmelsbach, **Malin Finkernagel**, Karin Klingel, Eberhard Hildt, Biochemical Journal, Jan 05, 2016, 473 (2) 145-155, impact factor: 4.40.

Restrictive influence of SAMHD1 on Hepatitis B Virus life cycle

Andreas FR Sommer, Lise Rivière, Bingqian Qu, Kerstin Schott, Maximilian Riess, Yi Ni, Caitlin Shepard, Esther Schnellbächer, **Malin Finkernagel**, Kiyoshi Himmelsbach, Karin Welzel, Nadja Kettern, Christian Donnerhak, Carsten Munk, Egbert Flory, Baek Kim, Stephan Urban, Renate König, Scientific Reports, May 27, 2016, 6:26616, impact factor: 5.578.

Comparative characterization of HBsAg derived from different HBV genotypes

Matthias Hassemer, **Malin Finkernagel**, Kai-Hendrik Peiffer, Dieter Glebe, Sami Akhras Andreas Reuter, Heinrich Scheiblauer, Lisa Sommer, Michael Chudy, Micha Nübling, Eberhard Hildt, Virology, Dec 02, 2016, 502 (2017) 1–12, impact factor: 3.20.

Table of contents

List of Abbreviations

A/H1N1	influenza virus A
aa	amino acid
AIDS	acquired immune deficiency syndrome
ALT	serum alanine aminotransferase
AP1G1	adaptor related protein complex 1 gamma 1 subunit
APCs	antigen presenting cells
APS	ammoniumperoxidisulphat
ARE	antioxidant response element
ASHV	arctic squirrel hepatitis virus
AST	aspartate aminotransferase
BatHBV	bat hepatitis B virus
BCA	bicinchoninic acid
bp	base pairs
BSA	bovine serum albumin
bZIP	basic leucine zipper
C	celsius
cccDNA	covalently closed circular DNA
CD	cluster of differentiation
CDC	Centers for Disease Control and Prevention
cDNA	complementary DNA
CHBV	crane hepatitis B virus
cIAP	cellular inhibitor of apoptosis proteins
CLSM	confocal laser scanning microscopy
CP	crossing point
CRISPR/Cas	clustered regularly interspaced short palindromic repeats
CTL	cytotoxic T cells
CYP	cytochrome P450
Da	dalton
DAPI	4,6-diamidino-2-phenylindol
DBP	vitamin D-binding protein
DC	dendritic cell
DENV	dengue virus
DEPC	diethylpyrocarbonat
DHBV	duck hepatitis B virus
DMEM	dulbecco`s modified eagle serum
DMSO	dimethyl sulfoxide
DNA	desoxyribonuclein acid
DTT	Dithiothreitol
DZIF	Deutsches Zentrum für Infektionsforschung
E. coli	*Escherichia coli*
EASL	European association for the study of the liver
EBV	Epstein-Barr virus
EDTA	Ethylendiamintetraacetate
EGFP	enhanced green fluorescent protein
ELISA	enzyme-linked immunosorbent assay
ER	endoplasmic reticulum
ERGIC	ER-Golgi intermediate compartment
ESCRT	endosomal sorting complex required for transport
FACS	fluorescence activated cell sorting,
FAK	focal adhesion kinase
FCS	fetal calf serum
FSC	forward scatter
GAPDH	glycerinaldehyd-3-phosphat-dehydrogenase
GCLC	glutamate-cysteine ligase catalytic subunit
GRASP	Golgi reassembly-stacking protein

GSHV	ground squirrel hepatitis virus
GSTs	glutathione S-transferases
HAPs	heteroaryldihydro-pyrimidines
HBcAg	hepatitis B core antigen
HBeAg	hepatitis B excreted antigen
HBHBV	African horseshoe bats hepatitis B virus
HBsAg	hepatitis B surface antigen
HBV	hepatitis B virus
HBV/A	hepatitis B virus genotype A
HBV/B	hepatitis B virus genotype B
HBV/C	hepatitis B virus genotype C
HBV/D	hepatitis B virus genotype D
HBV/E	hepatitis B virus genotype E
HBV/F	hepatitis B virus genotype F
HBV/G	hepatitis B virus genotype G
HBV/H	hepatitis B virus genotype H
HBV/I	hepatitis B virus genotype I
HBV/J	hepatitis B virus genotype J
HCC	hepatocellular carcinoma
HCV	hepatitis C virus
HHBV	heron hepatitis B virus
HIV	human immunodeficiency virus
HRP	horseradish peroxidase
HSPGs	heparan sulfat proteoglycane
ICTV	International Committee on Taxonomy of Viruses
IF	immunofluorescence
IFN	interferon
Ig	immunglobulin
IL	interleukin
IU	infectious units
Keap1	Kelch-like ECH-associated protein 1
LB	lysogeny broth
LBHBV:	Burmese long-fingered bats hepatitis B virus
LHBs	large hepatitis B surface
LPS	lipopolysaccharide
MCRA	most common recent ancestor
MHBs	middle hepatitis B surface
MHC-II	major histocompatibility complex-II
MOI	multiplicity of infection
mRNA	messenger RNA
MVB	multivesicular body
Mθ	macrophages
NFκB	nuclear factor 'kappa-light-chain-enhancer' of activated B-cells
NLSs	nuclear localization sequences
NQO1	NAD(P)H quinone oxidoreductase 1
Nrf2	nuclear factor (erythroid-derived 2)-like 2
nt	nucleotides
NTCP	Na^+-taurocholate cotransporting polypeptide
ORF	open reading frame
PAGE	polyacrylamid-gelelectrophorese
PAMPs	pathogen associated molecular pattern
PBS	phosphate-buffered salt solution
PCR	polymerase chain reaction
PDI	protein disulfide isomerase
PEG	polyethylene glycol
pegIFNα	pegylated interferon α
PEI	Polyethylenimin
PEI	Paul-Ehrlich-Institut

PFA	Paraformaldehyde
pgRNA	pregenomic RNA
PHBV	parrot hepatitis B virus
PhD	doctor of philosophy
PHH	primary human hepatocytes
PI	Propidium iodide
Prk2	prolin rich tyrosin kinase 2
PTH	parathyroid hormone
PTH	primary tupaia hepatocytes
PVDF	polyvinylidendifluorid
qPCR	quantitative real-time PCR
RBHBV	african roundleaf bats hepatitis B virus
rcDNA	relaxed circular DNA
RGHBV	ross goose hepatitis virus
RH-domain	RNase H-domain
RIG-I	retinoic acid-inducible gene
RIPA	radioimmunoprecipitation assay
RNA	ribonucleic acid
ROS	reactive oxygen species
rpm	rounds per minute
RT	room temperature
RT	reverse transcriptase
RT-qPCR	reverse transcriptase and quantitative real time PCR
RXR	retinoid X receptor
S	safty level
SHBs	small hepatitis B surface
SMP	skimmed milk powder
SN	supernatant
SNARE	soluble N-ethylmaleimide-sensitive factor attachment protein receptor
Src	sarcoma and cellular
SSC	side scatter
STHBV	stork hepatitis B virus
SVP	subviral particle
TAE	Tris-acetate-EDTA
TALEN	transcription activator-like effector nucleases
TB	tuberculosis
TBHBV	tent-making bats hepatitis B virus
TBS	Tris buffered saline
TEMED	N,N,N,N-Tetramethylethylendiamin
TF	transcription factor
TLM	translocation motif
TLRs	toll like receptors
TM	transmembrane region
TNF-α	tumor necrosis factor-α
TP-domain	terminal protein-domain
T_{Reg}	regulatory T cells
TRIS	tris(hydroxymethyl)-aminomethan
Triton	oktylphenolethoxylat
TSG101	tumor susceptibility gene 101
t-SNARE	target-SNARE
Tween	polyethylenglycolsorbitanmonolaurat
TXLNA	α-Taxilin
UV	ultraviolet
v/v	volume/volume
VDR	vitamin D receptor
VDRE	vitamin D response element
VP	viral particle
v-SNARE	vesicle-SNARE
w/v	weight/volume
WHO	World Health Organization
WHV	woodchuck hepatitis virus
WHV	woodchuck hepatitis virus
WMHBV	woolly monkey hepatitis B virus
ZFN	zinc finger nucleases

List of Figures

List of Tables

1. Introduction

Every year around 55 million people die worldwide, and a third of those estimated deaths is traced back to preventable infectious diseases like virus infections (Gannon, 2000). The awareness of the risk of HIV/AIDS rose during the last two decades remarkably; however, the consequences of viral hepatitis are still underestimated[1] (Lozano et al., 2012). In 2010, the WHO (World Health Organization) declared viral hepatitis as a public health problem with worldwide distribution (WHO, 2010). An aim of the WHO is to reduce new viral hepatitis infections by 90% and related deaths by 65% by 2030 (WHO, 2016).

1.1 Viral hepatitis

Hepatitis is an inflammation of the liver, often caused by infections with the hepatitis virus designated A to E. These viruses are the major cause for chronic hepatitis, liver cirrhosis, and HCC (hepatocellular carcinoma). The viruses cause similar pathological conditions, but differ fundamentally in their structure and virology (Shin, Sung, and Park, 2016; WHO, 2015). For a better understanding of the pathology, and to have new medical opportunities for treatment, it is a major aim of research to characterize the morphogenesis of those viruses. In this thesis, I will focus on the influence of the hormone vitamin D (calcitriol) on the life cycle of HBV (hepatitis B virus). Furthermore, a particular emphasis will be placed on the HBV genotypes, as not much knowledge exists about the molecular differences at all. Hitherto, the establishment of genotype-specific guidelines for treatment is neglected due to lacking information and awareness.

1.1.1 Course of diseases and pathogenesis

While an effective vaccine against HBV has been available since 1982, around 240 million people worldwide are chronically infected. Additionally, every year between 500,000 and 700,000 patients die in consequence of HBV infection (Mortality and Causes of Death Collaborators, 2015). Symptoms of acute infection appear after 30 to 180 days (on average 75 days) after the infection and include jaundice (increased levels of ALT (serum alanine aminotransferase) and AST (aspartate aminotransferase)), dark urine, extreme

[1] Estimated number of deaths per year: HIV/AIDS ~1.5 million, viral hepatitis ~1.4 million (Lozano, Naghavi et al. 2012).

fatigue, nausea, vomiting, and abdominal pain (CDC, 2015; Mortality and Causes of Death Collaborators, 2015; WHO, 2015). Infections may pass symptomless (65–80%), become acute (20–35%), or develop into chronic illness (10–20%), depending on the host (age, gender, genetic background and associated immune status) and the virus (HBV genotype, viral DNA levels) (reviewed in Chang and Lewin, 2007). For children, the rate of chronicity is much higher (Defresne and Sokal, 2016). In 0.5–1% of the cases, a fulminant hepatitis may develop with a lethality of 10–20% due to liver failure (reviewed in Liang, 2009; Tugendheim, 2016). Further atypical HBV infections are occult or latent HBV infections (reviewed in Liang, 2009).

The chronic infections are a major cause for the development of liver cirrhosis and are the chief cause for HCC, the most common type of primary liver cancer (see Figure 1) (reviewed in Petersen, Thompson, and Levrero, 2016). HBV-related-HCC is responsible for 5–10% of liver transplantations globally and a burden on the national health systems (reviewed in Yachimski and Chung, 2005).

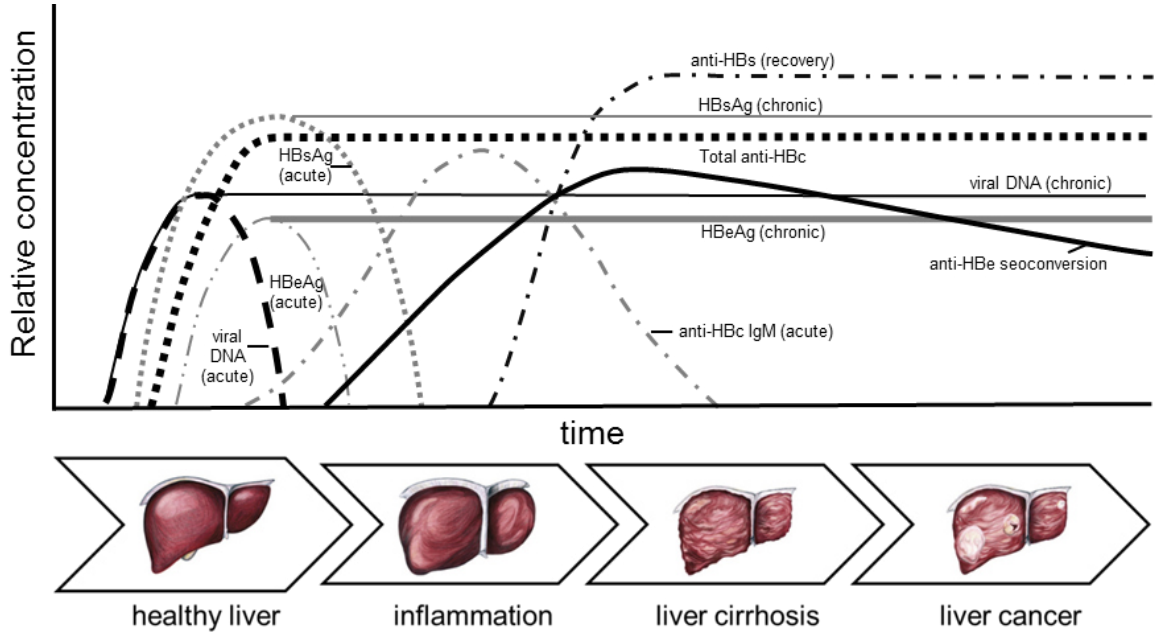

Figure 1: Time curve of serological markers and liver pathogenesis (modified from Hoffmann-La Roche AG, 2016; Sablon and Shapiro, 2005).
Serological markers differ in acute and chronic infection. HBV causes an inflammation of the liver, which can develop into a chronic infection and lead to liver fibrosis, liver cirrhosis, and HCC.

1.1.1.1 Acute infection

The acute phase of the infection, which can last from two weeks up to three months, is characterized by increasing levels of viral DNA, HBeAg (hepatitis B excreted antigen) and HBsAg (hepatitis B virus surface antigen) detected in blood samples of patients (see Figure 1) (reviewed in Liang, 2009). In this phase, IgM antibodies against HBcAg (hepatitis B core antigen) and HBeAg are being generated and the HBV DNA signal drops over time (see Figure 1). In the following phase (post-acute phase), which ranges from three up to six months, the titer of HBcAg specific-IgM-antibodies disappears. HBs specific-antibodies are being produced in the late phase during recovery or convalescence (reviewed in Liang, 2009). For the HBV clearance, the adaptive immune system is mainly responsible, due to the binding of antibodies to the circulating virus and the killing of the infected cells by CTL (cytotoxic T cells) (Chisari, Isogawa, and Wieland, 2010). CTLs lead to apoptosis of infected hepatocytes and the secretion of IFN γ (interferon γ), which triggers the inhibition of the HBV gene expression and replication (Guidotti et al., 1996). Furthermore, HBV replication is suppressed by IFN α/β stimuli, leading to a wide range of possibilities for the immune response to self-limit the infection (see 1.1.1.3) (Chisari, Isogawa, and Wieland, 2010).

1.1.1.2 Chronic infection

As previously described, 10−20% of the infections can develop into a chronic hepatitis. A majority of chronic hepatitis is caused by previous vertical transmission from HBV-infected mothers to the neonates (reviewed in Glebe and König, 2014). Chronically infected patients show a similar initial pattern of serological markers for the acute infection, but the dynamic course is variable (reviewed in Liang, 2009). However, in the early phase, viral replication is detectable by HBsAg, HBeAg and viral DNA in high titers (see Figure 1) (reviewed in Liang, 2009; Sablon and Shapiro, 2005). The immune tolerance phase is characterized by the persistence of high levels of HBeAg and viral DNA (reviewed in Liang, 2009). Nevertheless, HBeAg-negative chronic HBV patients are existing, who develop anti-HBe antibodies and lose in consequence HBeAg (reviewed in Liang, 2009). Furthermore, in samples of inactive carriers, HBeAg and HBV DNA cannot be detected (reviewed in Liang, 2009) and seroconversion of HBsAg- and HBeAg-antibodies does not occur (Halegoua-De Marzio and Hann, 2014). The prognosis of chronicity is directly related to the severity of the diseases (reviewed in Liang, 2009).

The chronic infection leads to persistent inflammation of the liver with the consequence of the elimination of liver cells, which are replaced by connective tissue and liver fibrosis, and cirrhosis occurs (see Figure 1) (reviewed in Hoffmann-La Roche AG, 2016; Liang, 2009). In one-third of the chronically infected patients, end-stage liver disease is the consequence of HBV infection. HBV itself does not lead to liver destruction directly, as there is no histological evidence of infected hepatocytes in the early phase (Chisari, 2000; Guidotti et al., 1999). Firstly, HBV bypasses the host viral defense, which makes it to a stealthy virus. The invisibility of the virus for the innate immune system is characterized by the abundance of the induction of IFN α/β target genes and therefore promotes the spread in the liver (Wieland et al., 2004). $CD4^+$ and $CD8^+$ T cell response (and dependent antibody response) are vigorous in acute infections, but are merely weak in chronic hepatitis (Chisari, Isogawa, and Wieland, 2010). In liver tissue of chronically infected patients, T cells are present but not able to clear infection. However, the cytopathic activity of $CD8^+$ T cells leads to inflammation and supports disease pathogenesis (Chisari, Isogawa, and Wieland, 2010). $CD4^+$ T cells are not directly involved in liver damage and clearance, but influence B and $CD8^+$ T cell response (Thimme et al., 2003). The integration of viral DNA triggers the carcinogenesis by the expression of oncogenic viral proteins and chronic immune-mediated hepatitis (Chisari, Isogawa, and Wieland, 2010).

1.1.2 Prevention and treatment

The major pathways of the transmission of HBV are body fluids (e.g. blood transfusions), sexual contacts, intravenous drug abuse with contaminated needles, and perinatal mother-to-child transmission (reviewed in Tugendheim, 2016). For the prevention, those transmission routes have to be eliminated by testing blood products, condom usage, and the utilization of disposable syringes and vaccine strategies in the early childhood (Defresne and Sokal, 2016). Post-exposure immunization for newborns of HBV-positive mothers and adults who came in contact with infectious material is highly effective (Polo Rodriguez et al., 2016).

Although chronically infected patients can be treated with pegIFNα (pegylated Interferon α) or antiviral agents like nucleos(t)ide (e.g. lamivudine, entecavir and tenofovir), the cure rate of HBV is very low (reviewed in Lin and Kao, 2016). HBV cure is defined by international guidelines as the loss of seroconversion of HBeAg/HBsAg for HBeAg-positive patients and HBsAg loss or seroconversion for HBeAg-negative patients (reviewed in Lin and Kao, 2016). However, the nucleos(t)ide analogs have the advantage of good tolerance, in contrast to IFN therapy, but their use is limited due to occurring drug

resistances (Petersen, Thompson, and Levrero, 2016). HBsAg clearance, caused by antivirals, is not a satisfactory therapeutic endpoint because of the existence of long-lasting cccDNA (covalently closed circular DNA) in the liver and associated hepatocarcinogenesis (see 1.1.4.5) (reviewed in Lin and Kao, 2016). Accordingly, the combinations of existing agents and novel drugs are under investigation (see Table 1) (reviewed in Lin and Kao, 2016). New therapeutic approaches should address the long-term suppression of HBV DNA, the regression of fibrosis and the reversal of cirrhosis, and the reduction of the risk of developing HCC (reviewed in Lin and Kao, 2016). Hence, novel antiviral strategies target the virus life cycle (see 1.1.4.5) by inhibition of the entry (NTCP (Na^+-taurocholate cotransporting polypeptide) inhibitors), the polymerase, the cccDNA (formation, silencing, and destruction), the capsid, and the HBV gene expression (secretory pathway, RNAi) (reviewed in Petersen, Thompson, and Levrero, 2016). Furthermore, new agents are designed to modulate the immune response via TLR (toll like receptor) ligands, RIG-I (Retinoic acid-inducible gene) ligands, cIAP (cellular inhibitor of apoptosis proteins), and therapeutic vaccines (see Table 1) (reviewed in Lin and Kao, 2016; Petersen, Thompson, and Levrero, 2016).

Table 1: Novel agents for chronic HBV therapy (modified from Lin and Kao, 2016; Petersen, Thompson, and Levrero, 2016)

Target	Strategy	Candidate	Clinical trial
NTCP (receptor)	Entry inhibitor	Myrcludex-B	Phase IIa
HBV polymerase	Polymerase inhibitor	Tenofovir alafenamide (GS-7340), Besifovir (LB80380)	Phase III, III
cccDNA	Site specific cleavage of DNA	ZFNs, TALENs, CRISPR/Cas	Pre-clinical
	Inhibition of relax-circular DNA to cccDNA conversion	CCC-0975, CCC-0346	Pre-clinical
Core	Inhibition of nucleocapsid assembly, Capsid inhibitor	AT-61, AT-130. By 41-4109 NVR-1221, HAPs, Pheylpropenamide	Pre-clinical Phase Ia, I, Pre-clinical
HBV RNA	Knock-down of HBV RNA, viral proteins and HBV DNA	ARC-520, TKM-HBV, ALN-HBV	Phase IIa, I, Pre-clinical
HBsAg	Blocks HBsAg secretion	REP9 AC, REP-2139-Ca	Phase II, II

Target	Strategy	Candidate	Clinical trial
Innate immunity	Induces APOBEC3A and APOBEC3B	Lymphotoxin-β receptor agonist	Pre-clinical
	Exogenous interferon stimulation	TLR 7 agonist GS9620	Phase II
Adaptive Immunity	Therapeutic vaccine	GS-4774, DV601, TG1050	Phase II, Ib, I
	Immune checkpoint inhibitor to activate $CD8^+$ T cells PD-1 (programmed death-1) inhibitor	Nivolumab, Pembrolizumab	Pre-clinical
	cIAP inhibitor	Birinapant	Phase I

1.1.3 HBV epidemiology

It is estimated that more than two billion people are positive for HBsAg antibodies and that the worldwide prevalence for HBsAg is regionally distributed (reviewed in Gerlich, 2013). In Sub-Saharan Africa and Southeast Asia the prevalence for HBsAg is higher than 8% in contrast to Europe and North America where the prevalence is lower than 2% (see Figure 2). The low prevalence rates are associated with the high coverage of vaccines, diagnostic testing, and the general knowledge about the potential transmission (reviewed in Tugendheim, 2016; WHO, 2015).

HBV is classified into eight different genotypes, entitled genotype A to H, which show a DNA variation of up to 8% due to deletions and insertions and which vary regionally (see Figure 2, 1.1.5). Until now, the number of subgenotypes is rising (entitled with additional numbers) and recently isolated virus of patients from Asia suggests two additional genotype strains, genotype I and J, which are not yet ratified by the ICTV (International Committee on Taxonomy of Viruses) (reviewed in Kim et al., 2011; Littlejohn et al., 2016).

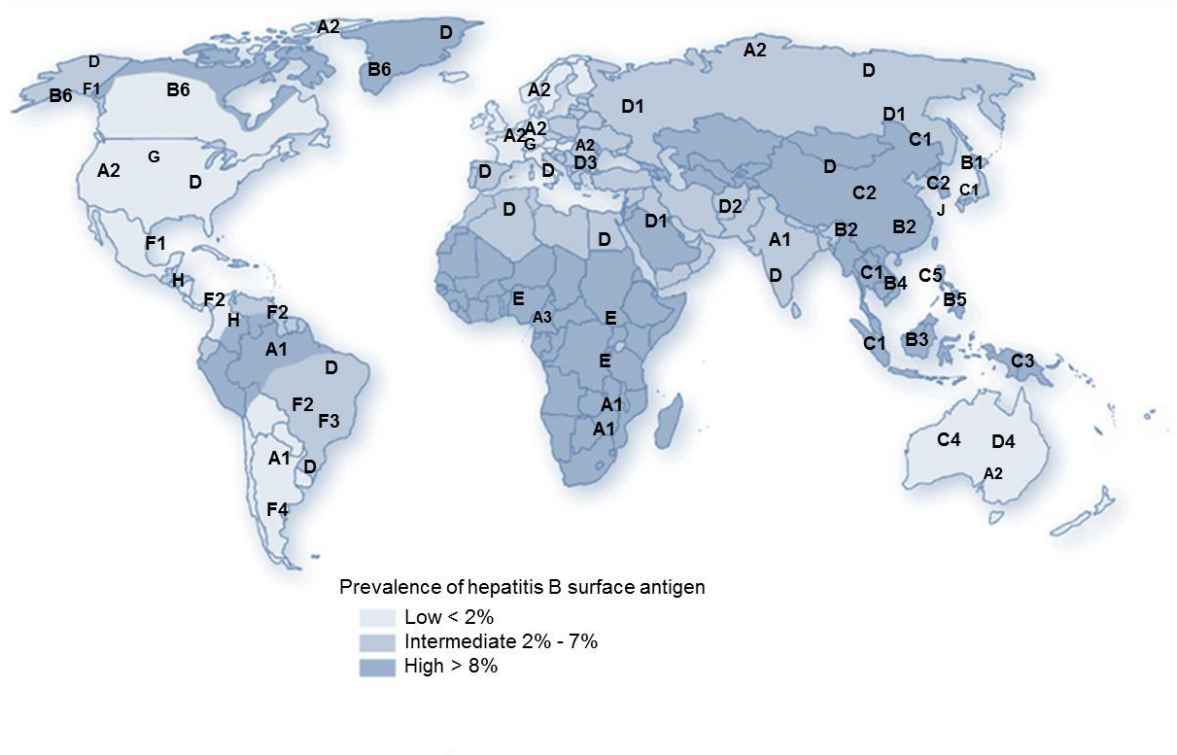

Figure 2: Prevalence of anti-HBsAg and distribution of HBV genotypes (modified from Averhoff, 2016; Kim, Revill, and Ahn, 2011).
Worldwide over two billion people are carrier of HBsAg antibodies. The prevalence for HBV is regionally distributed. High prevalence for HBsAg exists in Sub-Saharan Africa and Southeast Asia. Furthermore, HBV genotypes, which are entitled A-J, are regionally distributed. Subgenotypes are indicated with numbers.

1.1.4 Virology and replication

HBV was discovered in 1965 by Prof. Dr. Blumberg by the initial description of the Australia antigen which was later entitled as HBsAg (Blumberg, Alter, and Visnich, 1965; Sutnick et al., 1970). In 1976, Prof. Dr. Blumberg was awarded the Nobel Prize for his groundbreaking work in the field of infectious diseases (Datta and Datta, 1977).
HBV is a small, enveloped DNA virus with a size of 42 nm and it is a member of the family of the *Hepadnaviruses.* The family has two genera: the *Orthohepadnaviruses*, which HBV belongs to, and the *Avihepadnaviruses* (see 1.1.4.4). The family of *Hepadnaviridae* is comprised of very tissue-specific viruses whose replication is nearly restrictively limited to hepatocytes (Kumar et al., 2016). In addition to its tissue-specificity, HBV is a very species-specific virus and infects almost exclusively humans. Some animal viruses, such as BatHBV (bat hepatitis B virus), WHV (woodchuck hepatitis virus), or DHBV (duck hepatitis B virus), are closely related to HBV (Rasche, Souza, and Drexler, 2016; RKI, 2014).

1.1.4.1 Structure

HBV VPs (viral particles), also called Dane-particles, have a diameter of 42 nm (Dane, Cameron, and Briggs, 1970) (see Figure 3.1). The virus consists of an envelope composed of an icosahedral nucleocapsid, which encases the partial double-stranded viral DNA the so-called rcDNA (relaxed circular DNA) with a size of 3.2 kb. It is covalently bound to the viral polymerase. The virus surface is formed out of about 400 molecules of the three surface proteins LHBs, MHBs and SHBs (large, middle and small hepatitis B virus surface antigen) (Gerlich et al., 2010; Siegler and Bruss, 2013).

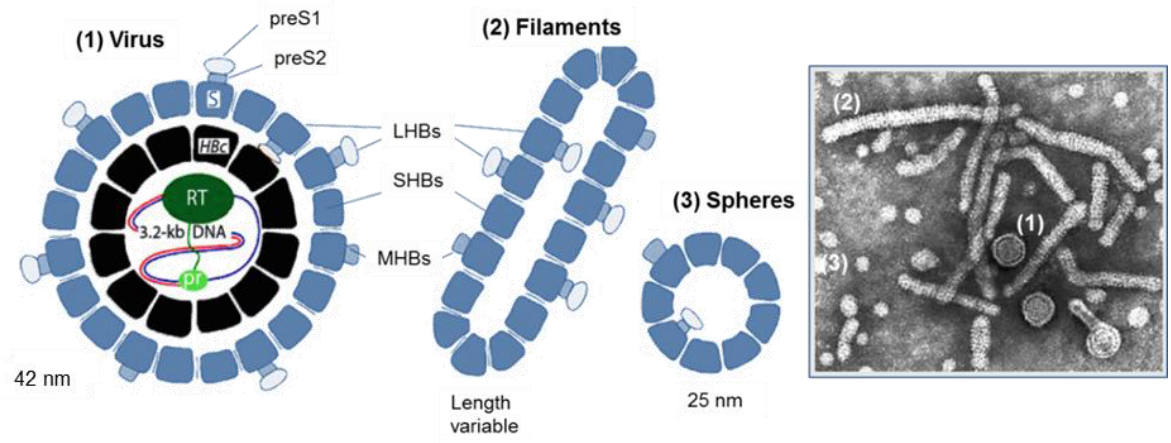

Figure 3: Viral and subviral particles.
HBV consists of VPs and SVPs. SVPs are subdivided into filaments and spheres. VPs have a size of 42 nm and spheres have a diameter of 25 nm. Filaments vary in their length.
Left figure: Illustration of viral particles (1), filaments (2), and spheres (3) (modified from Gerlich, 2013).
Right figure: Electron microscopy picture of purified HBV (modified from Stannard, 2016).
S: surface protein; HBc: Hepatitis B core protein, RT: Reverse transcriptase; pr: Polymerase; LHBs: Large Hepatitis B Virus Surface Protein; SHBs: Small Hepatitis B Virus Surface Protein; MHBs: Middle Hepatitis B Virus Surface Protein.

Infected hepatocytes release, in addition to the virus itself, huge amounts (1000−10,000-fold) of SVPs (sub viral particles) (Chai et al., 2008) which appear as filaments (see Figure 3.2) and spheres (see Figure 3.3). The SVPs merely consist of HBsAg and have no viral DNA and capsid (Chai et al., 2008). Spheres have a diameter of 25 nm, whereas the filaments can vary in their length. The composition of the surface proteins is differing in those particles, noticeably due to the fact that spheres contain less LHBs compared to filaments and VPs (Short et al., 2009). Hitherto, the function of the SVPs is not completely

understood, however, they might sequester antibodies of the immune system and increase the infection rates (Bruns et al., 1998). In addition to the VPs and the SVPs, HBV forms incomplete particles, the so-called naked capsids (Bardens et al., 2011). They are structured like viral patricles, but are lacking the viral surface proteins. Furthermore, empty virons lacking the viral DNA exist and can be released (Chou et al., 2015).

1.1.4.2 Viral proteins

The viral genome encodes for seven proteins: SHBs, MHBs, LHBs, Core, preCore, polymerase and HBx that are being described in the following in more detail.
As previously mentioned, the surface of HBV is formed of the three HBsAg proteins. All HBsAg types are encoded by one ORF (open reading frame) and differ in their composition of domains. The following domains are produced: preS1, preS2, and S. The SHBs contains only the S-domain, whereas the MHBs consist of the S- and the preS2-domain and the LHBs consists of the S-, preS2-, and preS1-domain (see Figure 4). The S-domain is built of 226 aa (amino acids), has a N-glycosylation site at Asn-146 and a molecular weight of 24 kDa (unglycosylated, p24) and 27 kDa (glycosylated, gp27) (Marion et al., 1979; Peterson, Roberts, and Vyas, 1977). The molecular weight of MHBs is 31 kDa, whereas the LHBs has a mass of 42 kDa. The LHBs and the MHBs both additionally feature the preS2-domain, nevertheless the glycosylation pattern in the two proteins is differing in this domain, characterized by an extra glycosylation site at Asn4 in MHBs, which is not used in LHBs. Moreover, there is another O-glycosylation site at Tyr-37 in the preS2-domain. Finally, for MHBs three forms can be distinguished: the unglycosylated (p30), the monoglycosylated (gp33) and the biglycosylated (gp36) form, whereas the LHBs is glycosylated only in the S-domain (p39, gp42).
HBsAg is an integral membrane protein of the ER and is anchored with its S-domain. The TM1 (transmembrane region 1) is located at the position aa8−22 and the growing protein chain is directed towards the cytoplasm (see Figure 4). An additional transmembrane region is located at aa80−98 (TM2). The hydrophobic C-terminus is composed of two further transmembrane regions TM3/TM4 and the last loop contains the major antigenic determinants of HBsAg (Eble et al., 1987). On closer observation, it becomes apparent that LHBs has a dual topology in the ER-membrane, which it keeps in the mature virions (Bruss et al., 1994; Ostapchuk, Hearing, and Ganem, 1994; Prange and Streeck, 1995). On one hand, the preS1-/preS2-domain and a part of the S-domain (with its TM1), up until aa79, are located in the cytoplasm. On the other hand, the preS1/preS2 is orientated to

the ER-lumen and forms the second topology (see Figure 4). By having this unusual dual topology, it is assumed that LHBs bears multiple responsibilities in the HBV life cycle such as virion-host interaction during infection (Prange and Streeck, 1995) (see 1.1.4.4).

In addition to HBsAg, another protein, the HBcAg also known as Core, subsists in the structure of HBV, which consists of 185 aa and has a molecular weight of 21 kDa. The protein has the ability for self-assembly to viral capsids and has a primary structure consisting predominantly of α-helices. Two α-helices (α3, α4) are connected to each other and form the central domain of the monomer. The proteins are forming dimers out of four α-helices which are crucial for the self-assembly process. There are two types of capsids formed: T=3 and T=4. The symmetry T=3 is formed out of 90 HBc-dimers, the T=4-symmetry is formed out of 120 and dominating during HBV infection (Nassal, 2008; Zhou and Standring, 1992; Zhou and Standring, 1991). In addition, a secreted version of HBcAg/Core the HBeAg/preCore exists. HBeAg has a molecular weight of 17 kDa and is formed by posttranslational processing and C-terminal cleavage of 34 aa (Garcia et al., 1988; Ou, Laub, and Rutter, 1986).

Beside the structure proteins, non-structure proteins are encoded by the viral genome. One of them is the 17 kDa large HBx-protein with 154 aa. In the family of the *hepadnaviridae,* HBx is not as highly conserved as the other proteins and its function is still under debate (Colgrove, Simon, and Ganem, 1989; Meyers et al., 1986). It is described for its regulating activity, but it is not essential for replication (Reifenberg et al., 2002). Despite all that, it seems to be a prerequisite for the development of HCC (Levrero and Zucman-Rossi, 2016).

Furthermore, the genome encodes for the viral polymerase (molecular weight: 90 kDa) - the only HBV protein with enzymatic activity. In each virion, only one polymerase molecule can be observed and it is covalently linked to the partially double-stranded viral genome. It consists of four domains: the TP- (terminal protein-) domain, the non-conserved spacer-domain, the RT- (reverse transcriptase-) domain, and the RH- (RNase H-) domain (Nassal, 2008). The enzyme has on the one hand the ability to act as a RT and as a DNA polymerase on the other hand. The RT-domain exhibits in its active site a highly conserved amino acid sequence (active site: YMDD) (Bartenschlager and Schaller, 1988). The TP-domain provides a primase activity and is essential for the priming mechanism for DNA-synthesis, whereas the RNA-template is degraded via the RH-domain (Bartenschlager, Junker-Niepmann, and Schaller, 1990).

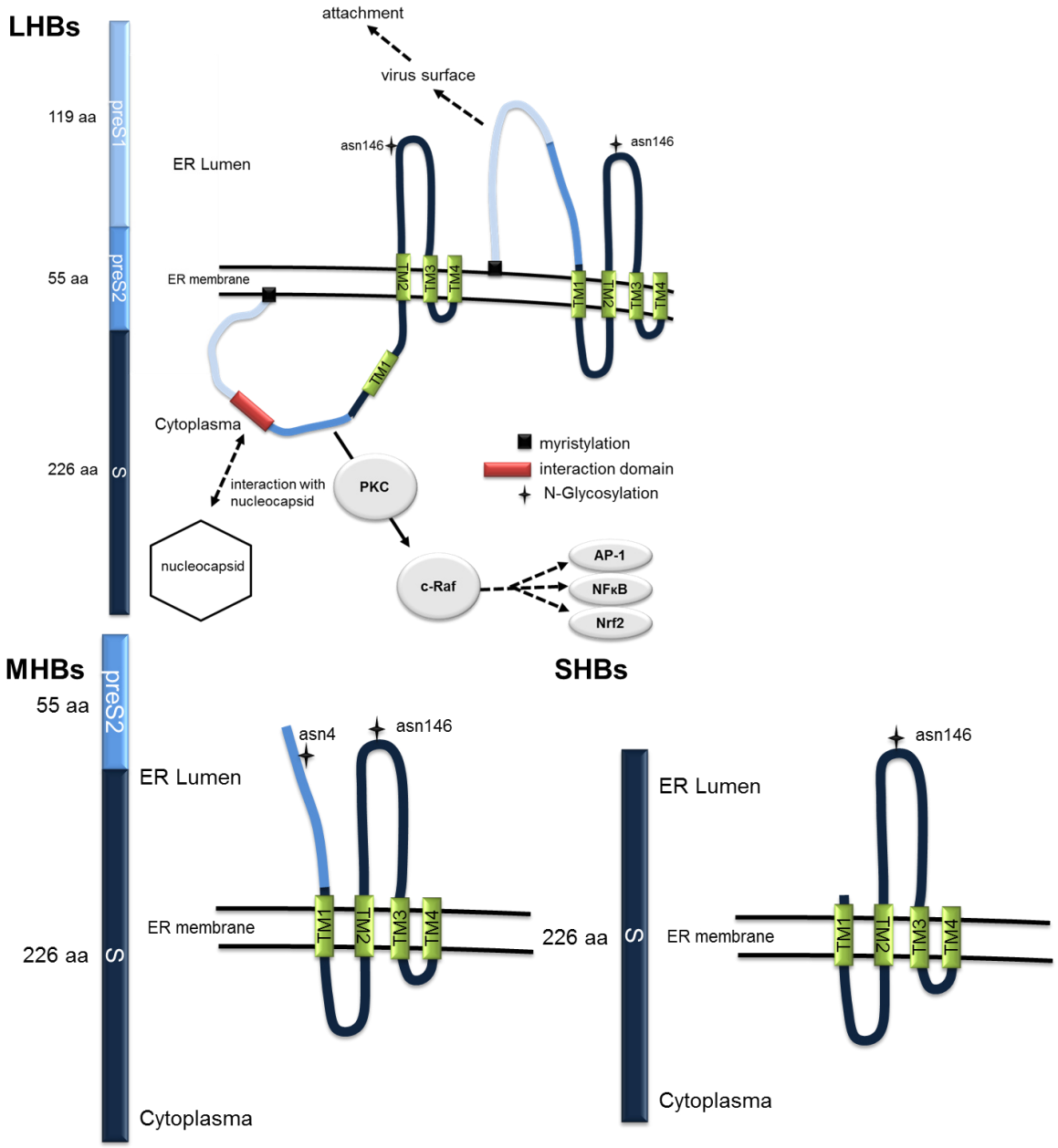

Figure 4: HBV surface proteins, domains and topology (modified from Schädler and Hildt, 2009).
HBsAg contains three the three surface proteins: LHBs, MHBs and SHBs. SHBs consists of the S-domain with 226 aa, MHBs consists of the S-domain and the 55 aa long preS2-domain and LHBs consists of the S-domain, the preS2-domain and the 119 aa big preS1-domain. All proteins show a specific membrane topology.

1.1.4.3 Molecular virology

As noted above, HBV has a partially double-stranded, circular DNA-genome. On the (-)-strand the polymerase is covalently bound, whereas the (+)-strand contains an eight to nine nucleotide long RNA-oligomer for the transcription start (Bartenschlager, Junker-Niepmann, and Schaller, 1990; Beck and Nassal, 2007). The circular configuration is ensured due to its termini with an overlap of 200 nt (nucleotides) (Micorbewiki, 2016). Four RNA constructs are transcribed and differ in size (see Figure 5). The mRNA encoding for Core/preCore has a size of 3.5 kb and is subdivided into preCore mRNA, which is leading to the preCore and HBeAg, and the 3.5 kb pgRNA (pregenomic RNA), encoding for the Core and the polymerase. The mRNA encoding for the LHBs with its preS1-, preS2- and S-domain has a length of 2.4 kb and the transcripts encoding for the MHBs and SHBs have a size of 2.1 kb. Last, the mRNA encoding for the HBx has a length of 0.7 kb. All transcripts have their own promotor and can therefore be regulated individually (Block, Guo, and Guo, 2007).

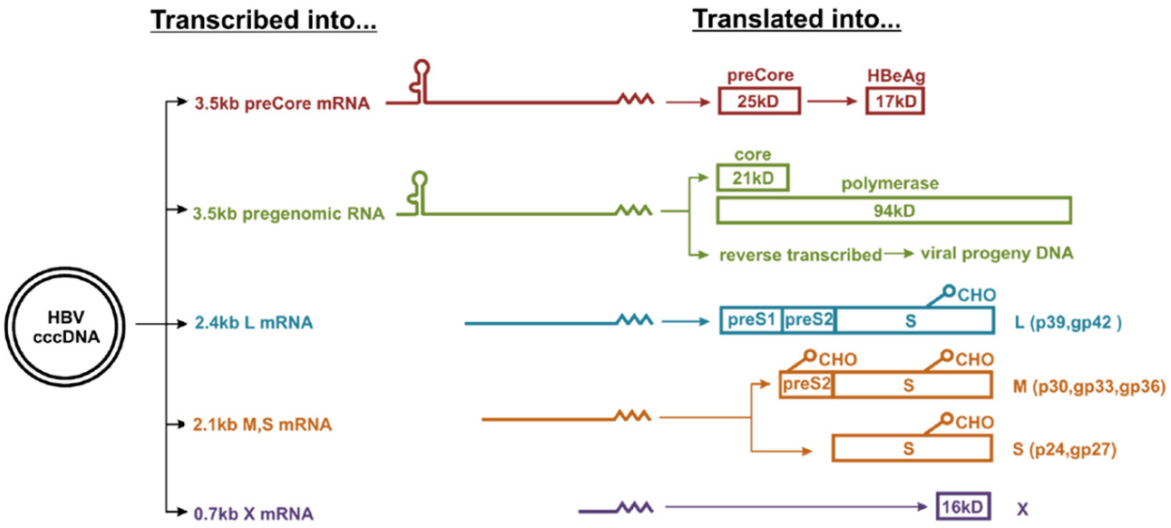

Figure 5: Viral transcripts (modified from Block, Guo, and Guo, 2007).
HBV cccDNA is transcribed into constructs differing in their size. The 3.5.kb constructs are encoding for the preCore/HBeAg and Core/polymerase. The 2.4.construct is translated into the LHBs. The M and SHBs protein is encoded by the 2.1.kb construct and the 0.7kb construct is translated into the regulatory HBx protein.
CHO: carbohydrate.

1.1.4.4 HBV life cycle

HBV has a unique life cycle, which is very complex due to several DNA/RNA intermediates and different release pathways of VPs and SVPs. Starting with the viral entry, the first steps of the HBV life cycle are mediated by the attachment of the virus with the S-domain of HBsAg to HSPGs (heparan sulfat proteoglycane) (Morikawa, Suda, and Sakamoto, 2016). A weak and unspecific binding drives this first contact of the virus and the hepatocyte. After the attachment, the receptor NTCP is leading to the intracellularly specific uptake of the virus (see Figure 6) (Yan et al., 2014). This process is triggered by the interaction of the preS1-domain of LHBs and NTCP and the clathrin-dependent endocytose (Huang et al., 2012). In the endosome, a pH-dependent structural change of preS2 leads to an exposure of the TLM (translocation motif) (Stoeckl et al., 2006). It is formed by an amphipathic helix and is membrane-permeable (Oess and Hildt, 2000). It leads to the uptake of the virus and the nucleocapsid is released into the cytoplasm (Morikawa, Suda, and Sakamoto, 2016). The viral DNA is directed to the nucleus via the microtubuli-system (Brandenburg et al., 2005; Rabe, Glebe, and Kann, 2006). NLSs (nuclear localization sequences) are located C-terminally of the Core and in the polymerase crucial for the import of the rcDNA (Lupberger et al., 2013; Schmitz et al., 2010). The entrance into the nucleus is followed by the conversion of the rcDNA into cccDNA under the involvement of host cellular factors (see Figure 6) (Knowles, Howe, and Aden, 1980; Königer et al., 2014). The cccDNA associates with nucleosomes and forms a minichromosome (Bock et al., 2001). Subsequently, the host RNA polymerase II uses the in the nucleus remaining cccDNA as a template for transcription, which might be regulated by HBx, Core and liver-specific TFs (transcription factors) (Lucifora et al., 2011; Tang and McLachlan, 2001).

The viral RNA utilizes a polyA-signal and thus is transported to the cytoplasm and translated into viral proteins. Hitherto, splicing variants are not described (Morikawa, Suda, and Sakamoto, 2016). Afterwards, the pgRNA is translated into the Core and the viral polymerase, whereas the structure proteins and the HBx are translated from the subgenomic RNA. The pgRNA as well as the polymerase are encapsidated within new Core particles for the formation of VPs (Urban et al., 2010). The rcDNA is built up from the pgRNA template by reverse transcription of the polymerase (Nassal, 2008). Nucleocapsids containing rcDNA can be recycled into the nucleus to form new cccDNA or are enveloped with the L-, M- and SHBs, which were formed at the ER, to build new VPs (see Figure 6) (Urban et al., 2010). The SVPs are formed out of HBsAg without a nucleocapsid with containing DNA.

As previously mentioned, SVPs and VPs leave the cells on different routes (see Figure 6). Recent studies showed that secretion of the VPs and filaments is carried out via MVBs (multivesicular bodies) due to ESCRT- (endosomal sorting complex required for transport) system (Jiang et al., 2015; Prange, 2012). However, spheres are transported in an ESCRT- and MVB-independent way and are released by an ERGIC (ER-Golgi intermediate compartment) by the secretory pathway (Watanabe et al., 2007).

1.1.4.5 HBV replication systems

During the last decades, studying the full HBV life cycle was not easy. Lacking knowledge about the HBV receptor made it difficult to have sufficient cell culture-based replication systems, inasmuch as common hepatoma cell lines do not express the HBV entry-relevant molecules.

Nowadays, wide ranges of replication systems are generated. Well-established cells for the analysis of replication of HBV are PHHs (primary human hepatocytes) and PTHs (primary tupaia hepatocytes), but with a variability of donors of liver tissue, infection rates can vary strongly. A revolution for HBV researchers occurred with the establishment of HepaRG cells (Gripon et al., 2002). This cell type can be differentiated with DMSO (dimethyl sulfoxide) and acquires some primary hepatocytes characteristics in order to make infections possible on a low level.

Addition of PEG (polyethylene glycol) during infection leads to a fusion of the virus with the host surface and to an increase in infection rates. With the discovery of NTCP as a receptor candidate in 2013, the generation of stably NTCP expressing HepG2 cell lines, which are susceptible to HBV, was possible (Yan et al., 2014). Nevertheless, as not all hepatocytes cell lines which are stably transfected with human NTCP are efficient for HBV infection (differential infectivity) and HBV has to be added with high MOIs (multiplicity of infection) in the presence of PEG, suggesting that other factors might be in all likelihood crucial for infectivity (Tong and Li, 2014). One of these factors might be TXLNA, which is located on the cell surface of PHHs, and differentiated HepaRGs (Hoffmann, 2013).

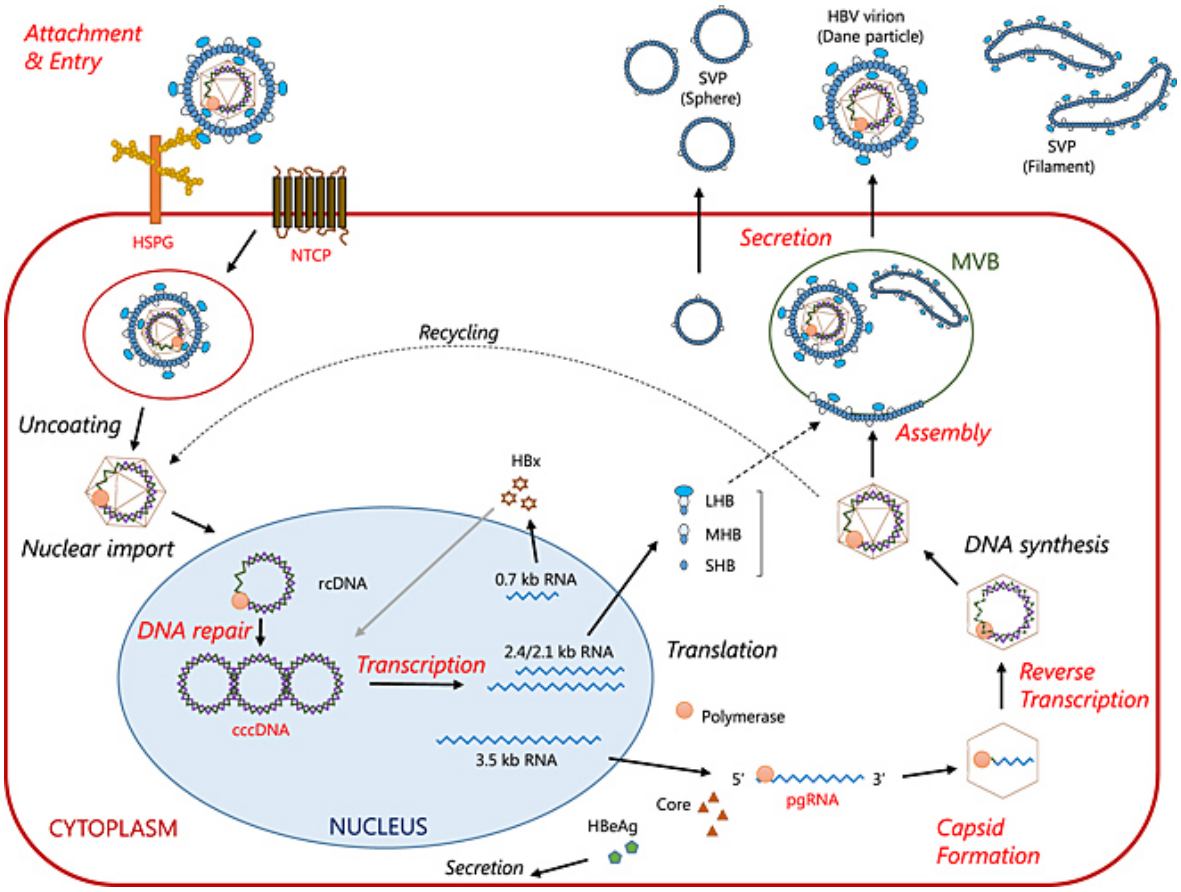

Figure 6: HBV life cycle (adapted from Morikawa, Suda, and Sakamoto, 2016).
The viral entry is mediated by the binding of HBV to its liver-specific receptor NTCP. VPs are endocytosed and within the endosomes, the nucleocapids are released into cytoplasm. Subsequently, the nucleocapsid is directed into the nucleus, viral DNA is released and forms cccDNA by cellular host factors. The cccDNA serves as template for the transcription. pgRNA including the polymerase is incorporated into forming capsids. Subsequently, pgRNA is built to rcDNA by the reverse transcriptase activity of the polymerase. These particles can be recycled to the nucleus to contribute to an accumulation of cccDNA or coated with HBsAg. VPs and filaments leave the cell MVB-dependently, whereas spheres are released by the ERGIC.
HBeAg: hepatitis B e-antigen; HBsAg: hepatitis B surface antigen; HBV: hepatitis B virus; HBx: hepatitis B x protein; HSPG: heparan sulfate proteoglycan; LHB: large hepatitis B surface protein; MHB: middle hepatitis B surface protein; SHB: small hepatitis B surface protein; MVB: multivesicular body; NTCP: sodium taurocholate co-transporting polypeptide; pgRNA: pregenomic RNA; SVP: subviral particle.

1.1.4.6 Vesicle transport and the viral factor TXLNA

As previously mentioned, the intracellular transport of viral proteins is important for the life cycle of the virus. One of the essential components for the cargo is the factor TXLNA (also known as α-taxilin, taxilin alpha, IL14, TXLN). It has the potential to be a HBV receptor candidate and is crucial for the release of VPs. Until today, three different proteins of the taxilin-family have been discovered, entitled α-, β- and γ-Taxilin. α- and β-Taxilin are

expressed ubiquitously, whereas γ-Taxilin is merely expressed in skeletal muscles and the heart (Nogami et al., 2004). Taxilins were identified as binding partners of syntaxin proteins. Syntaxins belong to the SNARE (soluble N-ethylmaleimide-sensitive-factor attachment receptor) -proteins that form complexes in the vesicles of eukaryotic cells. For vesicle fusion v-SNAREs (vesicle-SNAREs) and t-SNAREs (target-SNAREs) form so-called trans-SNAREs. It has been observed that TXLNA can bind to free syntaxin-3 and syntaxin-4 when they are not associated to SNAREs (Nogami et al., 2004). By this process, TXLNA prevents the complex formation and thereby inhibits the fusion of the vesicle membrane with the plasma membrane. The protein-protein interaction is mediated by a long coiled-coiled domain on the C-terminus of TXLNA, the late domain (Ohtomo et al., 2010). Furthermore, physiological functions of TXLNA are the involvement in Ca^{2+}-dependent exocytose in neuroendocrine cells (Nogami et al., 2003).
HBV positive cells show elevated amounts of TXLNA. The regulatory proteins HBx and preS2 of the LHBs activate the promotor region of *TXLNA* via c-Raf by triggering the PKC-dependent activation of c-Raf-1/Erk2 signaling (Hildt et al., 2002; Hoffmann et al., 2013). TXLNA was identified as a binding partner of the preS1-/2-domain of the LHBs. It leads to an interaction of the virus with the ESCRT-machinery by acting as an adaptor between the LHBs and the ESCRT-I protein TSG101. Finally, this interaction leads to the MVB-dependent release of HBV (Hoffmann et al., 2013).

1.1.5 Development of HBV genotypes

The true origins of HBV have been controversially discussed for a long time (Simmonds, 2001). For decades, it has been assumed that HBV, with its very species-limited replication, is unlikely to be a zoonosis. The discovery of BatHBV opened up a new debate (He et al., 2013). *In vitro* experiments confirmed the hypothesis that BatHBV can infect human hepatocytes and its preS1-domain carries the sequence crucial for the binding with the NTCP receptor (Drexler et al., 2013). With this knowledge, future public health studies should consider new possible routes of transmission. Interestingly, the BatHBV is phylogenetically very close to the HBV/F and WMHBV (woolly monkey hepatitis B virus) (Drexler et al., 2013).
HBV is a DNA virus and therefore much more stable in its sequence compared to RNA viruses. Nevertheless, the polymerase has no proofreading function and more mutations occur compared to other DNA viruses. The estimated mutation rate of HBV conducts $\sim 2 \times 10^{-5}$ nucleotide substitutions per site per year, with continuous virus replication in the host (reviewed in Littlejohn, Locarnini, and Yuen, 2016; Orito et al., 1989). Despite of this,

it has to be considered that the HBV genome is highly compressed. With overlapping ORF it has only a limited potential of mutations and the mutations might reverse back to its origin (Tedder et al., 2013).

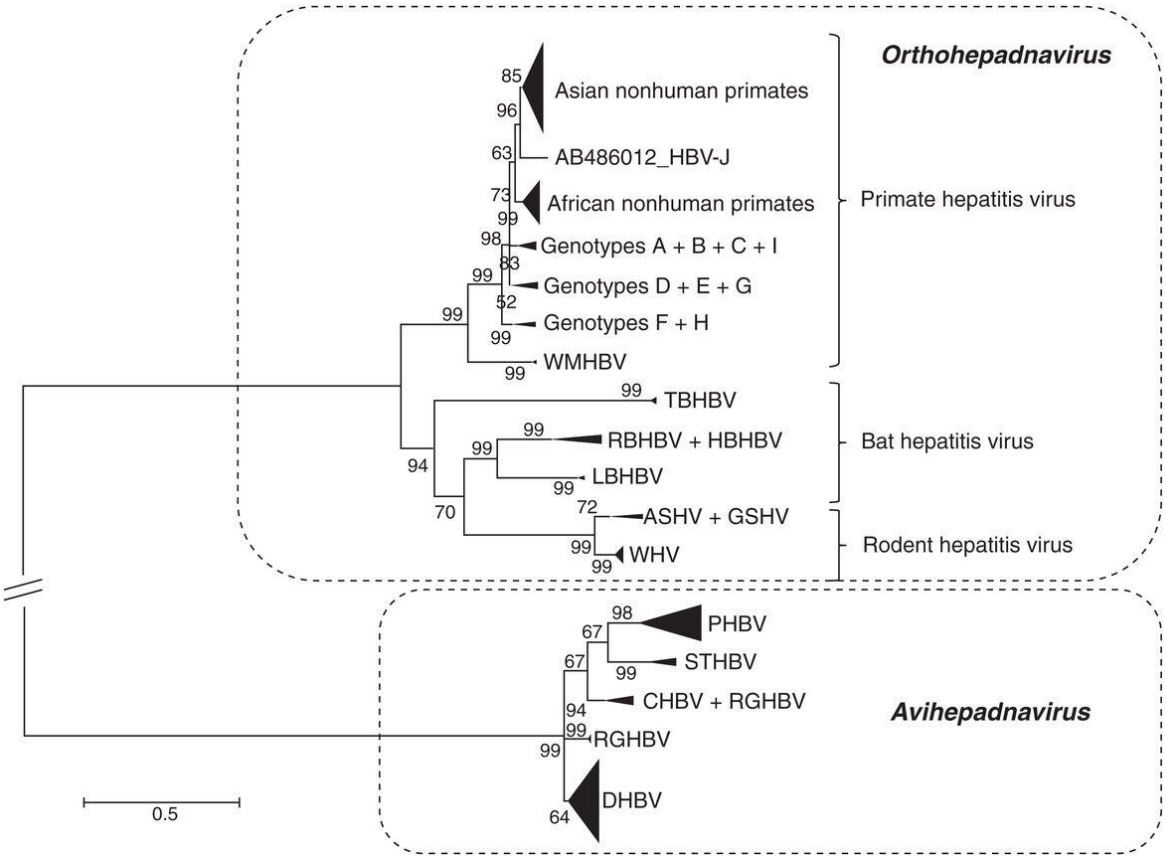

Figure 7: Phylogenetic tree of hepadnaviruses (adapted from Littlejohn, Locarnini, and Yuen, 2016).
Phylogenetic tree shows *Orthohepadnaviruses* and *Avihepadnaviruses*. BatHBV and WMHBV are close relatives to HBV/F.
WMHBV: woolly monkey hepatitis B virus; GSHV: ground squirrel hepatitis virus; ASHV: arctic squirrel hepatitis virus; WHV: woodchuck hepatitis virus; LBHBV: Burmese long-fingered bats hepatitis B virus; RBHBV: African roundleaf bats hepatitis B virus; HBHBV: African horseshoe bats hepatitis B virus; TBHBV tent-making bats hepatitis B virus; DHBV: duck hepatitis B virus; RGHBV: ross goose hepatitis virus; CHBV: crane hepatitis B virus; HHBV: heron hepatitis B virus; STHBV: stork hepatitis B virus; PHBV: parrot hepatitis B virus.

The MCRA (most common recent ancestor) seems to have existed in humans two to three thousand years ago (reviewed in Littlejohn, Locarnini, and Yuen, 2016). Regional distribution of the HBV genotypes gives evidence for its evolutionary history due to the migration of humans (reviewed in Littlejohn, Locarnini, and Yuen, 2016).

The most common genotypes in Europe and North America include HBV/A, D and G (see Figure 2) (Kato et al., 2002; Schäfer, 2007a; Vieth et al., 2002). Countries surrounding the Mediterranean Sea (Italy, Greece, Egypt, Algeria, Lybia and Spain) have a high prevalence for HBV/D, whereas in Eastern Europe (Poland, Czech Republic) HBV/A is more frequent (see Figure 2) (Basaras et al., 2007; Croagh, Desmond, and Bell, 2015; Dal Molin et al., 2006; Deterding et al., 2008; Hadziyannis, 2011; Saudy et al., 2003).

In Africa, genotypes A and E are the most common ones. HBV/A is predominantly found in East Africa and South Africa, whereas HBV/E is mostly found in West and Central Africa (Hasegawa et al., 2006; Huy et al., 2006; Kimbi, Kramvis, and Kew, 2004). In South and Middle America, for the most part HBV/F is recorded (Sanchez et al., 2002). In addition, genotype H is endemic in Middle America (Mexico and Nicaragua) (Sanchez et al., 2007).

Genotype B is the dominant genotype in Southeast Asia, China and Japan (Ding et al., 2001; Orito et al., 2001; Sakamoto et al., 2006). First reports about genotype I were published in 2000 (Hannoun, Norder, and Lindh, 2000). Its origin is located in Vietnam (Shen et al., 2015). Isolation of HBV/J took place in in 2009 from a patient in Japan (Tatematsu et al., 2009).

Apart from that, multiple genotypes are located in the same region; therefore coinfections of genotypes are likely and lead to the transfer of genetic material from one genotype to another (Croagh, Desmond, and Bell, 2015; Schäfer, 2007b). Likewise, subgenotypes distribute regionally. HBV/E and HBV/G have no subgenotypes (Schäfer, 2007b).

The HBV genotypes differ not only regionally, but also in clinical parameters and in the course of disease (see Table 2). Comparative analysis of carriers of different HBV genotypes showed divergence in their response to antiviral treatments (e.g. IFN α or Adefovir), virus load (serum HBV DNA level), risk for the development of HCC and the mode of transmission (Kao, 2002). For instance, HBV/C has a much higher tendency for chronicity and a lower response to IFN α treatment (Chan et al., 2003). Surveillance of genotypes is rare because of typically untested status in HBV carriers. Diagnostic methods like the first WHO international reference panel of viral DNA can expand the possibilities for collection of clinical data (Chudy et al., 2012).

Table 2: Clinical parameters in HBV genotypes (modified from Kneser and Wedemeyer, 2005)

Parameter	Comparison of genotypes	Source
Clinical outcome	B > C	Lindh et al., 1999
	A > D	Chan et al., 2003; Kao, 2000 & 2002; Kao et al., 2000
HBsAg clearance	A>B=D>C	Croagh, Desmond, and Bell, 2015
HBV viral load	C > B	Lindh et al., 2000
	B = C	Sugauchi et al., 2002
	D > A, B, C	Yuen et al., 2003
Progression of chronicity	A=C>B>D	Croagh, Desmond, and Bell, 2015
Response to Adefovir	A=B=C=D	Westland et al., 2003
Response to IFN α	A > B > C > D> G	Janssen et al., 2005; Liu and Kao, 2013
	A > B, C, D	Cooksley, 2003

The typical HBV genome has a size of 3215 nt (HBV/B, C, F, H). The length of other genotypes differ from 3182 nt (HBV/D) to 3248 nt (HBV/G) due to insertions and deletions (see Table 3) (Schäfer, 2007b). Furthermore, specific genotypes have a higher prevalence for mutations in patients under treatment. For example, the frequency of the mutation of the preCore A1896 in HBV/B and D is higher compared to HBV/A and C (Liu and Kao, 2013). Moreover, it can be pointed out that the O-glycosylation site at Tyr-37 in preS2 is varied in the genotypes. HBV/A is lacking of the Tyr in this position and therefore, the glycolysation site is not existing (Schmitt et al., 2004).

Table 3: Genome length of HBV genotypes (modified from Schäfer, 2007b)

Genotype	Genome length [bp}	ORF-differences
A	3221	Insertion of aa 153 and 154 in HBc
B	3215	
C	3215	
D	3182	Deletion of aa1-11 in preS1
E	3212	Deletion of aa11 in preS1
F	3215	
G	3248	Insertion of 12 aa in HBc, Deletion of aa11 in preS1
H	3215	

In summary, only limited data about the molecular virology and the influence on the infection process of the different HBV genotypes is available.

1.2 The nutrient vitamin D

Vitamin D is a fat-soluble prohormone which can be obtained from food sources (e.g. certain fish, milk, and mushrooms), but most of it is produced by the modification from a precursor substance in the skin due to sun exposure (Rahman and Branch, 2013). Vitamin D is traditionally associated with mineral metabolism and skeletal health (Prietl et al., 2013). The hormone regulates over 200 genes for cell proliferation, differentiation, and apoptosis, as well as immunomodulation and angiogenesis (Smyk et al., 2013). Worldwide vitamin D deficiency is a major health problem (DGE, 2012). The vitamin D status largely depends upon the production and is therefore influenced by factors such as genetic determinants, latitude, season, skin pigmentation, and lifestyle (Prietl et al., 2013).

1.2.4 Vitamin D biosynthesis

The first reaction of the production of vitamin D is driven by the absorption of UVB light in the epidermal layer. Under this photolytic reaction, the substance 7-dehycdrocholesterol is converted into vitamin D3 (also known as Cholecalciferol, Colecalciferol, or Calciol). After this reaction, vitamin D3 is transported via the DBP (vitamin D-binding protein) and serum proteins to its targeted tissues with the blood stream. Having reached the liver, the enzymes CYP27A1 and CYP2R1 hydroxylate vitamin D3 to 25(OH)D3 (25-hydroxyvitaminD3) (also known as Calcidiol or Calcifediol) (see Figure 8) (Prietl et al., 2013; Speeckaert et al., 2006). 25(OH)D3 has a half-life of several weeks (reviewed in White, 2012). After some further transportation steps, 25(OH)D3 is hydroxylated a second time in the kidney and other cells by the enzyme CYP27B1 (see Figure 8). The hormone PTH (parathyroid hormone) stimulates this hydroxylation process (reviewed in White, 2012). With this final conversion, vitamin D becomes the biologically active substance 1,α $25(OH)_2D$, entitled calcitriol (Prietl et al., 2013). The amount of calcitriol is strictly regulated by a negative feedback loop by the inhibition of CYP27B1 and the activation of CYP24A1 which inactivates calcitriol into calcitroic acid which is abolished in the bile (see Figure 8) (Prietl et al., 2013). The bioactive form of vitamin D, calcitriol can bind to its nuclear receptor, VDR (vitamin D receptor), and acts as a TF in the promoter region of targeted

genes on VDREs (vitamin D response elements) (Kitson and Roberts, 2012; Smyk et al., 2013). The vitamin D receptor is expressed in a wide range of cell types and involved in many physiological processes (Pike and Meyer, 2012).

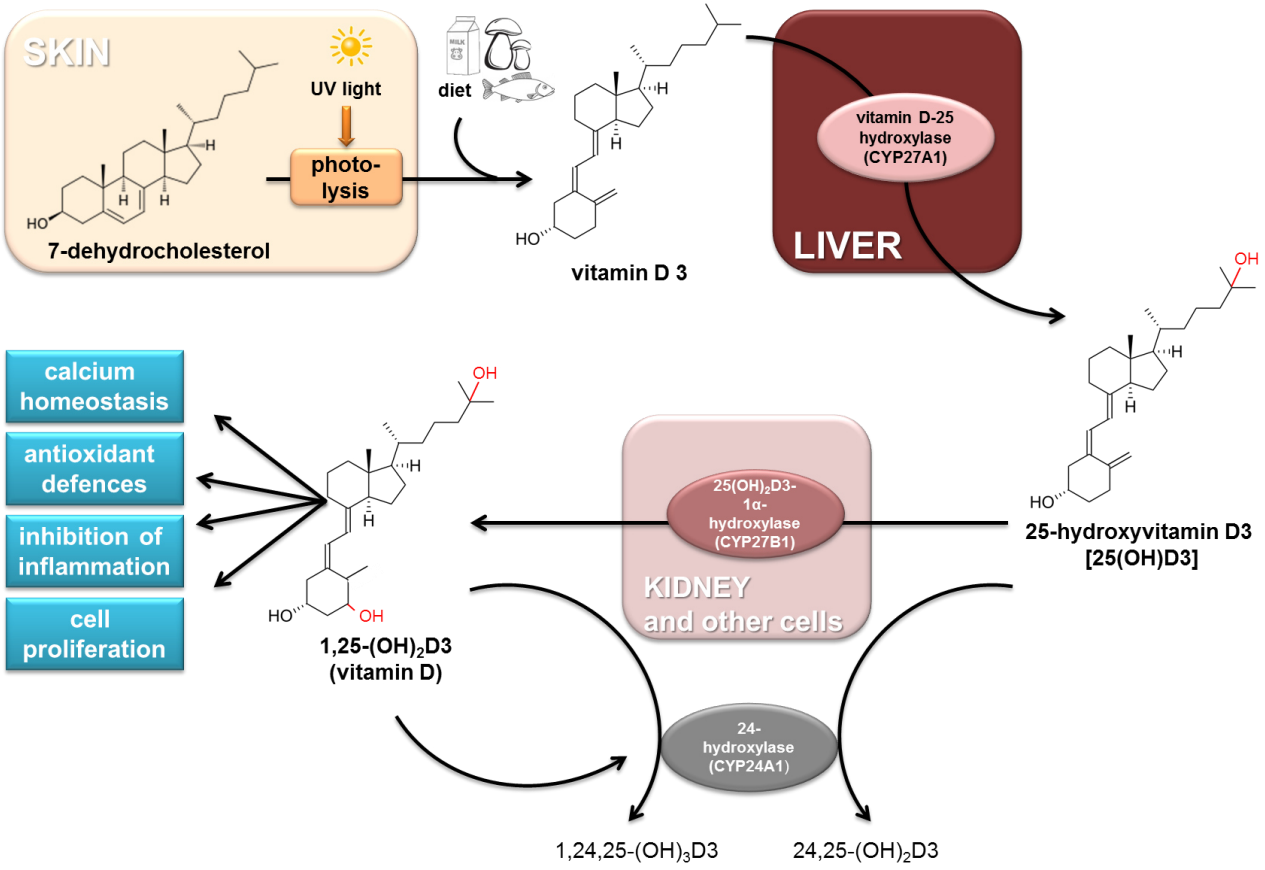

Figure 8: Biosynthesis of vitamin D (modified from Berridge, 2015).
Vitamin D is a nutrient which can be obtained from food sources like fatty fish, some types of mushrooms, and milk products. Nevertheless, most of it is produced by a photolytic reaction due to UV light. After further hydroxylation steps in the liver and the kidney, it becomes its bioactive form, calcitriol. Vitamin D can influence signaling pathways related to calcium homeostasis, antioxidant defense, and cell proliferation, and can inhibit inflammation.

1.2.5 Vitamin D signaling

Vitamin D is involved in many pathways of physiological interactions. It is mostly known for its involvement in calcium homeostasis, and it can regulate signals in quite a wide range of tissues. The VDR is a nuclear receptor, more precisely a ligand-activated TF, and has a highly conserved domain with which it binds to the DNA (reviewed in White, 2012). The binding of vitamin D leads to the formation of a heterodimer of VDR with RXR (retinoid X receptor) and by this, the recognition of VDRE is possible (reviewed in White, 2012). The recruitment of coregulatory proteins is necessary for the expression of target

genes. Thereby, histone modifications, chromatin remodeling, and the binding of RNA-polymerase II are mediated (reviewed in White, 2012). VDR is also able to activate and repress transcriptional activity by binding (Takeuchi et al., 1998).

1.2.6 Vitamin D and immunity

The positive, but functional unknown effect of vitamin D as treatment against infectious diseases has been used for a long time. Already in the mid-19th century, sun exposure was a common therapy in sanatoriums for TB (tuberculosis) infections (Moller et al., 2005). Additionally, cod liver oil, which contains large amounts of vitamin D, has been employed for treatment of a range of diseases (reviewed in Aranow, 2011). Vitamin D levels depend on the season and are caused by the different intensity of sun light (Maxwell, 1994). Seasonal variations are held responsible for a number of infectious diseases (Ladero et al., 2013; Prietl et al., 2013) and, accordingly, vitamin D deficiency (serum levels of 25(OH)D <50 nM) is associated with the susceptibility to a variety of infectious diseases (Watkins, Lemonovich, and Salata, 2015). For instance, clinical studies gave evidence that vitamin D supplementation plays a beneficial role in the prevention of seasonal A/H1N1 (influenza A) (Urashima et al., 2010).

Vitamin D is described to regulate both adapted and innate immunity via endocrine, paracrine, and intracrine mechanisms (Hewison, 2012; Szymczak and Pawliczak, 2016).

By the secretion into the bloodstream, vitamin D influences the activity of organs via the endocrine mechanism. The paracrine mechanism refers to effects in nearby cells, whereas the intracrine mechanism is associated with the hormonal activity of vitamin D inside the cell (see 1.2.2) (Szymczak and Pawliczak, 2016). The activity of vitamin D is associated to the expression of *VDR* and *CYP27B1* in immune cells. It is described that these co-expressed genes are activated (induced by immunological stimuli) in cells like T-lymphocytes ($CD4^+$ and $CD8^+$), B cells, neutrophils, DCs (dendritic cells) and Mθ (macrophages)/ monocytes (White, 2012).

For the innate immunity, TLRs are a major recognition site of antimicrobials and sense PAMPs (pathogen associated molecular pattern) (Watkins, Lemonovich, and Salata, 2015). Vitamin D induces the expression of CD14, which is involved in the recognition of LPS (lipopolysaccharide) by TLR4 (Fitch, Becker, and HayGlass, 2016). Moreover, calcitriol inhibits the expression of TLR2, TLR4, and TLR9. This is linked to the enhancement of vitamin D signaling by an upregulation of *VDR* and *CYP27B1*, due to TLR2 and TLR4 in monocytes and Mθ (Edfeldt et al., 2010; Szymczak and Pawliczak,

2016). Calcitriol impairs the expression of proinflammatory cytokines like TNF-α (tumor necrosis factor-α), IL-6 (interleukin), IL-12, and IL-23 and enhances chemotaxis and phagocytosis of macrophages (see Table 4) (Dickie et al., 2010). A deficiency of vitamin D impairs the maturation of Mθ and gives evidence that vitamin D stimulates the differentiation of monocytic precursors into mature cells (Di Rosa et al., 2011). For the response to pathogens, the transcription of genes encoding for the antimicrobial peptides defensin β2 and cathelicidin (hCAP18) is triggered by calcitriol (Szymczak and Pawliczak, 2016; Watkins, Lemonovich, and Salata, 2015). The induction of defensin β2 depends on NFκB (nuclear factor kappa-light-chain-enhancer of activated B-cells) and IL-1β (Doss et al., 2010).

It has been demonstrated that calcitriol modifies the morphology and the function of DCs upon suppression of its differentiation, maturation and immune stimulatory capacity (Szymczak and Pawliczak, 2016). Described in more detail, vitamin D induces tolerogenic properties in DCs, which results in a reduced antigen presentation to T cells and decreased secretion of IL-12. Furthermore, vitamin D decreases MHC-II (major histocompatibility complex-II) in Mθ, which is leading to a modulation of $CD4^+$ T cell response and inhibition of T cell proliferation by the decreased recognition of APCs (antigen presenting cells) (see Table 4) (Szymczak and Pawliczak, 2016). Vitamin D is crucial for the balance of Th-1 and Th-2 by suppressing pro-inflammatory signals and enhancing anti-inflammatory signals (see Table 4) (Hewison, 2012; Mahon et al., 2003; Sun, 2010; Szymczak and Pawliczak, 2016). T_{reg} cells (regulatory T cells), another subpopulation of T cells, suppress the immune system and hereby manage the immunological self-tolerance. Calcitriol stimulates the T_{reg} development, influences its differentiation, and functions (Di Rosa et al., 2011). It leads to a $FOXP3^+$ T_{reg} cell expansion and actively regulates the cytokine production (see Table 4) (Jeffery et al., 2009; Marinho et al., 2016).

As previously mentioned, *VDR* is expressed in B cells. Current studies reveal that B cells respond to vitamin D with a promotion of apoptosis of Ig-producing cells and the suppression of the generation of plasma and memory cells (Szymczak and Pawliczak, 2016). B cells show high levels of CYP24A1 upon vitamin D treatment, hence suggesting that B cells are influenced by the degradation of the hormone (Szymczak and Pawliczak, 2016). Additionally, calcitriol downregulates the nuclear factor NFκB and therefore influences the activity of its target genes (Lundqvist, Yde, and Lykkesfeldt, 2014).

In sum, vitamin D is crucial for the interplay of innate and adaptive immunity. On one hand, it suppresses the excessive response of the adaptive immune system and on the

other, it activates the response of the protective innate immunity (Sun, 2010; Szymczak and Pawliczak, 2016).

Table 4: Immunoregulation of vitamin D (modified from Di Rosa et al., 2011; McGregor et al., 2014; Mora, Iwata, and von Andrian, 2008)

Target	Function
Monocytes and Mθ	
	↑IL-1, ↓IL-6, ↓ IL-12, ↓TNF-α, ↓ IL-23, ↓GM-CSF, ↓GM-CSF
	↑Proliferation
	↑Cathelicidin, ↑β-Defensin
	↑VDR, ↑CYP27B1
DCs	
	↓Maturation
	↓MHC class II
	↓IL-12, ↑ or ↓ IL-10, ↓IL-6, ↓IL-23, ↓IFN-γ,
	↓CD40, ↓CD80, ↓CD86, ↑CD152
	↓NF-κB
T cells	
	Balance of Th-1/Th-2
	↓IL-2, ↓IFN-γ, ↑ or ↓IL-4, ↓IL-5, ↑IL-10, ↓IL-17, ↓IL-21
	↓Proliferation
	↓Cytotoxicity
	↑T_R1 and FOXP3$^+$ T_{reg} generation
	↓XBP1, ↓ERN1
B cells	
	↑ IL-10
	↓IgE, ↓IgM
	↓Proliferation
	↓Plasma cell differentiation
	↓NF-κB
	↑VDR, ↑CYP24A1
Chemokines	
	CXCL10 and CCL5

1.2.7 Crosstalk between VDR and Nrf2

ROS (reactive oxygen species) are reactive substances, which are produced as a consequence of the normal cell metabolism of oxygen. They can lead to intracellular oxidative stress and hereby to cellular damage. To protect the cell against these molecules, genes encoding for cytoprotective proteins are upregulated. For the detoxification of ROS for instance, GSTs (glutathione S-transferases), NQO1 (NAD(P)H quinone oxidoreductase 1) and GCLC (glutamate-cysteine ligase catalytic subunit) are activated. The promotor regions of the related genes harbor an ARE (antioxidant response element) for the binding of the TF Nrf2 (nuclear factor (erythroid-derived 2)-like 2). Nrf2 is a key TF to prevent intracellular oxidative damage. In the absence of oxidative stress, Nrf2 is located in the cytoplasm and bound to Keap1 (Kelch-like ECH-associated protein 1), which keeps Nrf2 inactive. Due to oxidative stress, Keap1 and Nrf2 disassociate and Nrf2 can form a heterodimer with MafG to activate ARE target genes (Itoh et al., 1997). Nrf2 is a TF of the bZIP (cap 'n' collar superfamily of basic leucine zipper).

The liver is the major organ for drug metabolism and detoxification of toxins and other chemicals and hereby permanently exposed to ROS (Aleksunes and Manautou, 2007). Thus, the proper activity of Nrf2 is crucial for the regeneration of the liver (Kohler et al., 2014). Astonishingly, HBV induces Nrf2 by its regulatory-proteins HBx and LHBs via the MAPK pathway, which leads to a protection against oxidative damage (Schädler et al., 2010).

Genome analysis for binding sites of VDR in DCs implicates that vitamin D leads to a modulation of metabolic pathways involving lipids, glucose, and oxidative phosphorylation for the response to the generation of ROS (Watkins, Lemonovich, and Salata, 2015). Recent studies reveal that alterations in the activity of Nrf2 might contribute to diseases, which are linked to vitamin D deficiency. Further evidence of the involvement of Nrf2 as key component of the vitamin D regulatory network are emphasized, due to expression analysis, which show that vitamin D controls the expression of *Nrf2 in vitro* and *in vivo* (Bobilev et al., 2011; Lin et al., 2002; Nakai et al., 2014). Furthermore, Nrf2 leads to an induction of Fos an JUN, which can increase the expression of *VDR* and *RXR* (reviewed in Berridge, 2015).

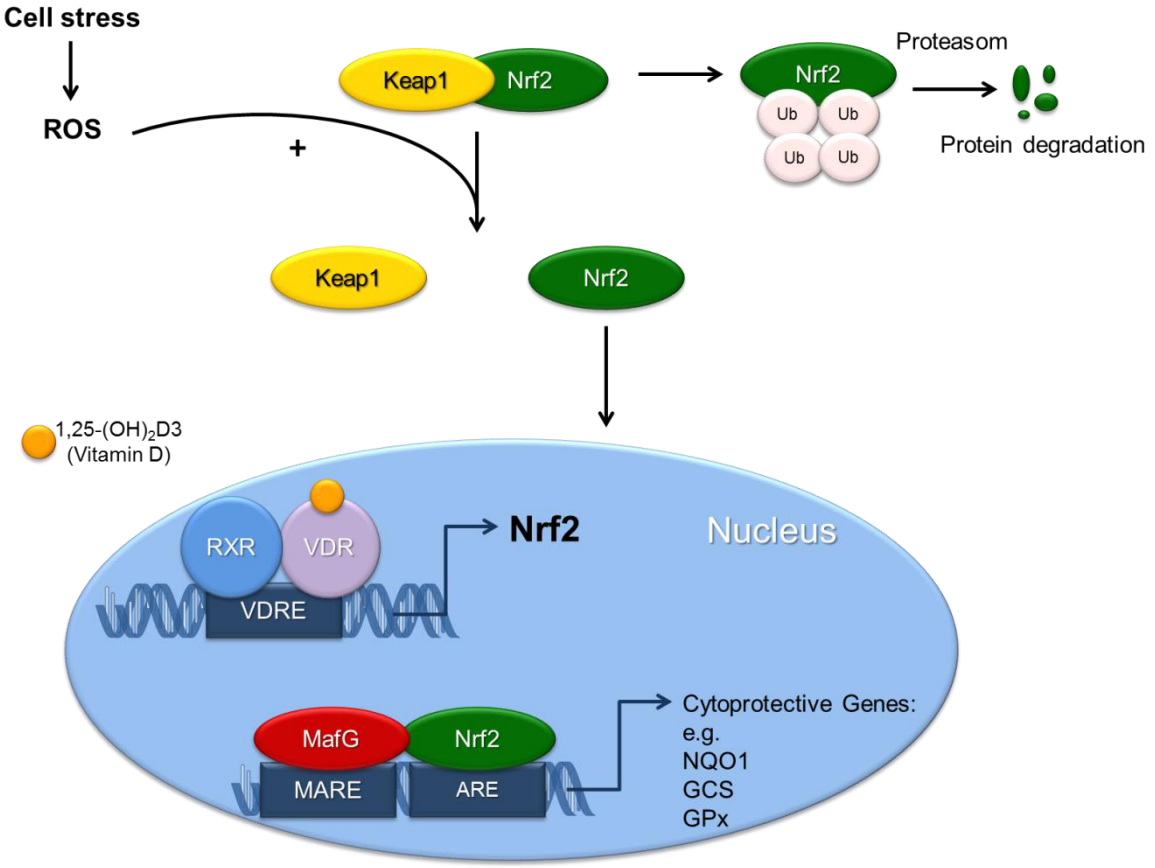

Figure 9: Crosstalk between VDR and Nrf2 (modified from Berridge, 2015).
Vitamin D leads to an activation of the TF Nrf2. In the absence of oxidative stress, Nrf2 is bound to Keap1 and is targeted for ubiquitination and proteasomal degradation. ROS lead to the dissociation of Nrf2 and Keap1 and the translocation of Nrf2 into the nucleus for the formation of a heterodimer with MAFG to activate cytoprotective genes.
RXR: retinoid X receptor, VDR: Vitamin D receptor, VDRE: Vitamin D receptor response element, MafG: small Mafs, Nrf2: nuclear factor (erythroid-derived 2)-like 2, MARE: Maf recognition element, ARE: antioxidant response element, Keap1: Kelch-like ECH-associated protein 1, Ub: Ubiquitin, ROS: reactive oxygen species.

1.2.8 Vitamin D status in HBV-infected patients

Clinical observations revealed evidence that in chronic HBV-infected patients, the virus load in taken blood samples varies seasonally. Chronically infected patients had increased virus replication rates during winter periods (Zhang et al., 2006). Due to the association of low bone mineral density in patients (a typical symptom of vitamin-deficiency), one possibility for a seasonally triggering factor might be vitamin D (Trautwein et al., 2000). Interestingly, in 2013, researchers from the *Goethe University Hospital* in Frankfurt published that chronically HBV-infected patients show low serum levels for

vitamin D with increasing virus load (Farnik et al., 2013). In the following years, further research groups could support the observation of a negative correlation of vitamin D levels and the viral DNA in patients (Chen et al., 2015; Mohamadkhani et al., 2015; Wong et al., 2015).

Moreover, genetic data give evidence for an involvement of vitamin D in the course of HBV infection. Polymorphisms in the *VDR*, *CYP27B1*, and *DBP* genes are associated with HCC development in patients suffering from chronic HBV (Huang et al., 2010; Peng et al., 2014; Yao et al., 2013; Zhu et al., 2012). An ongoing clinical trial analyzes the beneficial effects of vitamin D supplementation with pegIFNα or telbivudine monotherapy in patients suffering from chronic HBV infection (ClinicalTrials.gov, 2010).

1.3 Hypothesis and aim

This PhD project is part of the collaborative project *"Comparative analysis of HBV genotypes"* of the PEI in cooperation (sections *Molecular Virology of Hepatitis Viruses* (2/0) and *Molecular Virology* (2/4) within the *Division of Virology*) with the *National Reference Centre for Hepatitis B and D Viruses* in Gießen and the *Goethe University Hospital* in Frankfurt. The impact of the HBV genotypes with regard to pathogenesis, treatment, and diagnosis is still unanswered. Only limited data of the comparison of genotypes under standardized conditions *in vitro* exist. According to recent data, the need of further analyses of the HBV genotypes is critical and should be addressed in this project. Moreover, strong genetic and epidemiological data suggest that vitamin D is involved in the course of the HBV infection. Preliminary clinical data correlate vitamin D deficiency with the HBV-status. The aim of the project was to characterize the direct influence of vitamin D treatment on the life cycle of HBV *in vitro* and to identify a potential mechanism of inhibition. Finally, vitamin D should be used as a tool for the further comparative analysis of the HBV genotypes.

2. Material and Methods

2.1 Material

In the following chapter, all used material is listed.

Table 5: List of plasmids used

Name	Description	Producer
GRASP65-GFP	encodes for the GRASP65 genome-tagged with GFP	Prof. Dr. Rainer Duden. University Lübeck
pCEP-gtA-1.5	encodes for the 1.5-fold HBV genome genotype A with ampicillin resistance	PD Dr. Glebe, University Gießen; Peiffer et al., 2015
pCEP-gtA-AAVS1	encodes for the 1.5-fold HBV genome genotype A with Puromycin resistance	PD Dr. Glebe, University Gießen
pCEP-gtB-1.5	encodes for the 1.5-fold HBV genome genotype B with ampicillin resistance	PD Dr. Glebe, University Gießen
pCEP-gtC-1.5	encodes for the 1.5-fold HBV genome genotype C with ampicillin resistance	PD Dr. Glebe, University Gießen
pCEP-gtD-AAVS1	encodes for the 1.5-fold HBV genome genotype D with Puromycin resistance	PD Dr. Glebe, University Gießen
pCEP-gtG-1.5	encodes for the 1.5-fold HBV genome genotype G with ampicillin resistance	PD Dr. Glebe, University Gießen; Peiffer et al., 2015, Goethe University Frankfurt
pEGFP-N1	control vector with ampicillin resistance	Clontech Laboratories Inc., Heidelberg
pEGFP-Vps4A.wt	encodes for Vps4A	Prof. Dr. Prange, University Hospital Mainz
peYFP-Rab7	encodes for Rab7, a marker of MVBs	Prof. Dr. Munz, University Tübingen

Name	Description	Producer
pHBV1.2 (pJo19)	encodes for the 1.2-fold HBV genome genotype D (serotyoe awy) with ampicillin resistance	Dr. Lupberger, INSERM Strasbourg
pUC18	control vector with ampicillin resistance	Life Technologies GmbH, Darmstadt
Sec22-YFP	encodes for the Sec22 genome-tagged with YFP	Prof. Dr. Rainer Duden, University Lübeck

Table 6: List of cell lines used

Designation	Medium	Producer
Hek 293-T	cDMEM	provided from Prof. Dr. Barbara Schnierle
HepAD38 human hepatoma cell line, stably expressing 1,2-fold HBV genome (Tet-regulated, serotype *ayw*, genotype D); derived from HepG2 cell line	cDMEM (500ml) + - 5µg insulin - 25 µg hydrocortisone	Ladner et al., 1997
HepaRG human hepatoma cell line, by differentiation some characteristics of PHHs were received	Williams´ E Medium - 10% FCS - 100 U/ml penicillin - 100 µg/ml streptomycin - 2 mM L-glutamine - 25 µg/ml hydrocortisone - 5 µg/ml insulin - 10% DMSO	Gripon et al., 2002

Designation	Medium	Producer
HepG2 human hepatoma cell line	cDMEM	Knowles, Howe, and Aden, 1980
HepG2.2.15 human hepatoma cell line, stably expressing 2,15-fold HBV genome (serotype ayw, genotype D) ; derived from HepG2 cell line	cDMEM	Sells, Chen, and Acs, 1987
Huh 7.5 Huh 7 derived human hepatoma cell line	cDMEM	Blight, McKeating, and Rice, 2002
PHHs	Hepatocyte growth medium (Promo Cell) + supplement-mix: - 10 ng ml epidermal growth factor (recombinant human) - 5 µg/ml insulin (recombinant human) - 0.5 µg/ml Hydrocortisone - 10 µg/ml transferrin, holo (human) - 250 µg/ml ascorbic acid - 3.75 mg/ml bovine serum albumin fatty acid free (BSA-FAF)	Isolated from liver tissue of partial hepatectomies, Goethe University Hospital in Frankfurt or delivered from MHH Hannover, DZIF

Table 7: List of media and supplements of cell culture used

Designation	Producer
100x penicillin streptomycin	Lonza, Basel, Switzerland
Accutase	PAA, Linz, Austria
DMEM (Dulbecco's Modified Eagles' Medium)	Lonza, Basel, Switzerland

Designation	Producer
FCS (Fetal calf serum)	PAA, Linz, Austria
HBSS (Hanks Salt Solution without Ca^{2+}/Mg^{2+})	Thermo Scientific, Langenselbold
Hepatocyte growth medium	Promo Cell GmbH, Heidelberg
Hydrocortisone	Sigma-Aldrich, Seelze
Insulin, bovin (50 mg in ddH_2O)	Sigma-Aldrich, Seelze
LB (lysogeny broth) medium	Section 3/3, PEI, Langen
LB agar plates + ampicillin or kanamycin	Section 3/3, PEI, Langen
L-Glutamine	PAA, Linz, Austria, Lonza, Basel, Switzerland
PBS (phosphate-buffered salt solution), sterile	Section 3/3, PEI, Langen
Penicillin/streptomycin	PAA, Linz, Austria
Puromycin	Sigma-Aldrich, Seelze
SOC medium	Section 3/3, PEI, Langen
Trypsin/EDTA (ethylendiamintetraacetate)	Section 3/3, PEI, Langen

Table 8: List of bacteria used

Material	Designation	Producer
One Shot® TOP 10 *E. coli*	F-mcrAD(mrr-hsdRMS-mcrBC) φ80lacZDM15 DlacX74 nupG recA1 araD139 D(ara-leu)7697 galE15 galK16 rpsL(StrR) endA1λ	Life Technologies GmbH, Darmstadt

Table 9: List of primary antibodies used

Designation	Dilution	Producer
Anti adaptin-γ, mouse, monoclonal	WB: 1:500 in 10% SMP in TBS (Tris buffered saline)-T IF: 1:100 in 1% BSA in PBS	Thermo Scientific, Karlsruhe
Anti- LHBs (MA18/7), mouse, monoclonal	WB: 1:600 in 10% SMP in TBS-T IF: 1:150 in 1% BSA in PBS	Heermann et al., 1984, Göttingen University
Anti-β-Actin, mouse, monoclonal	WB: 1:10.000 in 10% SMP in TBS-T	Sigma-Aldrich, Seelze
Anti-HBcAg (K46), rabbit, polyclonal	WB: 1:5000 in 10% SMP in TBS-T	Prof Dr. Prange, University Medical Center of the Johannes Gutenberg University Mainz
Anti-HBcAg (mAB16990), mouse, monoclonal	IF: 1:200 in 1% BSA in PBS	Merck, Millipore, Darmstadt
Anti-HBsAg (HB01), mouse, monoclonal	WB 1:200 in 10% SMP in TBS-T IF: 1:100 in 1% BSA in PBS	PD Dr. Glebe,Justus-Liebig University Gießen
Anti-HBsAg, goat, polyclonal	IF: 1:200 in 1% BSA in PBS	Abcam, Cambridge. UK
Anti-TSG101, mouse, monoclonal	WB: 1:1000 in Roti-Block	Santa Cruz Biotechnology Inc., Santa Cruz, CA, USA
Anti-TXLNA (E-2) mouse, monoclonal	WB: 1:1000 in Roti-Block	Santa Cruz Biotechnology, Inc., Santa Cruz, CA, USA
Anti-TXLNA (H-66), rabbit, polyclonal	IF: 1:100 in 1% BSA in PBS	Santa Cruz Biotechnology Inc., Santa Cruz, CA, USA
Anti-human Tubulin	WB: 1:850 in 3% BSA in PBS	Santa Cruz Biotechnology Inc., Santa Cruz, CA, USA

Table 10: List of secondary antibodies used

Designation	Dilution	Producer
Anti-goat IgG-Alexa488, donkey, polyclonal	IF: 1:1000 in 1% BSA in PBS	Invitrogen, Karlsruhe

Designation	Dilution	Producer
Anti-mouse IgG-Alexa488 donkey, polyclonal	IF: 1:1000 in 1% BSA in PBS	Invitrogen, Karlsruhe
Anti-mouse IgG-Cy3, donkey, polyclonal	IF: 1:400 in 1% BSA in PBS	Jackson ImmunoResearch Europe, Suffolk, UK
Anti-mouse IgG-Cy5, donkey, polyclonal	IF: 1:400 in 1% BSA in PBS	Jackson ImmunoResearch Europe, Suffolk, UK
Anti-mouse IgG-HRP (horseradish peroxidase) sheep, polyclonal	WB: 1:2500 in 10% SMP	GE Healthcare, Freiburg
Anti-mouse IRDye® 680RD donkey, polyclonal	WB: 1:10000 in Roti-Block	LI-COR Biosciences GmbH, Bad Homburg
Anti-mouse IRDye® 800CW donkey, polyclonal	WB: 1:10000 in Roti-Block	LI-COR Biosciences GmbH, Bad Homburg
Anti-rabbit IgG-Alexa488, donkey, polyclonal	IF: 1:1000 in 1% BSA in PBS	Invitrogen, Karlsruhe
Anti-rabbit IgG-Cy5 donkey, polyclonal	IF: 1:400 in 1% BSA in PBS	Jackson ImmunoResearch Europe, Suffolk, UK
Anti-rabbit IgG-HRP	WB: 1:2500 in 10% SMP	GE Healthcare, Freiburg
Anti-rabbit IRDye® 680RD donkey, polyclonal	WB: 1:10000 in Roti-Block	LI-COR Biosciences GmbH, Bad Homburg
Anti-rabbit IRDye® 800CW donkey, polyclonal	WB: 1:10,000 in Roti-Block	LI-COR Biosciences GmbH, Bad Homburg

Table 11: List of kit systems used

Application	Designation	Producer
Cell viability kit	PrestoBlue® Cell Viability Reagent	Thermo Scientific, Karlsruhe
DNA isolation	- High Pure Viral Nucleic Acid Purification Kit	Roche GmbH, Mannheim
	- Blood And Tissue Purification Kit	Qiagen, Hilden

Application	Designation	Producer
ELISA (enzyme-linked Immunosorbent Assay)	Enzygnost HBsAg 6.0, Enzygnost HBeAg monoclonal	Siemens Healthcare Diagnostics Products GmbH, Marburg
Gelextraction	peQGold Gel Extraction Kit	PeqLab, Erlangen
Plasmid preparation	Qiagen Plasmid Maxi Kit	Qiagen, Hilden

Table 12: List of devices used

Machine	Designation	Producer
Analog tube rollers	Stuart Roller Mixer SRT9	Bibby Scientific, UK
Autoradiography cassette	Hypercassette™	GE Healthcare, Freiburg
Cell counter	Particle counter Z1	Beckman Coulter, Krefeld
Chemical flow	Captair Flex	Erlab, Cedex, France
Chemiluminescent western blot scanner	C-DiGit® Blot Scanner	LI-COR Biosciences, Bad Homburg
Clean bench	BBD 6220 SterilGard III Advance	Heraeus, Osterode The Baker Company, ME, USA
Counting chamber	Counting chamber	Carl Roth, Karlsruhe
Electrophoresis	Electrophoresis power supply EPS301	GE Healthcare, Freiburg
	Horizontal electrophoresis system HE33	GE Healthcare, Freiburg
	SE250 Series electrophoresis unit	GE Healthcare, Freiburg
	Semidry blotting chambers TE77 Semidry blotting chambers TE77 PWD	GE Healthcare, Freiburg
	Semiphor TE70 semi-dry transfer unit blotter	GE Healthcare, Freiburg
	Standard power pack P25	Biometra, Göttingen

Machine	Designation	Producer
FACS (fluorescence activated cell sorting)	BD Accuri C6	Becton, Dickinson and Company, Franklin Lakes, New Jersey, USA
Film processor	Curix 60	Agfa, Cologne
Gel documentation	INTAS-Imaging System	Intas, Göttingen
Infrared imaging system	Odyssey Sa Infrared Imaging System	LI-COR Biosciences, Bad Homburg
Magnetic stirrer	RCT classic	IKA, Staufen
Microplate reader	Tecan Infinite M1000	Tecan Group Ltd., Männedorf, Switzerland
Northern blot system	TurboBlotter Rapid Downward Transfer System	Schleicher & Schuell BioScience GmbH, Dassel
pH-meter	Seven Easy Mettler	Toledo GmbH, Gießen
Photometer	Ultrospec 3000	GE Healthcare, Freiburg
Pipettes	- Eppendorf Reference®, 1- canal, variabel (0,1–2,5 µl; 0,5–10 µl; 2–20 µl; 10–100 µl; 50–200 µl; 100–1.000 µl) - Eppendorf Reference® , 8- and 12-canal (10–100 µl; 30–300 µl) - Eppendorf Easypet® multistepper	Eppendorf, Hamburg
Precision balance	M-Power, LP 6000 200S	Sartorius, Göttingen
Rocking platform	Tumbling Table TT 30	Biometra, Göttingen
Shaking Incubator	Innova® 44/44R	Brunswick Scientific, Nürtingen
Spectrometer	Ultrospec 1100 pro	GE Healthcare, Freiburg
Thermomixer	- Thermomixer Compact - Thermoblock 1	Eppendorf, Hamburg Biometra, Göttingen

Machine	Designation	Producer
Ultrasound homogenizer	Sonopuls HD 2200	Bandelin GmbH, Berlin
UV/VIS spectrophotometer	DU®730 Life Science	Beckman Coulter, Krefeld
Water bath	- TW12 - 1228-2F	Julabo, Seelbach VWR, Darmstadt
Water purification system	Milli-Q® Advantage A10	Merck Millipore, Darmstadt

Table 13: List of microscopes used

Microscope	Producer
Axio Observer.Z1	Carl Zeiss AG, Jena
Axiovert 40C	Carl Zeiss AG, Jena
Confocal laser scanning microscope 510	Carl Zeiss AG, Jena
Electron microscope, EM-109 transmission electron microscope	Carl Zeiss AG, Jena
Infinity 2 Microscope Camera	Lumenera, Nepean, Canada
Leica, Leitz DM RBE	Leica, Wetzlar

Table 14: List of centrifuges used

Centrifuges	Producer
Sepatech Cryofuge 8500, Sepatech 6606 Rotor, Heraeus Fresco 17 centrifuge, Heraeus Multifuge 1S-R sorvall 75002000, Heraeus Sepatech varifuge RF, Sepatech 5315 rotor	Heraeus Holding GmbH, Hanau

Table 15: List of PCR cyclers used

Cycler	Producer
ABI TaqMan, Roche LightCycler	Roche, Basel, Switzerland
LC480, real time PCR system	Roche, Basel, Switzerland
Mastercycler gradient	Eppendorf, Hamburg
Mastercycler® Nexus	Eppendorf, Hamburg
TPersonal	Biometra, Göttingen

Table 16: List of expendable materials used

Material	Designation	Producer
Cassette	HypercassetteTM	GE Healthcare, Freiburg
Cell culture flask and dishes	Dishes: - NuncTM cell culture dishes 60 mm	Thermo Scientific, Karlsruhe
	CELLSTAR ® cell culture flasks (T25/75/175): - Standard cell culture flasks - Filter Top cell culture flasks CELLSTAR ® cell culture multiwell plates: - 6, 12, 24, 96 well format	Fischer, Hannover
Cell culture scraper	TPP cell scraper	TPP Techno Plastic Products AG, Trasadingen, Switzerland
Counting chamber	C-Chip Neubauer improved	Carl Roth, Karlsruhe
Cover slipes	P231.1, Ø (mm):12	Carl Roth, Karlsruhe
Developer solution	Developer type E 1-3	C & L GmbH, Planegg
Disposable pipettes	2 ml 5 ml 10 ml 25 ml	Material Storage, PEI, Langen

Material	Designation	Producer
Filter paper	Whatman Paper	GE Health Care, Freiburg
Fixer solution	Fixer type F 1+2	C & L GmbH, Planegg
Freezing tubes	Cryo.s™	Greiner Bio-One GmbH, Frickenhausen
Glass beads	EZ-Spread™ Plating Beads	Genlantis, San Diego, USA
Hyper films	Amersham hyperfilm ECL, (18 × 24 cm), (12.7 × 17.8 cm)	GE Healthcare, Freiburg
Light cycler plate	LightCycler® 480 multiwell plate 96	Roche, Basel, Switzerland
Microscope slides	Microscope slides standard	Carl-Roth, Karlsruhe
Phase lock gel Pipette tips	Phase lock gel heavy, 2 ml Pipette tips Pipette tips with filter	5 PRIME GmbH, Hilden Sarstedt, Nümbrecht 4titude, Berlin
Reaction tubes	1.5 and 2 ml reaction tube PCR tubes 0.2 ml (domed cap)	Eppendorf, Hamburg VWR International GmbH, Erlangen
Reaction tubes 15ml/ 50ml	15 ml/ 50 ml CELLSTAR® polypropylene tube	Greiner Bio-one, Frickenhausen
Scalpel	Surgical disposable scalpel	B. Braun, Melsungen
Specimen slide	Standard-Objektträger	Carl Roth, Karlsruhe
Syringes	Omnifix®-F syringes (1, 5, 10, 20 ml)	B. Braun, Melsungen
Transfer membranes	0.45 µm pore size hydrophobic PVDF transfer membrane for western blotting	Merck Millipore, Darmstadt
	926-31092 Odyssey® nitrocellulose membranes	LI-Cor Biosciences, Bad Homburg
	Amersham Hybond-N+	GE Healthcare, Freiburg

Material	Designation	Producer
Transparency film	Parafilm	Brand GmbH + Co KG, Wertheim

Table 17: List of chemicals used

Designation	Producer
5x reaction buffer for M-MuLV RT	Fermentas, St. Leon-Rot
Agarose LE	Genaxxon, Biberbach
Bromphenol blue	Merck, Darmstadt
Calcipotriol	Sigma-Aldrich, Seelze
Calcitriol	Sigma-Aldrich, Seelze
Chloroform	Carl-Roth, Karlsruhe
DAPI (4′,6-diamidin-2-phenylindol)	Sigma Aldrich, Seelze
DMSO (dimethyl sulfoxide)	Genaxxon, Biberach/Riss
dNTP-mix	Fermentas, St. Leon-Rot
EB1089	Dr. Christian Lange, Goethe University Hospital, Frankfurt
EDTA	Serva, Heidelberg
Ethanol (methylated)	Merck, Darmstadt
Ethanol 96%	Merck, Darmstadt
Ethidiumbromid	Applichem, Darmstadt
Glycerin 99.5%	GERBU, Heidelberg
Glycin	AppliChem, Karlsruhe
ddH_2O (sterile)	Section 3/3, PEI, Langen
Immobilon Western HRP Substrate	Merck, Darmstadt
Isopropanol	Merck, Darmstadt

Designation	Producer
Kanamycine	Carl Roth, Karlsruhe
Luminata Forte Western HRP Substrate	Merck, Darmstadt
Methanol	Carl Roth, Karlsruhe
Mowiol	Sigma-Aldrich, Seelze
n-Butanol	Merck, Darmstadt
Oxacalcitriol	Santa Cruz Biotechnology Inc., Santa Cruz, USA
Paricalcitol	Tocris Bioscience, Bristol, United Kingdom
peqGOLD TriFast	PeqLab, Erlangen
PFA (paraformaldehyde) 37%	Carl Roth, Karlsruhe
PFA 37% (for northern blot analysis)	The Baker Company, Sanford, USA
Phenol	AppliChem, Darmstadt
Polyethyleneimine (PEI)	Fermentas, St. Leon-Rot
Random Hexamer Primer (200 ng/ml)	Fermentas, St. Leon-Rot
Revert Aid*TM* H Minus M-MuLV RT	Fermentas, St. Leon-Rot
Roti ® Block (10x)	Carl Roth, Karlsruhe
Rotiphorese® 40 Acrylamid/Bisacrylamid (29:1)	Carl Roth, Karlsruhe
RQ1 stop solution	Promega, Madison, USA
SDS (sodiumdodecylsulfate) 10%	Carl Roth, Karlsruhe
SMP (skimmed milk powder)	Carl Roth, Karlsruhe
Sodium	Carl Roth, Karlsruhe
Sodium chloride	Carl Roth, Karlsruhe
Sodium deoxycholate	AppliChem, Darmstadt
SuperSignal ‘West Femto’ chemiluminescent substrate	Thermo Scientific, Karlsruhe
SuperSignal ’West Pico’ chemiluminescent substrate	Thermo Scientific, Karlsruhe

Designation	Producer
SYBR Green PCR Master Mix (2x)	Invitrogen, Karlsruhe
Tacalcitol	Dr. Christian Lange, Goethe University Hospital, Frankfurt
TEMED (tetramethylethylenediamine)	Merck, Darmstadt
Tris (tris(hydroxymethyl)aminomethane)	Carl Roth, Karlsruhe
Triton X-100	Fluka, Deisenhofen
TWEEN 20 (Polysorbat 20)	Serva, Heidelberg
Xylol	Merck, Darmstadt
β-Mercaptoethanol	Sigma-Aldrich, Seelze

Table 18: List of standards used

Designation	Name	Producer
DNA standards	Gene Ruler*TM* 1kb DNA ladder	Fermentas, St.-Leon-Rot
Protein standards	PageRuler*TM* prestained protein ladder	Fermentas, St.-Leon-Rot
	PageRuler*TM* Plus prestained protein ladder	

Table 19: List of enzymes used

Designation	Name	Producer
Accutase	Accutase cell detachment solution	Merck Millipore, Schwalbach
Collagenase	Collagenase (Typ IV)	Sigma, Seelze
DNase	RQ1 RNase-Free DNase	Promega, Madision USA
M-MuLV reverse transcriptase	RevertAid reverse transcriptase	Fermentas, St. Leon-Rot

Table 20: List of primers used

Catalog number Hildt's Lab	Name	Sequence	Published	Primer eff.
#185	HBV S fwd	aac atg gag aac atc aca tca g	Schädler et al., 2010	84.49%
#186	HBV S rev	tat acc caa aga caa aag aaa att gg	Schädler et al., 2010	
#405	HBV 3.5kb fwd	ctc caa gct gtg cct tgg g	Peiffer et al., 2015	92.89%
#406	HBV_3.5kb_rev	ccc acc cag gta gct aga g	Peiffer et al., 2015	
#280	α-Taxilin HS fwd	atg aag aac caa gac aaa aag a	Hoffmann et al., 2013	97.57%
#281	α-Taxilin HS rev	ctg gct gct gcc ggg ac	Hoffmann et al., 2013	
#835	RPL27 fwd	aaa gct gtc atc gtg aag aac	Sequence provided by the Institute of Molecular Biology and Tumor Research, Philipps University, Marburg, Adhikary et al., 2011	97.24%
#836	RPL27 rev	gct gct act ttg cgg ggg tag	Sequence provided by the Institute of Molecular Biology and Tumor Research, Philipps University, Marburg, Adhikary et al., 2011	
#763	CYP24A1 fwd	tgg aag gcc tat cgc gac ta	Schuster et al., 2006	94.55%
#764	CYP24A1 rev	gga ccc gct gcc agt ctt	Schuster et al., 2006	

Catalog number Hildt's Lab	Name	Sequence	Published	Primer eff.
#783	AP1G1 fwd	cca cac atc tgt agt cct cc	Wood et al., 2004	83.91%
#784	AP1G1 rev	aac cgc aaa att cgt acc tg	Wood et al., 2004	
*#3*61	TSG101 fwd	tat ttg gag atg aac ctc ca	Hoffmann, 2013	81.69%
*#3*62	TSG101 rev	atg gag aga tcc cac ctg gc	Hoffmann, 2013	

All oligonucleotides were produced by biomers.net GmbH.

Table 21: List of inhibitors used

Application	Name	Target	Producer
Proteases inhibitors	aprotinin	serine proteases	Sigma-Aldrich, Seelze
	leupeptin	serine- and cysteine proteases	
	pepstatin	spartyl proteases	
	PMSF	serine proteases	Carl Roth, Karlsruhe

Table 22: List of media and buffer used

Reagent	Content	Producer
Agarose gel solution	0.5–1.5% (w/v) agarose in TAE buffer	Section 2/0, PEI, Langen
APS (Ammoniumperoxidisulphat)	10% (w/v) in ddH_2O	Section 2/0, PEI, Langen
Anode buffer I	20% (v/v) ethanol 300 mM tris base	Section 2/0, PEI, Langen
Anode buffer II	20% (v/v) ethanol 25 mM tris base	Section 2/0, PEI, Langen
Blocking and antibody solution	10% (w/v) SMP in TBS-T buffer; 1x Roti® (v/v) in ddH_2O	Section 2/0, PEI, Langen Section 2/0, PEI, Langen
Cathode buffer (pH= 7.6)	20% (v/v) ethanol 40 mM 6-aminohexanoic acid 10 mM tris-HCl	Section 2/0, PEI, Langen
DNA loading dye (6x)	0.03% bromophenol blue 0.03% xylene cyanol 60% glycerol 60 mM EDTA	Section 2/0, PEI, Langen
Ethidiumbromide	1-5 µl ethidiumbromid stock solution (10 mg/ml) in 60 – 100 ml agarose gel solution	Applichem, Darmstadt, Section 2/0, PEI, Langen
FACS blocking solution	10% FCS in PBS	Section 2/0, PEI, Langen
FACS buffer	1% BSA in PBS	Section 2/0, PEI, Langen
LB agar	15 g agar ad 1 l LB medium + antibiotics	Section 3/3, PEI, Langen
LB medium	pepton and casein, 10 g yeast-extract, 5 g NaCl, 10 g ad 1 l ddH_2O	Section 3/3, PEI, Langen

Reagent	Content	Producer
20x MOPS	1 M MOPS 1 M tris(hydroxymethyl)-aminomethan 69.3 mM SDS 20.5 mM EDTA ad 10 l ddH_2O	Section 3/3, PEI, Langen
Mowiol (pH= 8.5)	10% (w/v) mowiol 25% (w/v) glycerol 100 mM tris/ HCl	Section 2/0, PEI, Langen
Northern blot denaturing buffer	500 µl deionized formamid 120 µl 37% formaldehyd 200 µl 10x MOPS 10 µl ethidiumbromid	Section 2/0, PEI, Langen
Northern blot stop buffer	50% glycerol 0.25% bromphenol blue	Section 2/0, PEI, Langen
10x PBS (pH= 7.4)	80.0 g NaCl 2.0 g KCl 14.4 g Na_2HPO_4 2.4 g KH_2PO_4 ad 1 l ddH_2O	Section 3/3, PEI, Langen
RIPA (radioimmunoprecipitation assay) buffer (pH= 7.2)	50 mM tris-HCl 150 mM NaCl 0,1% (w/v) SDS 1% (w/v) sodium desoxycholat 1% (v/v) triton X-100 1 µM aprotinin 4 µM leupeptin 1 µM pepstatin 1 mM PMSF	Section 2/0, PEI, Langen
4x Sample buffer (pH= 6.8)	4% (w/v) SDS 125 mM tris-HCl 10% (v/v) glycerol 10% (v/v) β-mercaptoethanol 0.02% (w/v) bromphenol blue	Section 2/0, PEI, Langen

Reagent	Content	Producer
10x SDS running buffer (pH= 8.3)	0.25 M tris 2 M glycin 1% (w/v) SDS	Section 2/0, PEI, Langen
Separation gel buffer (pH= 8,8)	1.5 M tris-HCl 0.4% (w/v) SDS	Section 2/0, PEI, Langen
SOB-Medium	bacto-tryptone, 20 g bacto yeast-extract, 5 g NaCl, 0.5 g ad 1 l ddH_2O	Section 3/3, PEI, Langen
SOC-Medium	SOB-medium, 26.6 g glucose-solution, 20 ml ad 1 l ddH_2O	Section 3/3, PEI, Langen
20x SSC	1753.2 g NaCl 882.3 g tri-natriumcitrat x $2H_2O$ ad 10 l ddH_2O	Section 3/3, PEI, Langen
Stacking gel buffer (pH= 6.7)	0.5 M tris-HCl 0,4% (w/v) SDS	Section 2/0, PEI, Langen
20x TAE (tris-acetate-EDTA) buffer (pH= 8.0)	tris(hydroxymethyl)-aminomethan, 968 g 50% acetic acid, 457 ml EDTA 0.5M pH 8.0, 400 ml ad 10 l ddH_2O	Section 3/3, PEI, Langen
10x TBS-T (Tween 20)	200 mM tris-HCl pH 7.8 1.5 M sodium chloride 0.5% tween 20	Section 3/3, PEI, Langen
Trypsin-EDTA (0.05%trypsin) (pH= 7.1)	trypsin 250. 5 g titriplex III, 2 g ad 10 l PBS	Section 3/3, PEI, Langen

Table 23: List of internet resources used

Application	Website
Literature research	*http://www.ncbi.nlm.nih.gov/*
Protein sequences	*http://www.uniprot.org/*
Restriction of DNA sequences	*http://tools.neb.com/NEBcutter2/*
Translation from DNA to protein sequence	*http://web.expasy.org/translate/*

Table 24: List of software used

Designation	Name	Producer
Analysis of Light Cylcer Runs	LightCycler 480 Software, Version 1.5	Roche Diagnostics GmbH
Gel Documentation	Intas GDS	Intas, Göttingen
Image program	- Irfan View - Photoshop CS6 - ImageJ	Irfan Škiljan Adobe, US Wayne Rasband, NIH, US
CLSM (confocal laser scanning microscopy) program	ZEN Lite 2012	Zeiss, Jena
Presentation program	PowerPoint 2010	Microsoft Windows
Table calculation	Excel 2010	Microsoft Windows
Text program	Word 2010	Microsoft Windows
Citation program	Endnote X4	Thomson Reuters

2.2 Molecular biological methods

Molecular biological methods are common techniques for analyzing the interactions of cell components by the manipulation of DNA, RNA, and proteins.

2.2.1 Cultivation of bacteria

The cultivation of bacteria was used to amplify different plasmids. In order to prepare bacteria such as *E. coli* (*Escherichia.coli*) for transformation, the heat shock method was used.

2.2.2 Heat shock transformation of E. coli

E. coli (TOP10), stored at -80 °C, were thawed on ice and 10 ng of the desired plasmid was added to 50 µl of the cell suspension, incubated for thirty minutes on ice and the heat shock occurred for one minute at 42 °C. Afterwards, the cells were cooled down for two minutes on ice, and 1 ml of the SOC-medium was added. The preparation was incubated for ninety minutes at 37 °C and at a shaking rate of 800 rpm. Following, the cells were centrifuged for two minutes at 2000 g and 750 µl of the SN was quashed. Thereafter, bacteria were resuspended in the remaining 300 µl. This suspension was plated by means of autoclaved glass beads on antibiotics containing LB agar plates. The plates were afterwards incubated overnight at 37 °C.
Exclusive bacteria, which took up the plasmid with the antibiotic resistance, were capable of growing on the LB agar plates. On the following day, single bacteria colonies were picked by means of a sterile tip of a pipette. The picked clones were cultivated in 500 ml LB medium by shaking at 37 °C overnight.

2.2.3 Preparation of bacterial glycerol stocks

For the preparation of a bacterial glycerol stocks, 500 µl of the overnight culture were mixed with glycerol (80% v/v). The storage was carried out in cryovials at -80 °C. The glycerol stocks could be used for a plasmid amplification without previous heat shock transformation by directly adding 10 µl of the glycerol stock to 500 ml antibiotic containing LB medium.

2.2.4 Plasmid preparation

The isolation and purification of plasmid DNA was performed with the *QIAGEN Plasmid Maxi Kit* according to manufacturer's instructions. The method bases on the lysis of bacteria under alkaline conditions in the presence of SDS (Birnboim and Doly, 1979). The pellet was solubilized in ddH_2O and purified plasmids were stored at -20 °C.

2.2.5 Determination of DNA and RNA concentrations

DNA and RNA concentrations were measured spectrophotometrically with the *Implen's NanoPhotometer*®. The advantage of this device compared to other photometers is that the required sample size for measurement is heavily reduced (1.5 µl sample were used). The different nucleic acids are quantified by measuring absorption at different wavelengths. Delocalized π-electrons of the heterocyclic rings of the DNA/RNA bases were excited (λ= 260 nm). Proteins show an absorption maximum of λ= 280 nm, which represents the absorption of aromatic amino acids. It is possible to determine the concentration of nucleic acids and protein contamination with the Lambert-Beer law ($E= \varepsilon * c * d$; E= Absorbance, ε= Molar attenuation coefficient, c= concentration, d= path length) (Lambert et al., 1931).

2.2.6 Restriction analysis

To analyze constructs and vectors, the DNA was fragmented by restriction. To prepare an agarose gel, the agarose was dissolved in TAE buffer and boiled in a microwave. After adding 20 µg ethidiumbromide to the solution, the gel was poured into a chamber and cured. The samples were applied to the gel with 6x DNA gel loading dye (see Table 22). The separation took place in 1x TAE buffer within an electric field with a voltage of 80 V. The added dye ethidiumbromide intercalates in the DNA and makes it possible to visualize the probe by using UV light. The 1 kb marker of *New England Biolabs* served as DNA standard.

2.2.7 DNA isolation from agarose gels

For the DNA isolation from agarose gels, the *QIAquick Gel Extraction Kit, Qiagen*, was used according to manufacturer's instructions.

2.2.8 DNA isolation from cells

For the isolation of DNA from cell culture, the *Blood & Tissue Kit, Qiagen*, was used according to manufacturer's instructions.

2.2.9 Isolation of viral nucleic acid

The isolation of viral nucleic acids from blood samples and cell culture SN was performed with the *Roche viral nucleic acid purification kit* according to manufacturer's instruction. As input, 200 µl cell culture supernatant (SN) were used.

2.2.10 Sequencing of DNA

DNA sequencing was performed by *SEQLAB Sequence Laboratories Göttingen GmbH*.

2.2.11 RNA isolation

The RNA of cells was isolated by means of phenol-chloroform extraction. Firstly, cells were seeded confluent on cell culture dishes, washed with PBS once and lysed with *peqGOLD TriFast*™ (200 µl for one well of a confluent 6-well plate). Afterwards, cell fragments were removed by centrifugation at 4 °C and 13,300 rpm (*Heraeus*™ *Fresco*™ *Microcentrifuge*). By adding chloroform (80 µl for 400 µl starting material of *peqGOLD TriFast*™) and an additional centrifugation step, a phase separation occurred. The RNA containing upper phase was transferred into a fresh reaction tube and precipitated by adding 300 µl of isopropanol. The mix was incubated for ten minutes at RT followed by a thirty minutes centrifugation at 4 °C and 13,300 rpm. The pellet was washed with 75% ethanol and centrifuged for eight minutes at 13,300 rpm and dried. The resulting RNA was dissolved in DEPC-H_2O and the quality and quantity was tested, using agarose gel electrophoresis and the *Implen's NanoPhotometer*®.

2.2.12 Complementary DNA (cDNA) synthesis

The first step to convert RNA into cDNA is to remove contaminations with remaining DNA. Therefore, the DNA was digested with DNAse for one hour at 37 °C.

2.2.13 Reverse transcription

cDNA was synthesized with reverse transcriptase for one hour at 42 °C.

Table 25: Schema for cDNA synthesis

	Reagent	Time	Temperature
DNA digest	5 µg RNA 1 µl DNaseI 1 µl 10xDNaseI buffer (with MgCl2) ad 10 µl DEPC-H_2O	1 h	37 °C
Stop of DNA digest	1 µl stop solution	10 min	65 °C
Synthesis of the prime strand	1 µl Random Hexamer Primer (500ng/µl)	5 min	65 °C
Reverse transcription	2 µl dNTPs (10mM) 4 µl 5xRT buffer 1 µl reverse transcriptase (200U/µl) (*RevertedAid H Minus Reverse Transcriptase*) ad 20 µl ddH_2O	10 min 1 h	RT 42 °C
Stop reaction		5 min	72 °C

2.2.14 PCR (polymerase chain reaction)

PCR is a method developed in the 1980s for the amplification of DNA fragments *in vitro* (Mullis et al., 1986). The method bases on a temperature profile leading to denaturation, annealing, and extension of the DNA with primers targeting a specific fragment of interest, which should be amplified.

Table 26: Schema of a PCR mix

Reagent	Amount
Template	variable
dNTPs (10 mM)	1 µl
Fwd. primer (10 µM)	0.5 µl
Rev. primer (10 µM)	0.5 µl
10x buffer	2.5 µl
polymerase	1 U
ddH_2O	ad 25 µl

Table 26 shows an example for pipetting a PCR-mix. The supplementation of $MgCl_2$ and commercial enhancers were used to optimize the PCR conditions. As polymerases *Taq DNA Polymerases (NEB)*, *Q5® High-Fidelity DNA Polymerase (NEB)*. or *TaKaRa-Taq™-Polymerase (Clontech)* were used.

2.2.14.1 Touchdown PCR

Touchdown PCR is a specific type of PCR for avoiding unspecific primer binding. In each cycle, the annealing temperature is decreased. The annealing temperature is crucial for the specificity of primer binding; at high temperatures, only specific binding can occur.

Table 27: Temperature profile of touchdown PCR

Temperature	Duration	Number of cycles
95 °C	5 min	1x
95 °C	30 sec	
67-57 °C	45 sec	20x
72 °C	2 min	
95 °C	30 sec	
57 °C	45 sec	20x
72 °C	2 min	
72 °C	5 min	
4 °C	hold	∞

2.2.14.2 qPCR (quantitative real-time PCR)

qPCR is a method based on a normal PCR but gives the additional opportunity to quantify the generated DNA. The fluorescence dye SYBR Green I binds to double-stranded DNA, which is produced by the amplification and leads to the quantification. For qPCR, the *Light Cycler® 480 System* of *Roche Germany Holding GmbH* was used.
As control of the successful of the previous DNA digest, one sample was measured by means of qPCR without previous RT. Furthermore, the primer efficiency was measured and considered for analysis (see Table 20).

Table 28: Composition of the master mix for qPCR

Reagent	Volume
Fwd. primer (10 µM)	0.25 µl
Rev. primer (10 µM)	0.25 µl
Maxima SYBR green qPCR Master Mix (2x)	5 µl
Ultra-pure H_2O	ad 10 µl

Table 29: qPCR program

Program	Temperature [°C]	Time [sec]	Temperature decrease [°C/sec]	Cycle
Initial denature	95	600	20	1x
Denature	95	15	20	
Annealing	56	30	20	45x
Elongation	72	30	5	
Melting curve	95	60	20	
	60	30	20	1x
	95	0	0.1	
				∞
Cooling down	40	30	20	

For analyzing gene expressions by RT-qPCR, the ΔΔct method was used (housekeeping gene *RPL27*) (Livak and Schmittgen, 2001). Quantitative analyses (e.g. of the SN of virus producing cells) were calculated by referring to standards of defined amounts.

2.2.15 Northern blotting

The northern blot analysis is a method for studying RNA and mRNA. The RNA of interest is separated by electrophoresis according to its size and transferred to a membrane. The detection results from hybridization of a ^{32}P-labeled probe and related autoradiography.
In the experimental setting denaturing buffer was added to 10 µg RNA (50% v/v) and incubated for ten minutes at 65 °C. The reaction was stopped by adding stop buffer (see Table 22). Afterwards, the RNA was separated on a 1% agarose gel in 1x MOPS and 1.5% formaldehyde (running buffer 1x MOPS). Finally, the RNA was transferred to a membrane by blotting due to capillary force (transfer buffer, SSC buffer) and visualized.

2.3 Cell biological methods

Cell cultures provide the basis for analyzing scientific tasks in specific cell types and to simplify the complexity of an organism in an experimental setting. The conducted cell culture work was performed under a clean bench in the BSL3** facility of Division 2/0 of PEI. All the materials and flasks were autoclaved or disinfected before usage. The regular control of the cultivated cells was performed by inverse light optical microscope (*Axiovert 40C, Zeiss*).

2.3.1 Cultivation of cells

The cell lines were cultivated in 25–175 cm^2 cell culture flasks and 6-, 12-, 24-, and 96-well plates for the conduction of experiments. The used incubator had a temperature of 37 °C, 5% CO_2 and a humidity of 95%, and the cells were split every three to four days by trypsinization (0.05% Trypsin in PBS). PHHs were seeded directly in the needed format and used for experiments without further transfer. All of the used media were preheated to 37 °C in a water bath.

2.3.2 Storage of mammalian cell lines

Cell lines were stored by cryopreservation in a N_2-tank. For storage, the cells were suspended in medium containing 20% FCS and 10% DMSO.

2.3.3 Determination of cell number

Cell numbers were determined with a Neubauer chamber or with a cell counting device (*Z1 COULTER COUNTER® Cell and Particle Counter, Beckman*).

2.3.4 Cell viability

The cell viability was measured by means of trypan blue as exclusion test or PrestoBlue®-Assay. The PrestoBlue® reagent is based on the blue dye resazurin. Living cells reduce the dye and a fluorescence red/pink color appears, which can be used for photometric quantification (Thermofisher, 2016).

2.3.5 Transfection with PEI

Transfection describes the uptake of foreign DNA into a eukaryotic cell. The PEI stock solution (1 mg/ml in PBS) was sterile-filtered (0.22 µm filter) before usage and stored at -20 °C. The cells were transfected in 6-well plates at a confluency of 75% and six to twenty-four hours after the seeding. The transfection mixture was composed of PBS in an amount of 1/10 of the final media volume, 0.2 µg–1 µg plasmid, and of the 10 µl PEI solution per µg plasmid per well. The components were combined in exactly this order and vortexed for thirty seconds. After an incubation period of thirty minutes at RT, the transfections mix was added dropwise into the medium of the culture dish. The medium of transfected cells was changed after sixteen hours.

2.3.6 Isolation of PHHs (primary human hepatocytes)

The isolation of PHHs was performed in the laboratory of the clinic for general and visceral surgery of the *Goethe University Hospital* in Frankfurt, Germany. The liver tissue was obtained from liver fragments resected for different medical purposes such as metastasis, hepatocellular carcinoma (with no HBV or HCV causing liver pathogenesis), or other pathologies. Tissue was processed immediately after excision and the PHHs were isolated by a two-step perfusion (Strom et al., 1982). Therefore, all the open vessels, except one large branch of a vein, had to be closed using histoacryl gluten and the remaining open vein was used for the perfusion. The resected tissue was washed for ten to twenty minutes by perfusion with continuously replaced fresh HBSS (Hank's Balanced Salt Solution) with the addition of 20 mM HEPES and 10 µg/ml gentamycin (see Figure 10). For the dissolving of cell-cell contacts and avoiding further blood coagulation, the resectate was perfused with 0.5 mM EGTA in HBSS for fifteen to thirty minutes, depending on the size of the tissue and washed afterwards with HBSS. To open up the cells, the extracellular matrix was digested with HBSS-$CaCl_2$-Collagenase solution containing 250 mM $CaCl_2$ and 0.05% (w/v) collagenase for ten to forty-five minutes. The tissue was cut with a scalpel and cells were scratched out into surrounding medium. The remaining capsid and connective tissue were discarded. Afterwards, the suspension was filtered through a strainer on ice. The hepatocytes were washed twice with HBSS and centrifuged for five minutes with 200 g and 4 °C. Following sedimentation, the cells were resuspended in *Hepatocyte Growth Medium*. Finally, 1.5–2 million cells per well were seeded in collagen-coated 6-well plates. The cells were cultured over fourteen days with a medium exchange every 48 hours.

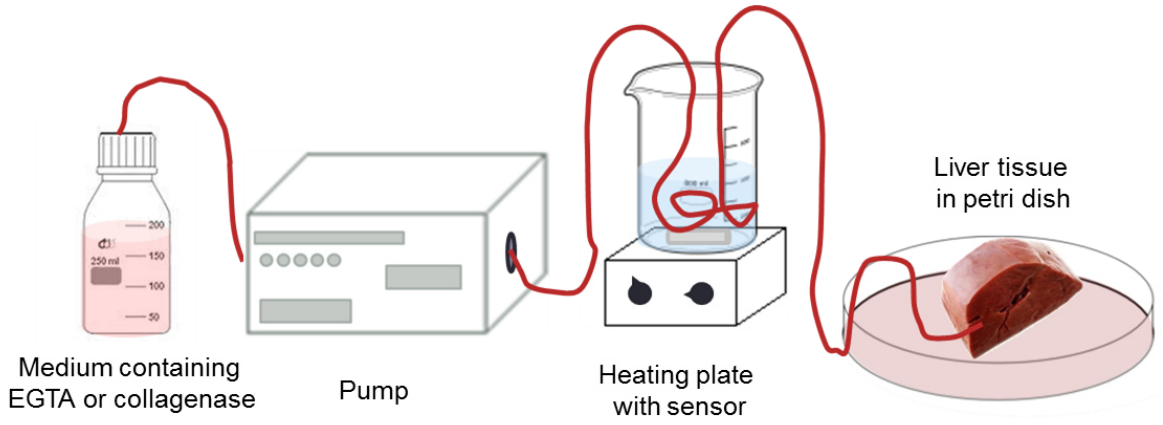

Figure 10: Construction of perfusion-aperture.
The liver resectat was constantly perfused with preheated medium. The tissue was digested by a two-step perfusion −first by EGTA and afterwards by collagenase.

2.3.7 Infection of PHHs with HBV

PHHs were infected with SN of HBV producing cells (HepAD38) or patient serum. Patient sera were obtained from the Division *Molecular Virology* (2/4) of PEI and IUs (infectious units) were measured beforehand by means of a CE-based test. The infection was carried out sixteen to fifty hours after the isolation of the cells. The cells were infected for sixteen hours with a MOI of 100–1000 in *Hepatocytes Growth Medium* by adding 4% PEG 6000 and 2% DMSO.

2.3.8 Mycoplasma test

For testing cell lines for mycoplasma, cells were seeded on cover slides on a regular basis and stained with DAPI. If microscopy analysis gave evidence for contamination, a PCR with mycoplasma specific primer was performed (*PCR Mycoplasma Test Kit, Applichem)*. Cell lines with positive results were treated according to manufacturer's instructions *LookOut® Mycoplasma Elimination Kit, Sigma* or replaced by freshly thawed cells.

2.3.9 Preparation of cell lysates

For the preparation of cell lysates, cells were harvested with a density of around 80%, washed with PBS and detached with a cell scratcher. The cells were lysed with RIPA buffer with added protease inhibitors on ice.

2.4 Protein biochemistry

2.4.1 Determination of protein concentrations

For the quantification of protein concentration in total cell lysates, the Bradford reagent was used (Bradford, 1976). The determination is based on the shifting of the absorption maximum of the dye Coomassie Brilliant Blue G-250 from 470 nm to 595 nm by complexing proteins. The measurement was carried out with the *Tecan reader Infinite M1000* in a 96-well plate. A standard row of a protein (BSA) with defined concentration was used to quantify absolute values.

2.4.2 SDS-PAGE (sodium dodecyl sulfate polyacrylamide gel electrophoresis)

SDS-PAGE is a method to separate proteins in a polyacrylamide gel based on the molecular weight. The proteins were charged with SDS to cover their own charge. Before loading the sample on a gel, it was boiled at 95 °C for ten minutes to dissolve the secondary and tertiary protein structures.

Table 30: Composition for ten mini polyacrylamide gels

	Separation gel			**Stacking gel**
	10%	**12%**	**14%**	**4%**
Acrylamide (Rotiphorese 40 (29:1)) [ml]	20	24	28	6
APS (10%) [µl]	800	800	800	600
ddH_2O [ml]	40	36	32	45
Buffer [ml]	20	20	20	15
TEMED [µl]	80	80	80	60

2.4.3 Western blotting

The designation western blotting orginates on a developed blotting technique of DNA, entitled southern blotting by its inventor Edwin Southern (Southern, 1975). Therefore, the blotting of proteins was termed as western blotting (Burnette, 1981). Before the blotting, proteins have to be separated by SDS-PAGE and afterwards, can be transferred from the polyacrylamide gel to a PVDF (polyvinylidenfluorid) membran by impressed voltage. The transferred proteins were visualized by dint of immune detection.

For the transfer of proteins onto a membrane, the semidry method was applied (Towbin, Staehelin, and Gordon, 1992). A blotting sandwich, consisting of filter papers, gel and membrane, was placed horizontally between two plate electrodes (Kyhse-Andersen, 1984). Before the usage of the membrane, it was activated for thirty seconds by the incubation with methanol. The filter papers were soaked in the respective buffers (see Figure 11) and it was ensured that no air bubbles impair the blotting procedure. The run-time was sixty minutes with 80 mA per SDS mini gel.

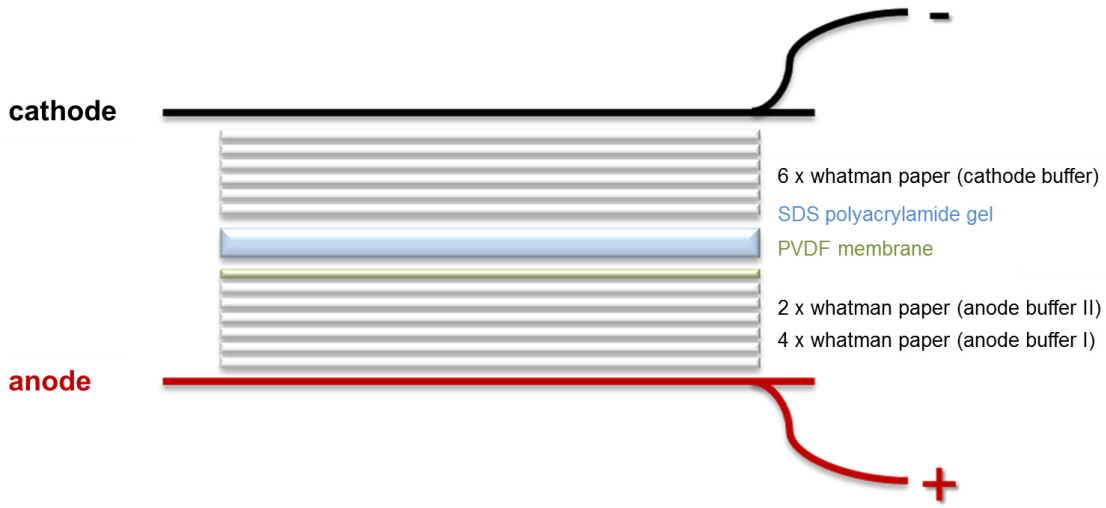

Figure 11: Structure of the blotting sandwich (modified from Finkernagel, 2012).
An impressed voltage leads to the transfer of proteins from the SDS gel to the PVDF membrane.
red: Anode; black: Cathode; grey: Whatman Paper; blue: SDS polyacrylamide gel; light green: PVDF membrane

The proteins on the membrane could be visualized by the binding of a primary antibody, which was targeting the protein of interest (washing steps inbetween antibody incubation

in TBS-T, three times for 10 minutes). The secondary antibody detects the species the primary antibody was originated from. The secondary antibody was labeled with a fluorescence dye or HRP. For fluorescence detection, the *Odyssey ® CLx Imaging System* was used, for HRP an ECL substrate and *Amersham Hyperfilm ECL, GE Healthcare* were used. Blocking of unspecific binding was prevented by usage of blocking reagents such as *Roti®-Block* or 10% SMP in TBS-T.

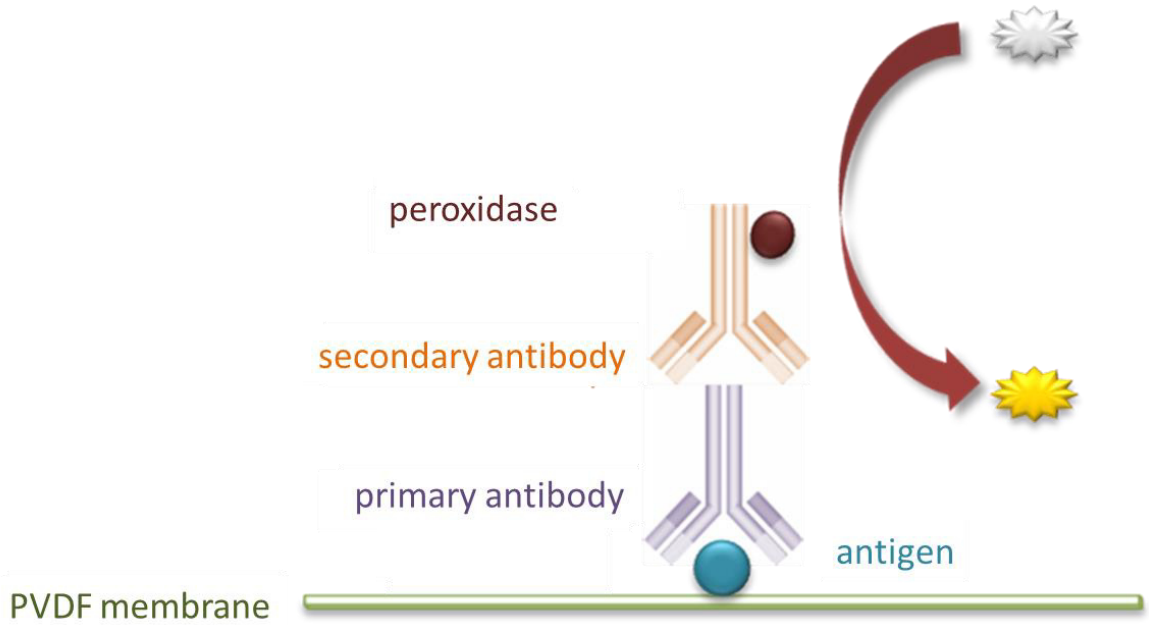

Figure 12: Immune detection of proteins on a PVDF membrane (modified from Finkernagel, 2012).
Proteins blotted on the membrane are detected by means of binding the primary antibody. Secondary antibodies target the species-specific Fc-fragment of the primary antibody. Secondary antibodies can be coupled to a fluorescence dye or a peroxidase, and detection is possible by converting a substrate and the dye or the peroxidase is leading to a signal.
Lightgreen: PVDF membrane; blue: Antigen; purple: Primary antibody; orange: Secondary antibody; red: Peroxidase; yellow: Converted substrate.

2.4.4 Stripping of membranes

For the removal of bound antibodies, PVDF membranes were stripped by incubation with hot 10% SDS in ddH_2O for three minutes (10% SDS was boiled in the microwave).

2.5 Immunological methods

Immunological methods are based on the detection of antibodies and/or antigens. They allow for instance the quantification of proteins.

2.5.1 ELISA

ELISA is an immunological method for the detection of proteins. In this project, the sandwich ELISA technique was performed. HBsAg and HBeAg ELISA were used according to manufacturer's instructions (*Siemens*).

2.5.2 FACS analysis

FACS analysis is a method to distinguish single cells based on their protein production. The cell suspension is aspirated into a capillary of the machine and accelerated. The cells pass a laser in a laminar flow singularly. Antibodies (coupled with fluorophores) label target proteins, and therefore the fluorescence signal can be measured (Biosciences, 2016).
For the FACS staining, $1*10^6$ cells were seeded in a 6-well plate and washed with PBS. The cells were detached by incubation for ten minutes at 37 °C with accutase and washed twice with FACS buffer by centrifugation of 1000 g at 4 °C for five minutes. The cells were dissolved in 100 µl of the blocking solution and incubated for fifteen minutes on ice. Afterwards, the cells were washed again with FACS buffer, and the primary antibody incubation was carried out for at least one hour at 4 °C, and the washing step was repeated. The secondary antibody was incubated for thirty minutes at 4 °C in the dark. After two further washing steps, the cells were resuspended in FACS buffer and at least 10,000 living cells were recorded with the *BD Accuri C6*. A PI (propidium iodide) staining served to distinguish living and dead cells.

2.6 Microscopy

Microscopy is a technique for visualizing specimens.

2.6.1 Immunofluorescence staining and CLSM

The CLSM is a method for visualizing cells with fluorescence dyes. If cells were transfected, transfection was carried out before the seeding to cover slips to avoid contaminations of free plasmid DNA. All staining steps were performed at RT. For the fixation, the cells were washed twice with PBS and incubated with 4% PFA in PBS for twenty minutes. After an intense washing (three times with PBS), the cells were permeabilized with 0.5% Trition-X100 for ten minutes. Following, the cells were washed again and blocked with 3% BSA for thirty minutes. The antibody incubation was conducted in 1% BSA in PBS for one hour. After the antibody incubations, the cells were washed three times with PBS. The cell nuclei were stained with DAPI and cover slips were fixed on slides with mowiol. Due to the light sensitivity of antibodies coupled with fluorochromes, the slides were stored in the dark.

2.6.2 Transmission electron microscopy

With transmission electron microscopy, magnifications of 10,000,000x can be reached. This method was used for the visualization of HBV particles. For isolation of VPs and SVPs, 10 ml SN of transfected Huh 7.5 cells were harvested and centrifuged on a 20% sucrose cushion for eighteen hours with the SWR41Ti rotor and 41,000 rpm. Glow-discharged carbon-coated nickel grids were prepared in section 3/3, PEI, Langen by Regina Eberle. The grids were incubated with the sample for three minutes and washed four times with PBS. Negative contrasting was carried out by the incubation with 2% uranyl acetate for ten seconds. The samples were analyzed by *Zeiss EM-109* transmission electron microscope.

2.7 Statistics

The statistical analysis and significance was calculated by two-tailed t-test using *Microsoft Excel 2010* and error bars represent the standard deviation σ. Only the positive error bars are illustrated in the figures. The p-values were defined as follows:

Table 31: Significance of data

p-value	Definition
n.s.	$p > 0.05$
*	$p \leq 0.05$
**	$p \leq 0.01$
***	$p \leq 0.001$

2.8 Vitamin D treatment

For the project, commercially produced calcitriol (abbreviation: *#1*), the bioactive form of vitamin D, in addition to five vitamin D analogs (abbreviation: *#2 - #6*), were chosen to analyze the influence of the substances on the morphogenesis of HBV (see Table 32). Concentrations for treatment in experimental settings were adapted to physiological conditions. The optimal vitamin D concentration in humans is greater than 70 nM in blood serum. Concentrations of less than 50 nM are defined as vitamin D insufficiency (Prietl et al., 2013). For the analysis in cell culture systems, concentration ranges between 1 nM and 1 µM were used. The successful treatment was analyzed by the expression of *CYP24A1*.

All treatments were carried out for twenty-four to thirty hours. The medium was refreshed after six hours and vitamin D treatment was repeated. All the negative controls, which are entitled as 'untreated control', were treated with the vehicle substance of the vitamin D and its analogs, pure ethanol in the same dilution as for treatment with metabolites. For simplifying the workaday laboratory life and the labeling of figures, the analogs were referred to as *#1 - #6*:

Table 32: List of used vitamin D analogs (modified from PubChem, 2016)

	Vitamin D analog	Synonyms	Formular	Molecular weight [g/mol]	Chemical structure
#1	Calcitriol CID: 5280453	- 1 alpha, 25 dihydroxy 20 epi Vitamin D3 - 1 alpha,25 Dihydroxycholecalciferol - 1 alpha,25-DihydroxyVitamin D3 - Bocatriol - Calcijex - Decostriol - MC 1288 - Silkis - Sitriol - Soltriol - Tirocal -	$C_{27}H_{44}O_3$	416.64	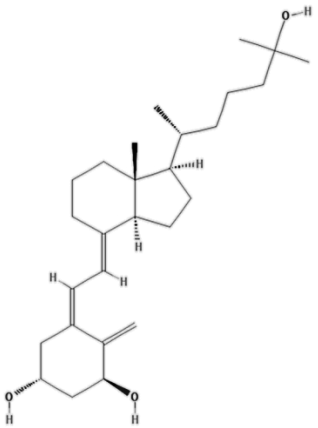
#2	Seocalcitol CID: 5288149	- EB 1089	$C_{30}H_{46}O_3$	454.68	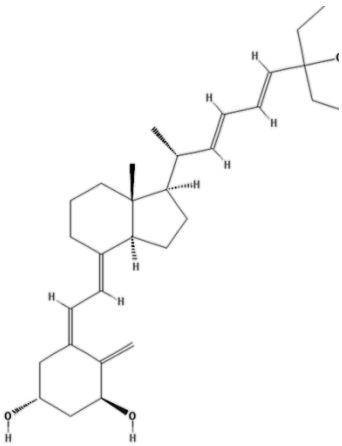
#3	Oxa-calcitriol CID: 6398761	- 1,25-dihydroxy-22-oxaVitamin D3 - 22-oxa-1,25-dihydroxyVitamin D3 - 22-oxa-calcitriol - Maxacalcitol - Maxacalcitriol - Oxarol -	$C_{26}H_{42}O_4$	418.61	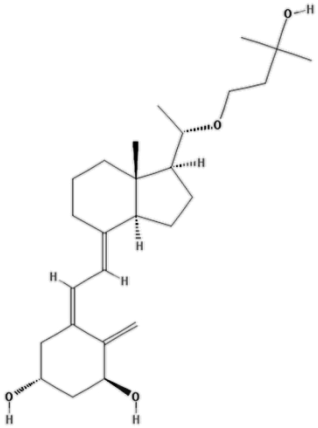

	Vitamin D analog	Synonyms	Formular	Molecular weight [g/mol]	Chemical structure
#4	Tacalcitol CID: 5283734	- 1,24-dihydroxycholecalciferol - 1,24-dihydroxyVitamin D3 - Curatoderm - PRI-2191 - Bonalfa	$C_{27}H_{44}O_3$	416.64	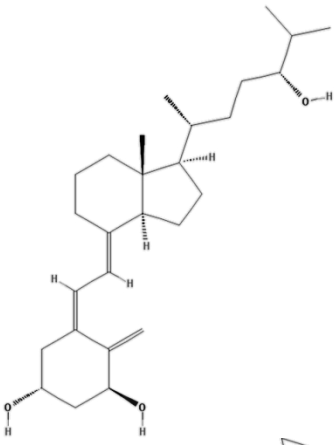
#5	Calcipotriol CID: 5288783	- BMS-181161 - Calcipotriene - Daivonex - Divonex - Dovonex - MC-903 - Psorcutan - STF-115469 - Sorilux	$C_{27}H_{40}O_3$	412.61	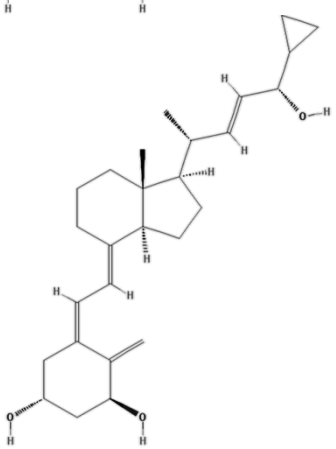
#6	Paricalcitol CID: 5281104	- 19-Nor-1alpha,25-dihydroxyVitamin D2 - 19-Nor-1,25-$(OH)_2$D2 - 131918-61-1	$C_{27}H_{44}O_3$	416.64	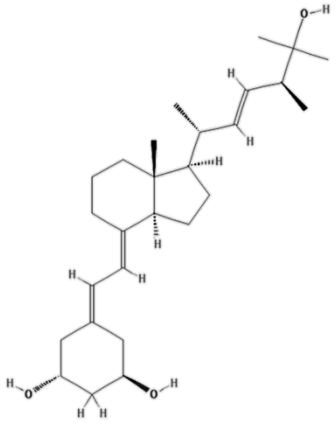

3. Results

In the following chapter, the data of the main project are illustrated.

3.1 Cultivation of PHHs

PHHs are a feasible tool for the analysis of a wide range of scientific questions. They are singularly useful for studying *in vivo*-like expression levels and for the investigation of the influence of physiopathological stimuli. Furthermore, they are an effective tool for *in vitro* evaluation of drugs and xenobiotics metabolism, drug-drug interactions, hepatotoxicity, and transporter activities. Moreover, PHHs can be used as infection system for hepatitis viruses. PHHs were isolated during the experimental phase of the PhD thesis on a regularly basis. In addition to my own research, PHHs were used for HCV research in the Division of Virology at the PEI and contributed to one co-authorship (Elgner et al., 2016a) and acknowledgments of two further publications (Elgner et al., 2016b; Ren et al., 2016).

For access to patient material, a cooperation with Prof. Dr. Bechstein and Elsie Oppermann of the Department of General and Visceral Surgery at the *Goethe University Hospital* in Frankfurt was established. The local and national ethics committees gave their approval beforehand (ethic committee of the *Goethe University Frankfurt*, agreement number 343/13), and the medical doctors Dr. Juliane Liese and Kerstin Lang obtained informed consents from patients.
The cells were directly seeded in the format of the respective experiment and the cell viability was analyzed with trypan blue exclusion before seeding and for several days with light microscopy (see Figure 13). The PHHs showed a good cell viability up to fourteen days after isolation (data not shown).

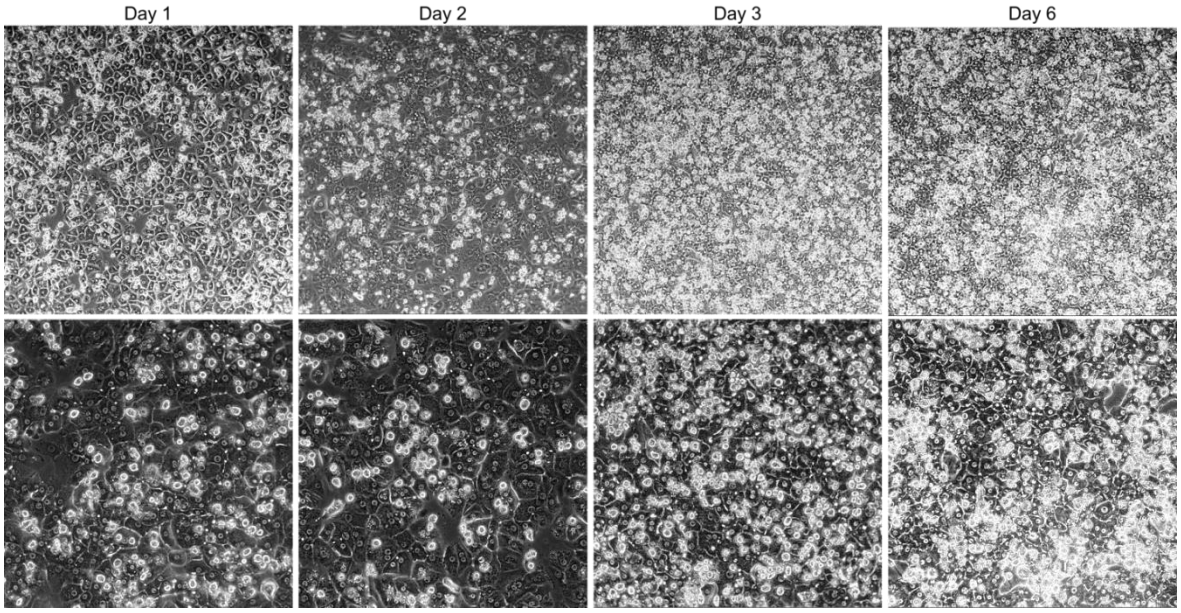

Figure 13: Cell viability of PHH.
Uninfected PHHs were cultivated for six days after isolation. The viability and differentiation was monitored with light microscopy. The upper row shows a magnification of 20x, the lower row of 40x.

3.1.1 Monitoring of HBV infection in PHH

As previously described in the chapter *Introduction*, immortalized hepatocyte cell culture systems have only a very limited potential to be susceptible to HBV (see 1.1.4.5). In light of this, PHHs were used as infection system for this project.
The generation of PHHs from liver tissue was performed in the *Goethe University Hospital* in Frankfurt as described in 2.3.6. The cultivated cells were transported to the laboratory facilities of the PEI and used for experiments. The cells were infected as described in chapter 2.3.7.

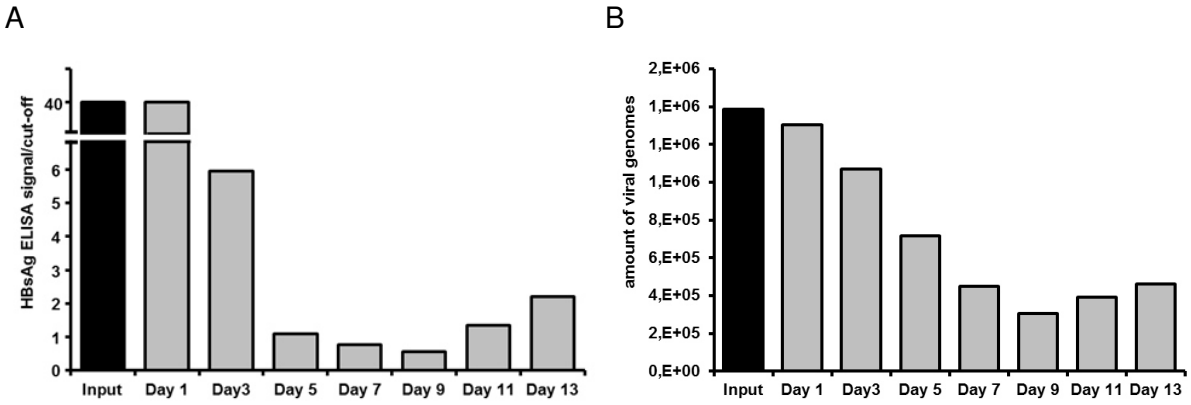

Figure 14: Monitoring of HBV infection in PHH.
PHHs were infected with a MOI= 500 of HBV/A. IUs were measured with a CE-based test beforehand. The infection was carried out for sixteen hours. The SN was changed every forty-eight hours for thirteen days and stored at 4 °C. SN was analyzed (A) with HBsAg-ELISA and (B) qPCR. Signal/cut-off was referred to internal controls of HBsAg-ELISA (Siemens). The amount of viral genomes was referred to an internal standard of Division 2/0, PEI.

PHHs were infected overnight (sixteen hours) and subsequently washed to remove the input of HBV positive material. The medium was replaced every forty-eight hours and the vitamin D treatment renewed. The infection was monitored for thirteen to fourteen days by the presence of HBsAg and viral genomes in the SN of infected cells. The presence of the virus was determined with HBsAg-ELISA (Figure 14A) and purified viral DNA was measured with qPCR relative to internal standards (see Figure 14B, 2.2.9). A successful infection is characterized by a drop of the HBV signal to a basal level over the first days (day one to day seven) and followed by an increase of signal intensity caused by the production of HBV of infected cells (day nine to day thirteen). Exemplary results in Figure 14 indicate a successful infection of PHHs with HBV. For all of the following illustrated experiments, this infection-characteristic time course was observed; otherwise, data were rejected for the analyses.

3.2 Influence of vitamin D on the life cycle of HBV

Although the involvement of vitamin D in the course of disease of HBV-infected patients has been discussed for many years, so far no published study has focused on the effect of vitamin D on the HBV life cycle *in vitro*. Several analyses were performed focusing on the association of replication rates and vitamin D deficiency and polymorphisms of genes

involved in vitamin D metabolism in chronically infected patients (reviewed in Luong and Nguyen, 2012).

Therefore, the aim of this project was to characterize the influence of vitamin D on the life cycle of HBV. For this purpose, HBV expressing hepatoma cell cultures and infection systems were used.

3.2.1 Vitamin D analogs have no cytotoxic effect on hepatocytes

For the analyses, six different vitamin D derivates were chosen to investigate the effect on HBV lifecycle (see 2.8). Firstly, it was essential to test the selected vitamin D analogs for cytotoxicity on relevant cell lines. Human hepatoma cell lines Huh 7.5 and HepG2 as well as stably HBV expressing HepG2 cells (HepAD38 and HepG2.2.15) were tested for their viability with a PrestoBlue® assay under the previously described experimental settings (see Figure 15). Huh 7.5 cells treated with 1 µg/ml of the antibiotic Puromycin served as positive control for the assay implementation.

The PrestoBlue® assay implementation was successful, indicated by a significantly reduced cell viability in Huh 7.5 cells after Puromycin treatment in contrast to the untreated control cells (see Figure 15E). In general, for all vitamin D analogs and tested cell lines no crucial impairment on viability was observed. The substance *#5* showed a slight but significant reduction in the viability in Huh 7.5 of 10.9% (see Figure 15A) and in HepG2 of 16.3% (see Figure 15B). Furthermore, for substance *#6* a significant reduction on cell viability in Huh 7.5 of 15.8% (see Figure 15A) and in HepG2 of 15.9% (see Figure 15B) was observed. In stably HBV expressing cells, no significant reduction was determined at all. All the other tested analogs showed no significant cytotoxicity. Collectively, these results indicate that the chosen vitamin D analogs in a concentration of 10 nM are feasible for hepatoma cell lines.

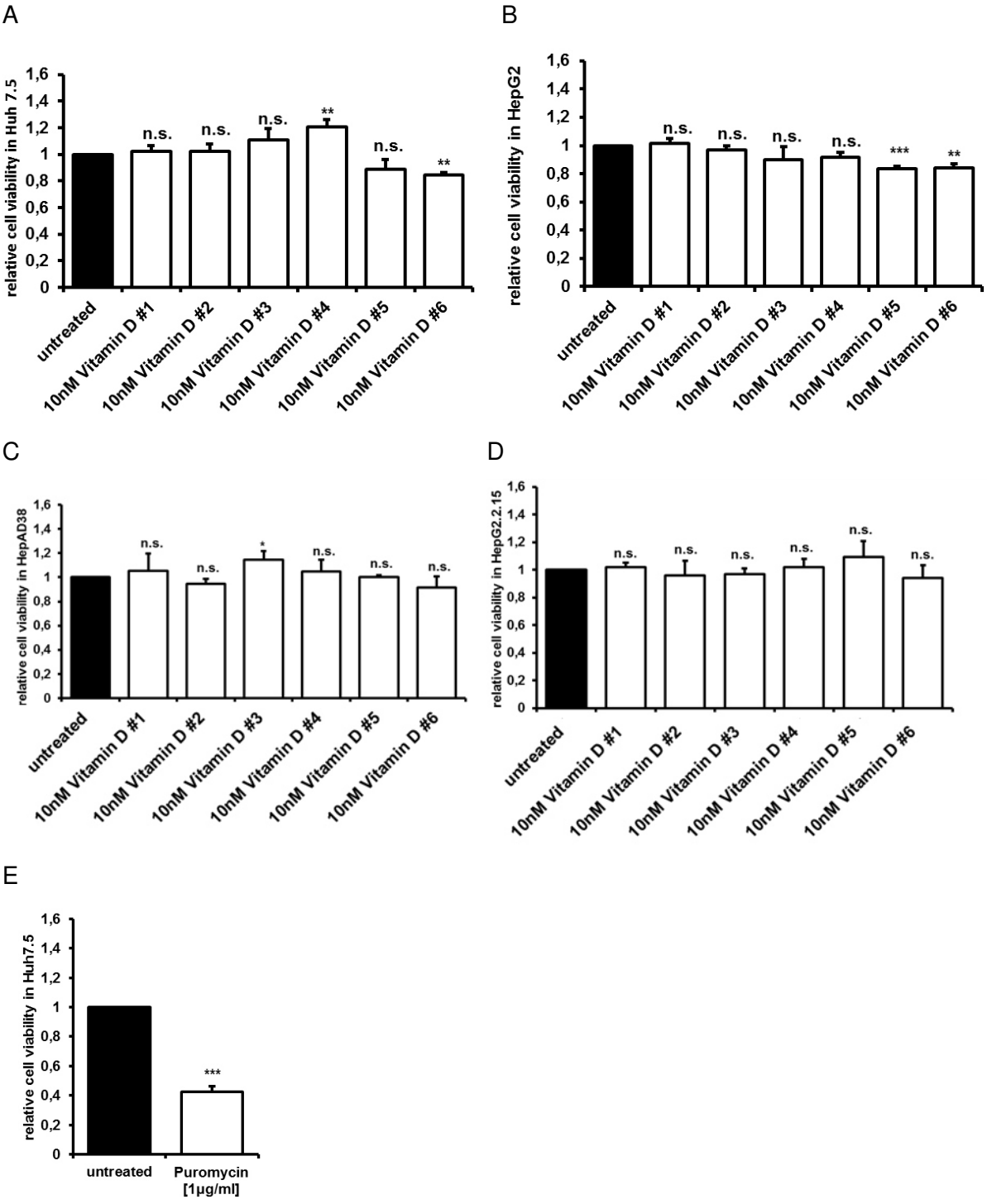

Figure 15: Cell viability of different hepatoma cell lines after thirty hours of vitamin D analog treatment.

Hepatoma cell lines Huh 7.5, HepG2, HepAD38 and HepG2.2.15 were tested for cell viability with a Presto Blue® Assay after thirty hours of vitamin D analog treatment. The cells were treated with 10 nM of vitamin D analogs. The values were normalized to the untreated control. n= 3.

A: Huh 7.5 cells were tested. n= 3, p-values= 0.511; 0.557; 0.054; 0.004; 0.200; 0.007.

B: HepG2 cells were tested. n= 3, p-values= 0.541; 0.507; 0.129; 0.122; 0.0009; 0.001.

C: HepAD38 cells were tested. n= 3, p-values= 0.559; 0.284; 0.038; 0.4337; 0.992; 0.224.

D: HepG2.2.15 cells were tested. n= 3, p-values= 0.744; 0.432; 0.585; 0.708; 0.308; 0.271.

E: Huh 7.5 cells were treated with 1µg/ml Puromycin. n= 3.

3.2.2 Reduction of HBsAg in the SN upon vitamin D analog treatment

To analyze the influence of vitamin D on the HBV life cycle, the release of HBsAg was investigated in stably or transiently HBV expressing cells. HepAD38 and HepG2.2.15 stably express HBV/D (serotype *ayw*). Furthermore, Huh 7.5 cells were transiently transfected with HBV/A (pCEP-gtA-1.5). All cell lines were treated with 10 nM of the vitamin D analogs *#1 - #6* as described in chapter 2.8. The SN was harvested and the release of HBsAg was measured by means of HBsAg-ELISA. The values were normalized to the untreated control.

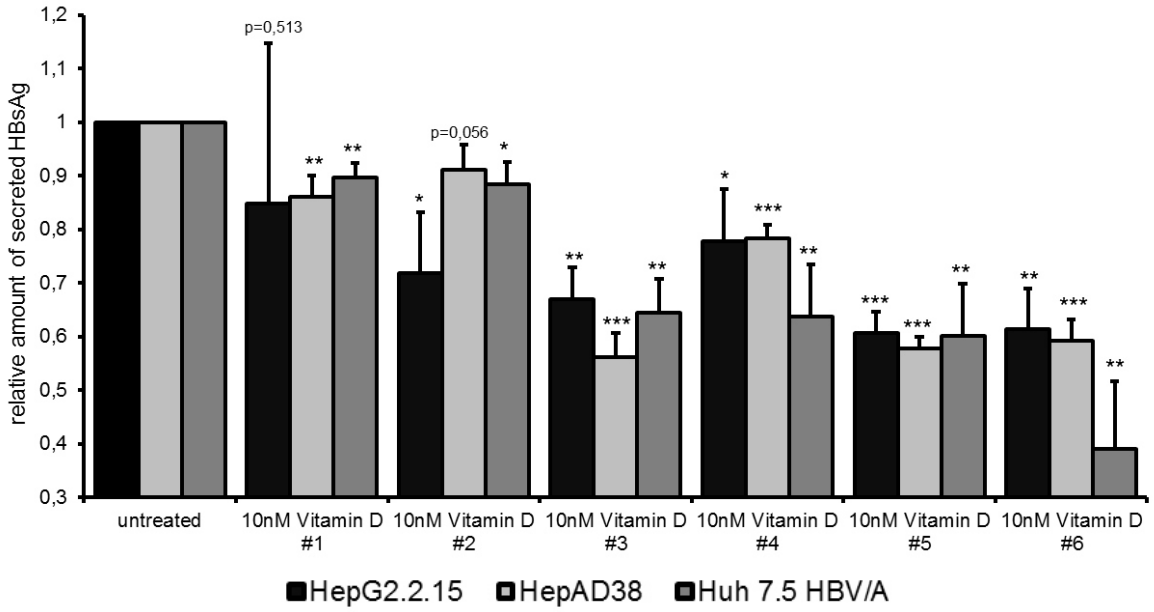

	Vitamin D induced reduction of HBsAg in the SN					
	#1	***#2***	***#3***	***#4***	***#5***	***#6***
HepG2.2.15	15.14%	28.17%	32.94%	22.26%	39.33%	38.52%
HepAD38	13.94%	8.91%	43.88%	21.64%	42.30%	40.79%
Huh 7.5 HBV/A	10.26%	11.65%	35.62%	36.25%	39.81%	61.04%

Figure 16: Reduction of HBsAg in the SN of HBV expressing cells.
Stably HBV expressing HepG2.2.15 and HepAD38 cells were treated with six vitamin D metabolites. The SN was harvested after thirty hours. The amount of HBsAg was measured with HBsAg-ELISA. Huh 7.5 cells were transiently-transfected with pCEP-gtA-1.5. The treatment with the vitamin D analogs was started sixteen hours after transfection. The amount of reduction was related to the untreated control cells. The table shows the percentage of reduction in different cell lines for vitamin D analogs. n= 3.

An influence of vitamin D and its analogs on the HBV life cycle was observed by a reduction of HBsAg in the SN of treated HBV expressing cells (see Figure 15). All tested substances showed a significant reduction of secreted HBsAg. The effect was observed in all used cell lines with no clear result to the question, whether one of the tested cell lines is more sensitive to the treatment than another is. The effectivity of the vitamin D analogs could be analyzed comparatively. The biologically active form of vitamin D calcitriol (*#1*) showed for a concentration of 10 nM only a moderate reduction (10.26% to 15.14%). The most inhibiting effect in all cell lines showed the vitamin D analog *#3*, oxacalcitriol, and substance *#5*, calcipotriol. Substance *#3* showed a diminished HBsAg signal of 32.94% to 43.88% and substance *#5* a reduction of 39.81% to 42.30%. In addition to that, paricalcitol (*#6*) showed for Huh 7.5 HBV/A cells a reduction of 61.04%, but it has to be considered that this substance showed a slightly cytotoxic effect in Huh 7.5 (see 3.2.1).

The substances with the most inhibiting effect in HepAD38 cells, oxacalcitriol (*#3*) and calcipotriol (*#5*) and also calcitriol (*#1*), were used for treatment in concentrations of 1 nM to 1 µM (see Figure 17).

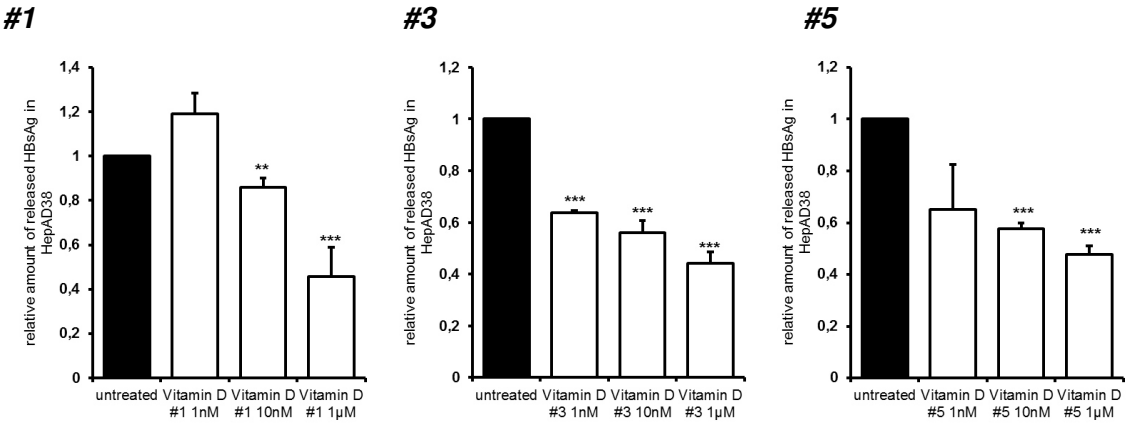

	Vitamin D induced reduction of HBsAg in the SN of HepAD38		
	#1	***#3***	***#5***
1 nM	-19.09%	36.15%	34.91%
10 nM	13.94%	43.88%	42.30%
1 µM	54.16%	55.84%	52.31%

Figure 17: Dose-dependent vitamin D-induced reduction of HBsAg in the SN of HepAD38.
HBV expressing HepAD38 were treated with vitamin D analogs in concentrations of 1 nM to 1 µM as described before. The amount of released HBsAg was measured in the SN with HBsAg-ELISA. The Values were normalized to the untreated control. n= 3.

The three tested substances showed a dose-dependent reduction on the release of HBsAg measured by means of HBsAg-ELISA. Calcitriol (*#1*) showed none or only a moderate effect for an impaired HBsAg release in lower concentrations, whereas treatment with a concentration of 1 µM had a comparable effect to substance *#3* and *#5* results (*#1*: 54.16%, *#3*: 55.84%, *#5*: 52.31%). In the following experiments, the focus lay on oxacalcitriol (*#3*) and calcipotriol (*#5*) because of their strong reductive effect and nearly no cytotoxic effect on hepatocytes.

The data listed above indicated a reductive effect of vitamin D analogs on the release of HBsAg. In the following, it was tempting to study whether vitamin D can cause the same effect in an infection system. Therefore, PHHs were infected with HBV and vitamin D treatment with 10 nM of substance *#5* was carried out during infection and for thirteen days after the infection. The medium was replaced every forty-eight hours with fresh vitamin D containing medium.

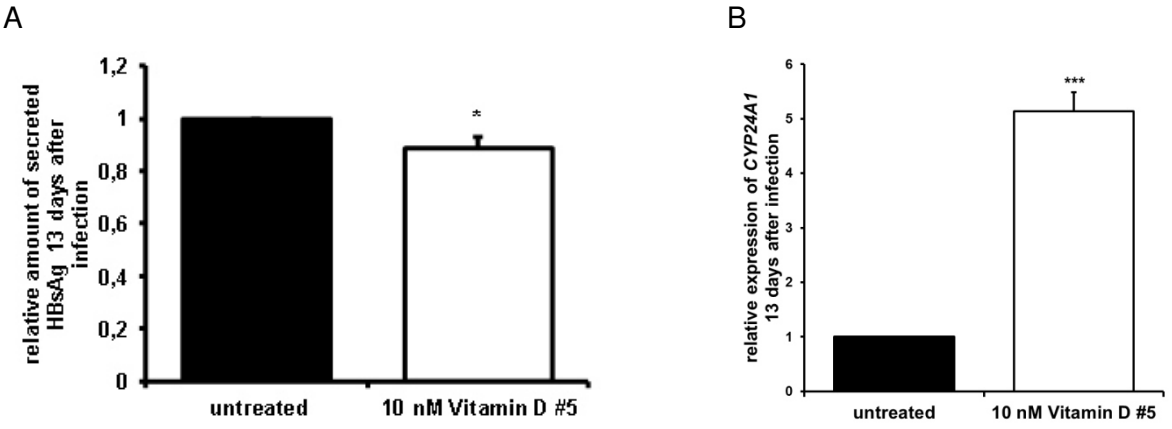

Figure 18: Release of HBsAg by vitamin D treatment in PHH.
PHHs were infected with HBV/A MOI= 500. IUs were measured with a CE-based test beforehand. The cells were treated with 10 nM vitamin D *#5* while and after the infection. The infection was monitored as described before.
A: SN of day 13 was measured with HBsAg-ELISA. The signal was referred to the untreated control. n= 3.
B: RNA was isolated on day 13 and converted into cDNA. Expression of *CYP24A1* was measured with qPCR. Values were referred to the housekeeping gene *RPL27* with the ΔΔct method. n= 3.

The release of HBsAg was measured with an HBsAg-specific ELISA on day thirteen after the infection. The signal was normalized to the untreated control. The success of infection was monitored as described before (see 3.1.1). The cells were lysed on day thirteen after the infection, and RNA was isolated and transcribed into cDNA. The expression of

CYP24A1 was measured with qPCR and the efficiency of the primers was calculated beforehand (see Table 20). Vitamin D substance *#5*-treated cells showed an induction of *CYP24A1* gene, implicating a successful treatment and long-term activation of VDR (Figure 18B).

The PHHs treated with oxacalcitriol (*#5*) showed a moderately but significantly lower signal of 11.30% for HBsAg in contrast to the untreated control. These results reinforced the observations that vitamin D leads to a reduction of the release of HBsAg.

3.2.3 Vitamin D reduces the secretion of VPs

After successful analysis of HBsAg in the SN by ELISA of HBV expressing and HBV infected cells, it was interesting whether vitamin D would selectively influence the release of VPs, filaments, and spheres because the particles leave the cell on different routes (see 1.1.4.4).

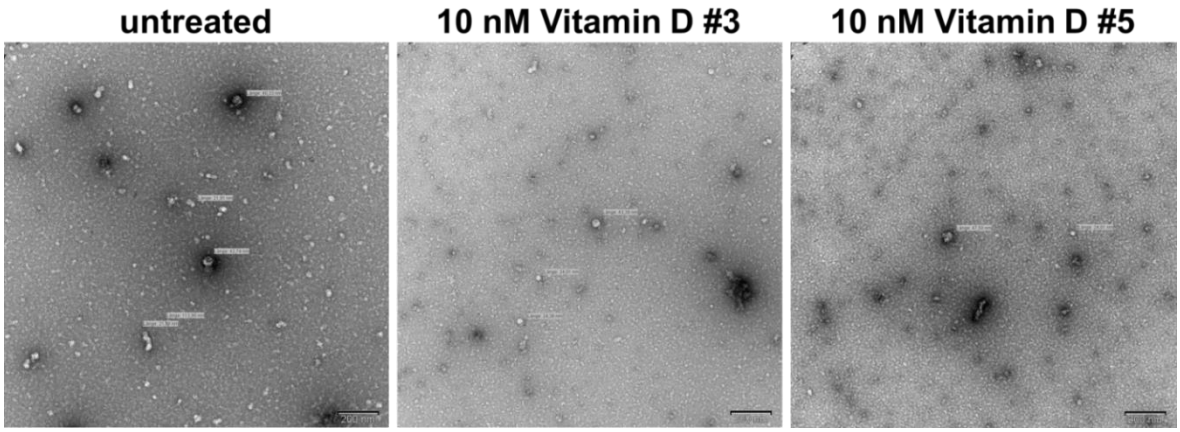

Figure 19: Electron microscopy picture of enriched HBV particles of the SN of Huh 7.5 HBV/A-treated cells.
Huh 7.5 cells were transiently transfected with pCEP-gtA-1.5. Sixteen hours after transfection, vitamin D treatment was carried out as described before with 10 nM of substance *#3* and *#5*. 10 ml of the SN was harvested and HBV particles were enriched with sucrose cushion centrifugation. The samples were visualized with negative contrast staining and electron microscopy. Representative pictures are illustrated.

For assessing this, SN of HBV/A-expressing Huh 7.5 cells was harvested and particles were enriched with sucrose cushion centrifugation. The particles were visualized with electron microscopy. The size of detected structures fitted to the presence of VPs (ca.

45-55 nm), spheres (ca. 20-30 nm), and filaments (size variable). In all samples, regardless whether treated with vitamin D analogs or not, VPs and SVPs were observed. Samples treated with vitamin D analogs *#3* and *#5* gave the impression of a reduction of particles in the SN (see Figure 19).

To review the objective observation of electron microscopy analysis, the SN of treated cells was further analyzed. Since the VPs and SVPs have a different structural composition (see 1.1.4.1), these characteristics were adduced for analysis. These characteristics are on the one hand the differences in the ratio of HBsAg of VPs, filaments and spheres and on the other hand the presence of viral DNA and HBcAg in the VPs in contrast du SVPs.

3.2.4 Vitamin D influences the ratio of HBsAg

The VPs and SVPs are composed differently with regard to the ratio of HBsAg (Patient, Hourioux, and Roingeard, 2009). All types of particles are consisting of the three surface proteins, but spheres are predominantly composed of SHBs, whereas VPs and filaments are composed in higher amounts of LHBs (Short et al., 2009).

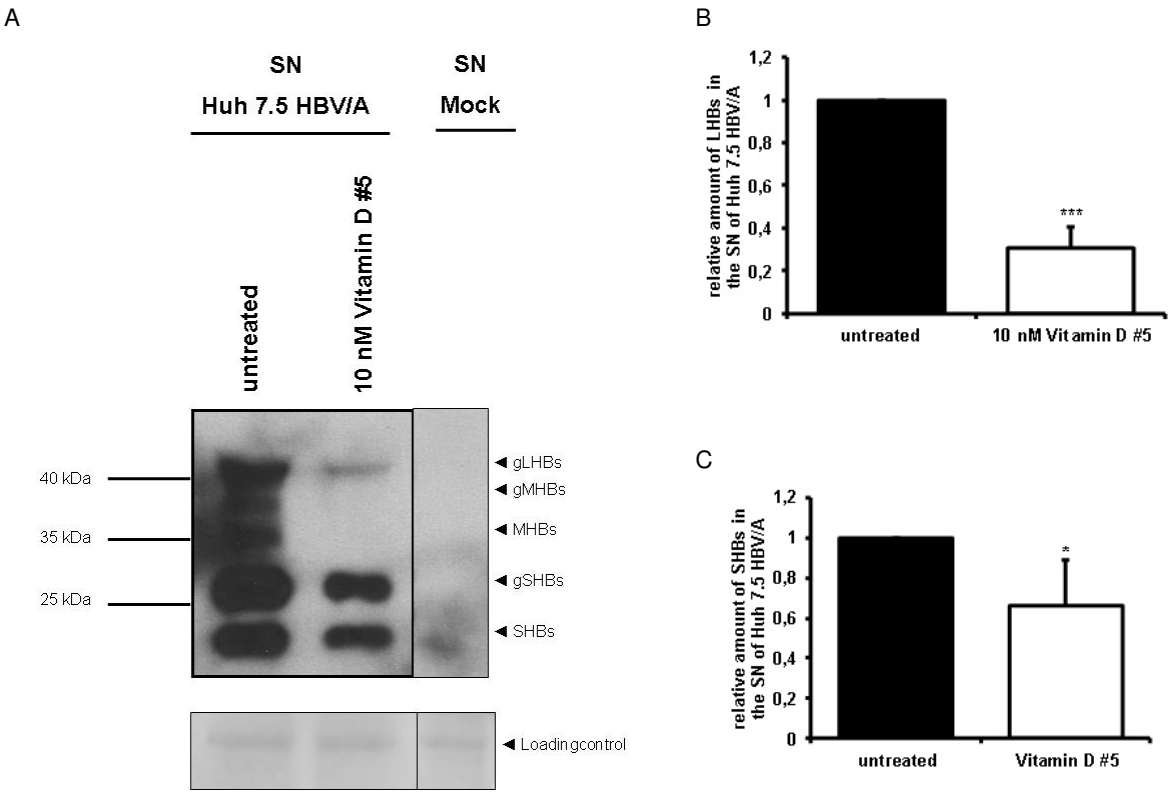

Figure 20: Ratio of LHBs and SHBs due to vitamin D treatment.
Huh 7.5 cells were transiently transfected with pCEP-gtA-1.5. After treatment with 10 nM of vitamin D analog *#5,* the SN was analyzed by western blot with an HBsAg-specific antibody (HB01).
A: Proteins were separated on a 12% SDS-gel. A ponceau-staining served as loading control.
B, C: Western blots were quantified and relative amounts of LHBs and SHBs are illustrated. Values were normalized to the untreated control. B: n= 3; C: n= 4.

To investigate the ratio of HBsAg, western blot analyses of the SN derived from vitamin D *#5*-treated HBV expressing cells were performed. Proteins were detected with an HBsAg-specific antibody (HB01). The epitope of the antibody is located in the S-domain of HBsAg and therefore detects LHBs, MHBs, and SHBs. The western blot signals were of the expected size, and detection of glycosylated and unglycosylated proteins was possible. The analysis implicated a reduction for all surface proteins upon vitamin D treatment. Interestingly, the quantification revealed that the reductive effect is stronger on LHBs (69.03%) (see Figure 20 B) compared to SHBs (34.07%) (see Figure 20C). No differences in posttranslational modifications, like glycosylations, were observed (visualized in this method by their differing molecular weight). In conclusion, a notable change in the ratio of LHBs and SHBs was observed.

3.2.4.1 Treatment with vitamin D results in an impaired secretion of viral genomes

As previously described consist the SVPs only of HBsAg and bear no genetic material. Hence, with quantification of viral genomes in the SN, it should be further investigated whether vitamin D influences the release of the particles in a distinguishable manner.

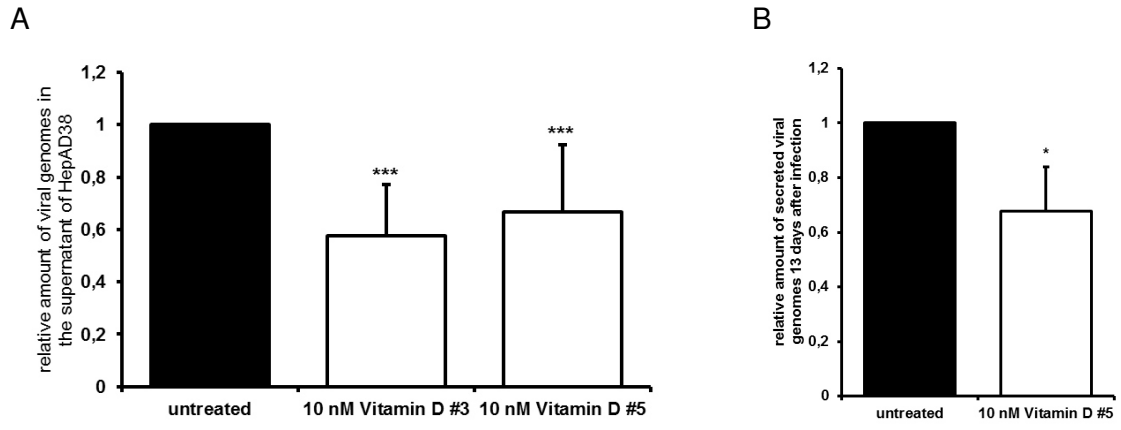

Figure 21: Release of viral genomes.
A: HepAD38 cells were treated with 10 nM vitamin D analog *#3* and *#5*. Viral DNA was purified and the viral genomes were measured with qPCR. The number of genomes was relative to standards and normalized to untreated cells. n= 10.
B: PHHs were infected as described before with HBV/A. The vitamin D treatment was carried out as listed above. The viral DNA was purified from the SN and measured with qPCR. The number of genomes was referred to existing standards and normalized to untreated cells. n= 3.

First of all, the viral genomes of stably HBV expressing HepAD38 cells were isolated and quantified with qPCR. The absolute number of viral genomes was determined by referring the values to existing standards. The values were normalized to the untreated control. The analysis showed a considerable reduction for the treatment with vitamin D analog *#3* (42.32%) and *#5* (33.36%) (see Figure 21A). Next, the influence of vitamin D *#5* on infected PHHs (HBV/A) was analyzed and the experimental setting for infection was conducted as described before. PHHs treated constantly with vitamin D *#5* showed a reduction of viral genomes of 32.30% in contrast to the untreated control. These results indicated that the vitamin D treatment impairs the release of viral genomes in HBV expressing and HBV-infected cells and consequently might influence the release of VPs or naked capsids.

3.2.4.2 HBcAg levels in the SN of HBV expressing cells are reduced upon vitamin D treatment

The vitamin D treatment leads to a reduction of viral genomes in the SN of HBV expressing and replicating cells (see 3.2.3.2) and consequently to a reduction of VPs or naked capsids, the only particles containing viral DNA. In the following section, the influence of vitamin D was further investigated by analyzing HBcAg in the SN of treated cells.

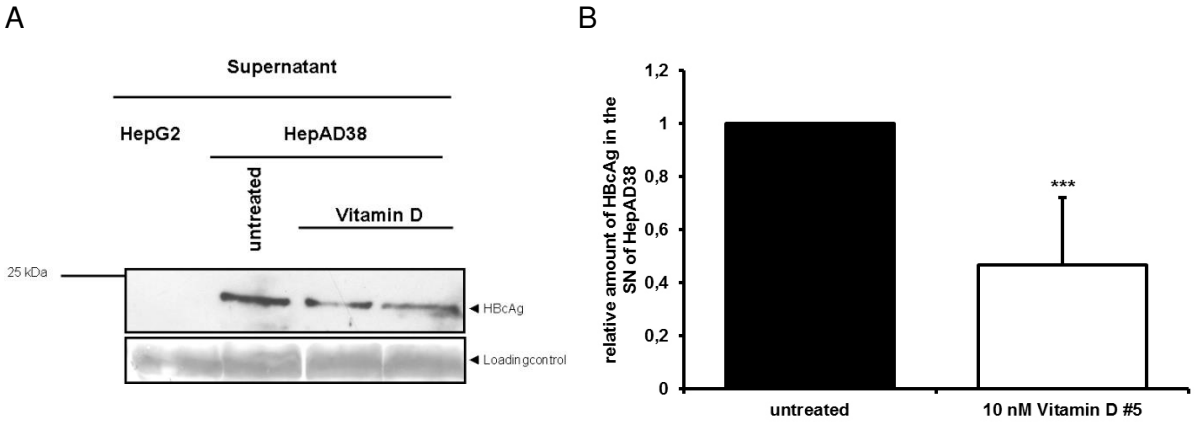

Figure 22: Influence of vitamin D on HBcAg.
HepAD38 cells were treated with 10 nM vitamin D analogs *#3*, *#5*.
A: The SN was analyzed by western blot with an HBcAg-specific antibody (K46). The proteins were separated beforehand on a 14% SDS-gel. A ponceau-staining served as loading control. The SN of HBV negative cells (HepG2) served as negative control.
B: Western blots signals for HBcAg were quantified normalized to untreated cells. n= 6.

The SN of HepAD38 cells treated with 10 nM vitamin D analog *#3* and *#5* was separated by SDS-page and further analyzed by western blot analysis with an HBcAg-specific antibody (K46). A specific signal of the right molecular weight (estimated 22 kDa) was visible in the lanes of HBV positive SN. The SN of vitamin D-treated cells showed a weaker signal in contrast to the untreated control (see Figure 22A). The quantification of the western blot of the SN of cells treated with substance *#5* showed a reduction of the HBcAg signal of 53.55%. Taken together, these data indicated that vitamin D causes a reduction in the release of VPs.

3.2.5 Secretion of HBeAg is not affected by vitamin D treatment

HBeAg is a serological marker for acute virus infection and secreted by the cells by the secretory pathway. In the following, the effect of vitamin D on the release of HBeAg was tested. For this, Huh 7.5 HBV/A and HepAD38 cells were treated with 10 nM of the vitamin D analogs *#3* and *#5* as described before and the SN was analyzed by an HBeAg-specific ELISA.

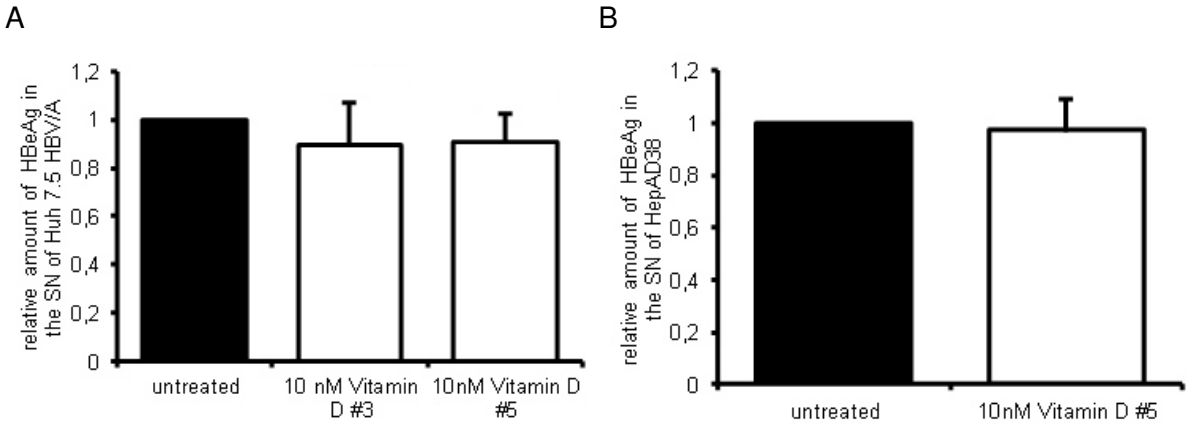

Figure 23: Secretion of HBeAg by vitamin D treatment.
HBeAg in the SN was measured by an HBeAg-specific ELISA, and the signal was normalized to the untreated control.
A: Huh 7.5 cells were transiently transfected with pCEP-gtA-1.5. Sixteen hours after transfection, vitamin D treatment was carried out as described before with 10 nM of the substance *#3* and *#5*. n= 3, p-value =0.497, p-value= 0.432.
B: HepAD38 cells were treated with 10 nM substance *#5*. n= 3, p-value=0.775.

Analysis of HBeAg of the SN of vitamin D-treated cells showed in contrast to untreated cells no significant change, neither for transiently transfected Huh 7.5 HBV/A-treated cells nor for stably HBV expressing HepAD38. This observation implied that the secretion of HBeAg is not affected upon vitamin D treatment. Furthermore, this result gave evidence that vitamin D is not impeding the secretory pathway, as HBeAg is still secreted.

3.2.6 Vitamin D and its effects on the amounts of intracellular viral proteins

The hitherto presented data showed that vitamin D treatment successfully leads to a reduction of HBV in the SN of treated cells. In the following section, it will be further demonstrated which mechanism might be causative for this reduction. Firstly, the intracellular amounts of HBsAg and possible alterations in ratio were analyzed.

A

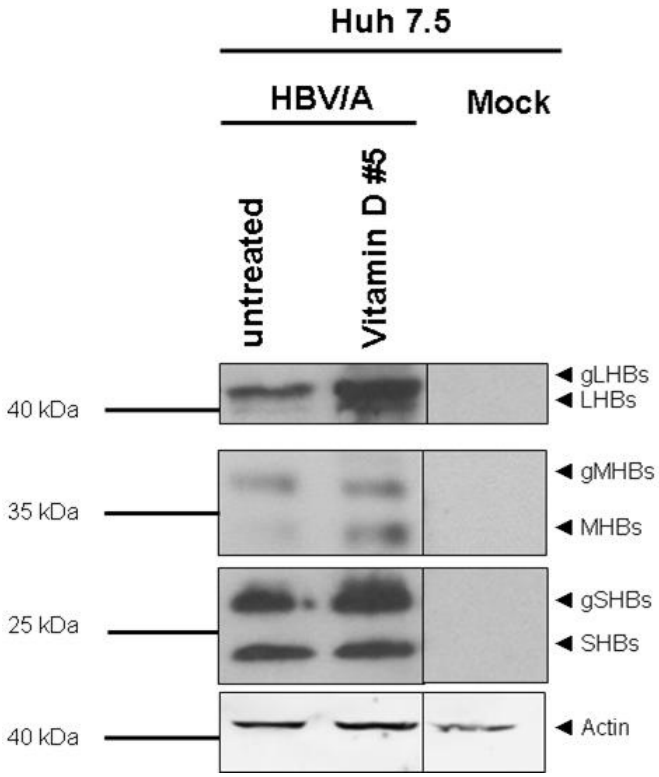

B

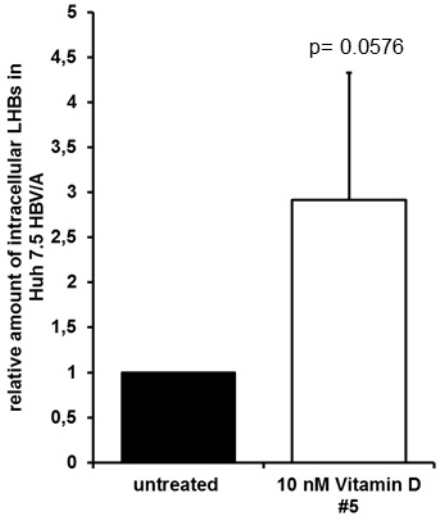

C

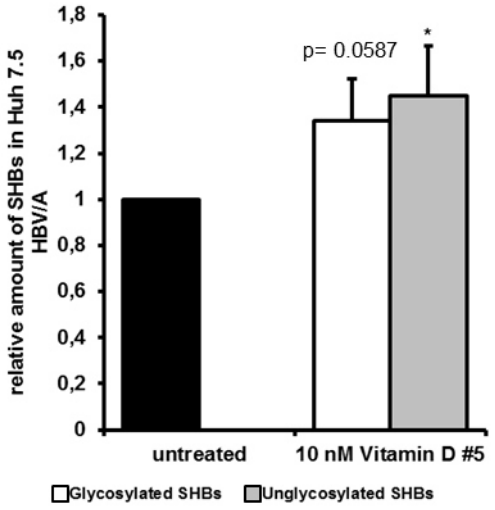

Figure 24: Intracellular amounts of HBsAg by vitamin D treatment.
Huh 7.5 cells were transiently transfected with pCEP-gtA-1.5. pUC18 transfected cells served as mock control. Sixteen hours after transfection vitamin D treatment with 10 nM *#5* was carried out as described before.
A: Corresponding cellular lysate were separated on a 12% SDS-gel. Samples were analyzed by western blot analysis with an HBsAg-specific antibody (HB01). An Actin-blot served as loading control.
B, C: Western blots were quantified by referring to Actin-loading control. Values were normalized to the untreated control. B: Quantification of LHBs n= 4; C: Quantification of glycosylated and unglycosylated SHBs n= 3.

The analyses of HBsAg by western blot revealed intracellularly elevated amounts for all three surface proteins (see Figure 24 A). Interestingly, the quantification showed that the elevation of LHBs (see Figure 24 B) is more pronounced in contrast of SHBs (see Figure 24 C). The LHBs signal was 2.9-fold increased, whereas SHBs signal was induced 1.34-fold for the glycosylated SHBs and 1.45-fold for the unglycosylated form of SHBs. The comparison of the glycosylation patterns of SHBs in treated and untreated cells showed no selective influence caused by vitamin D (see Figure 24 C).
These results fit to previously obtained data of the extracellular ratio of HBsAg (see 3.2.5). The same pattern on alteration on HBsAg induced by vitamin D was observed. The LHBs was altered considerably stronger in contrast to the SHBs.

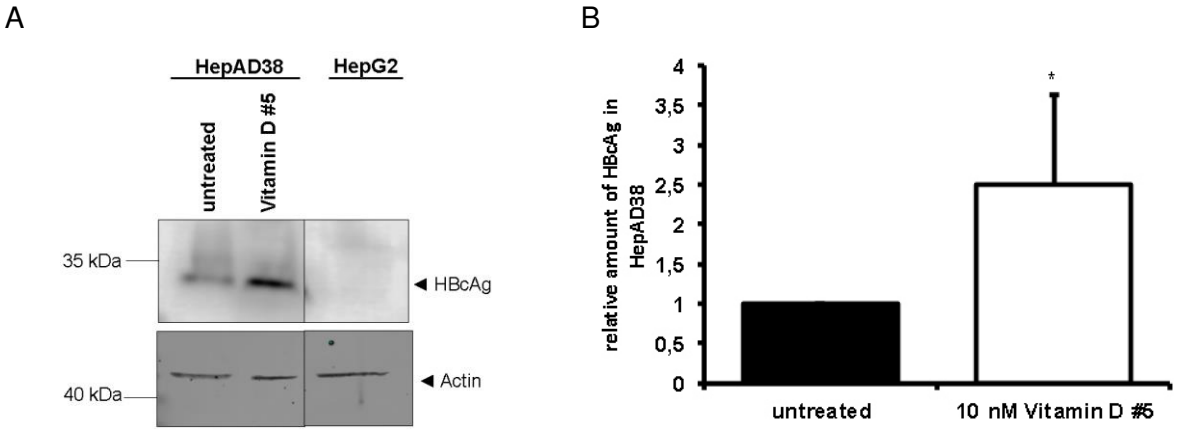

Figure 25: Intracellular amount of HBcAg by vitamin D treatment.
HepAD38 cells were treated with 10 nM vitamin D analog *#5*. The cells were lysed and separated on a 14% SDS-gel.
A: By means of an HBcAg-specific antibody (K46) western blot analysis was performed. Actin served as loading control.
B: For quantification, the signal was referred to the Actin control. The values were normalized to the untreated control. n= 5.

For further analysis of the effect on VPs, intracellular HBcAg was quantified by western blot (see Figure 25). The intracellular amount of HBcAg in vitamin D-treated cells was 2.5-fold and significantly elevated compared to the untreated cells.
Collectively, these results gave further evidence in favor of the hypothesis about an influence of vitamin D on VPs. All the proteins important for the structure of VPs, like HBsAg and Core, showed intracellularly elevated amounts in vitamin D-treated cells.

3.2.7 Vitamin D has no effect on HBV transcripts

To further investigate the influence of vitamin D on the HBV life cycle, the intracellular virus constructs were analyzed. As previously described, vitamin D treatment leads to reduced amounts of VPs and a drop down of HBsAg (mostly representing spheres) extracellularly, but to intracellularly elevated amounts of HBsAg and HBcAg. Therefore, it was rewarding to further investigate the influence of vitamin D on HBV transcripts. For this purpose, the HBV 3.5 kb mRNA was quantified. Total RNA of HepAD38 and Huh 7.5 HBV/A cells was isolated and measured with RT-qPCR. The calculation was carried out with the ΔΔct-method by referring values to the CPs (crossing points) of the housekeeping

gene *RPL27*. The expected vitamin D response was verified by means of measurement of *CYP24A1* gene expression.

A

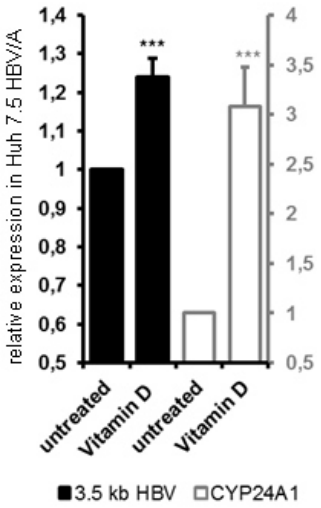

B

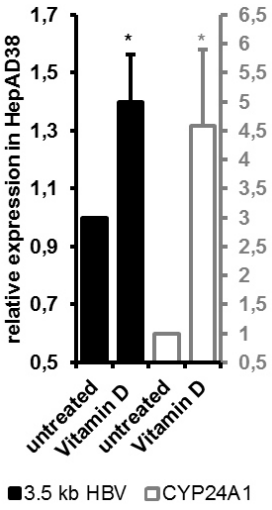

Figure 26: Relative amount of 3.5 kB mRNA in HBV expressing cells after vitamin D treatment.
Total RNA was isolated and transcribed into cDNA. qPCR measurement was performed with the LC480 Roche system. 3.5kb mRNA specific-primers detect HBV mRNA. The values were referred to the housekeeping gene *RPL27* with the ΔΔct method. *CYP24A1* expression served as positive control for successful vitamin D treatment.
A: Huh 7.5 cells were transiently transfected with pCEP-gtA-1.5. Sixteen hours after transfection, vitamin D treatment was carried out as described before with 10 nM of substance *#5*. n= 4.
B: HepAD38 cells were treated with vitamin D analog *#5* as described before. n= 3.

Huh 7.5 HBV/A (see Figure 26 A) and HepAD38 (see Figure 26 B) showed slightly significantly elevated amounts for HBV 3.5 kb mRNA. The Huh 7.5 HBV/A cells demonstrated an increase of 1.24-fold, and HepAD38 cells showed an increase of 1.40-fold.

To ensure those observations further analysis with northern blot were performed. With the northern blot method it was possible to analyze whether the ratio of the RNA constructs of HBV, characterized by different size, were influenced by vitamin D distinguishably.

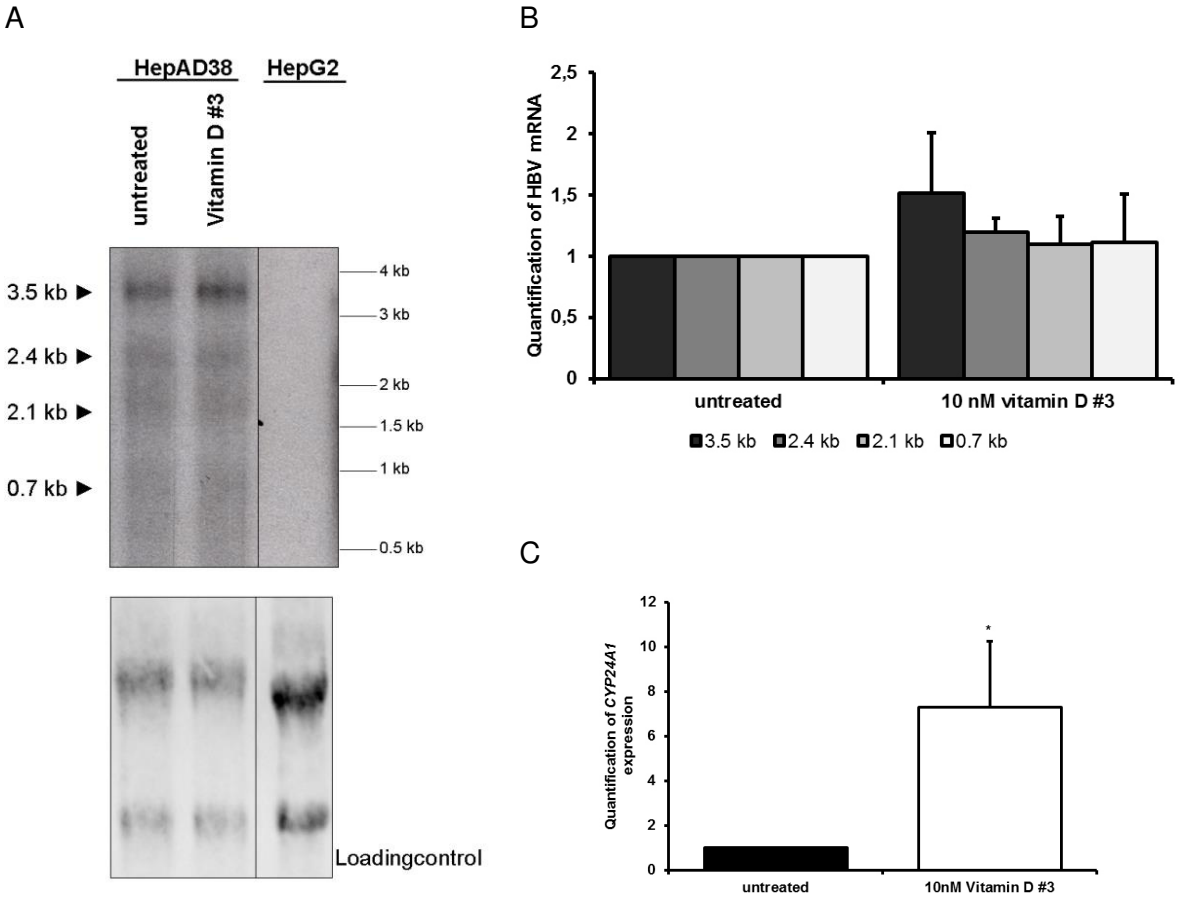

Figure 27: Northern blot analysis of HBV RNA constructs after vitamin D treatment.
HepAD38 cells were treated with 10 nM vitamin D analog *#3* and *#5* as described before.
A: RNA was separated with agarose-gel electrophoreses and northern blot was performed with an HBV specific-probe. One representative blot is illustrated. A picture of the membrane showing the ribosomal RNA served as loading control.
B: HBV mRNA was quantified by referring the values to the 28S rRNA. The values were normalized to untreated control n= 3. p-value 3.5 kb= 0.212; p-value 2.4 kb= 0.076; p-value 2.1 kb= 0.578; p-value 0.7 kb= 0.701.
C: RNA was converted into cDNA and expression of *CYP24A1* as measured with qPCR. *#3*: n= 3.

By northern blot analysis with an HBV-specific probe, the four different HBV transcripts were visualized. Specific bands of a size of 3.5, 2.4, 2.1, and 0.7 kb were observed (see Figure 27A). The analysis indicated that the HBV transcripts are not influenced differently upon vitamin D treatment. The 3.5 kb mRNA band of the northern blot was quantified and a 1.52-fold induction was observed upon treatment with vitamin D analog *#3* (see Figure 27B). For all the other constructs, no significantly altered values were measured. As a positive control for vitamin D treatment, the same RNA was quantified for *CYP24A* expression by RT-qPCR (see Figure 27C).

To sum it up, vitamin D has no influence on the HBV constructs tested by RT-qPCR and northern blot analysis. The intracellularly elevated amounts of viral proteins HBsAg and HBcAg are not caused by an induction of HBV transcripts.

3.2.8 Vitamin D influences the intracellular distribution of viral proteins

For the further characterization of the influence of intracellularly elevated levels of viral proteins, the distribution of LHBs, SHBs, and HBcAg was analyzed in HepAD38 and Huh 7.5 transiently expressing HBV/A with immunofluorescence analysis.

In general, in the untreated control a distribution of LHBs all over the cell was observed. The staining was specific for LHBs because HBV negative cells showed no signal (see cells with white stars). The cells, which were treated with 10 nM vitamin D analog *#5*, showed a different distribution of LHBs in contrast to the untreated control. An intracellularly accumulation of the LHBs was observed in all tested cell lines (see Figure 28, arrows).

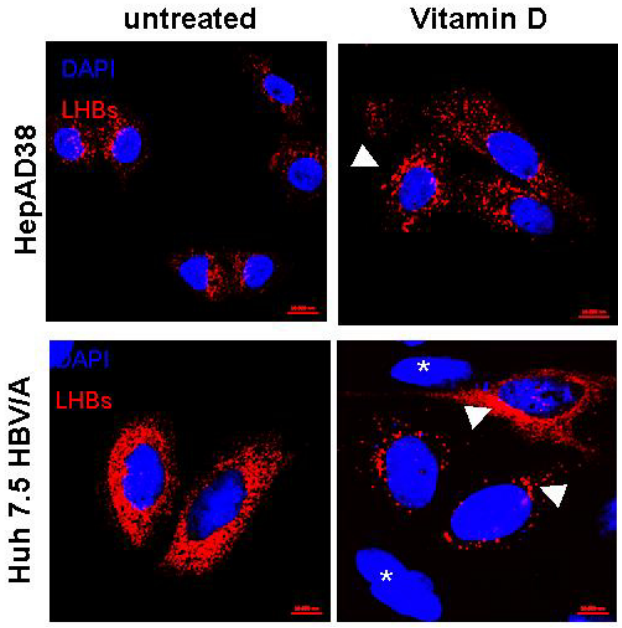

Figure 28: Distribution of LHBs in vitamin D-treated cells.
HepAD38 cells and transiently HBV/A-expressing Huh 7.5 cells were treated with 10 nM vitamin D analog *#5*. The cells were stained with a LHBs-specific antibody (Ma18/7). Nuclei were visualized by DAPI staining. Pictures were taken with CLSM magnification 100x. Representative pictures are illustrated.

Further immunofluorescence analyses were performed to reveal the localization of the accumulation. Therefore, Huh 7.5 cells were transiently co-transfected with pCEP-gtA-1.5 and plasmids encoding for molecules tagged with GFP/YFP. Those tagged proteins acted as markers for different cell compartments. Sec22 was used to target the ER, Grasp65 to visualize the Golgi, Rab7 as marker for MVBs and finally Vps4A as component of the ESCRT-machinery.

For all the used markers co-localizations with LHBs (indicated by yellow areas) were observed for the untreated control (see Figure 29). These co-localizations were also present in vitamin D analog *#5*-treated cells. For the further analysis, the overlap coefficient of whole cells of LHBs and the marker protein were measured and correlated to the untreated controls. The differences of the overlap coefficient of LHBs with GRASP65 (see Figure 29B) and Rab7 (see Figure 29C) showed no significant differences, whereas the overlap coefficient of LHBs with Sec22 was significantly increased (10%) (see Figure 29A) and the overlap coefficient of LHBs and VPS4a was significantly decreased (10.11%) (see Figure 29 D).

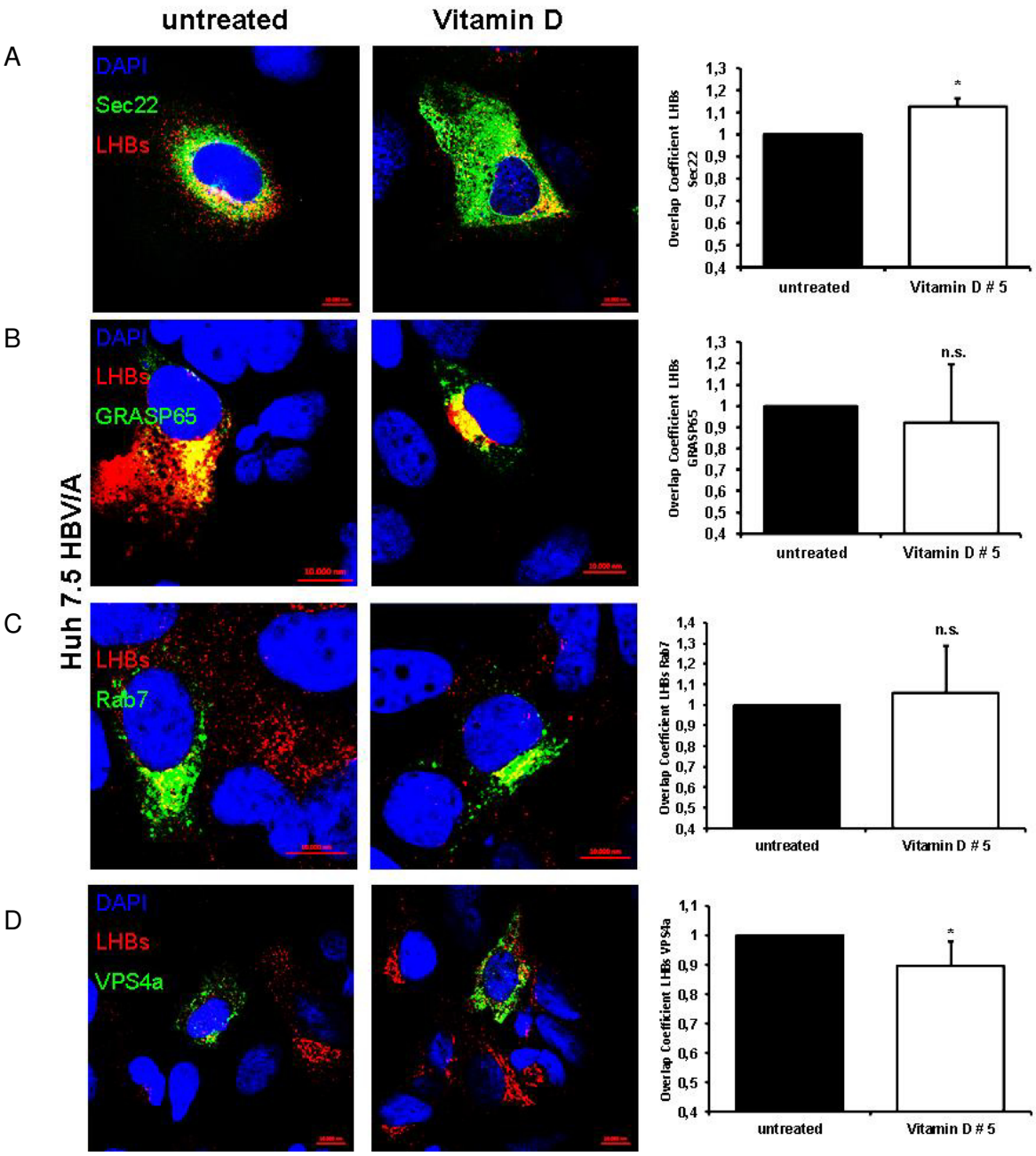

Figure 29: Distribution of LHBs in vitamin D-treated cells with marker proteins.
Huh 7.5 cells were co-transfected with pCEP-gtA-1.5 and marker plasmids (Sec22-YFP, GRASP65-GFP, peYFP-Rab7 and pEGFP-Vps4A.wt). The cells were treated with 10 nM vitamin D analog *#5* and stained with a LHBs-specific antibody (Ma18/7). Nuclei were visualized by DAPI staining. Pictures were taken with CLSM. Overlap coefficient was calculated for the whole cell with the Zeiss Zen software. The values were normalized to untreated control. Sec22-YFP n= 10, GRASP65-GFP n= 22, p-value= 0.471, peYFP-Rab7 n= 10; p-value= 0.474; PEGFP-VpsA.wt n= 6. Representative pictures are illustrated.

In the following experiments, the distribution of the viral proteins HBsAg, predominantly representing SHBs, was analyzed in more detail. Therefore, HepAD38 and transiently transfected Huh 7.5 HBV/A cells were stained with an anti-HBsAg-specific antibody. A specific staining was visualized by CLSM (see Figure 30, negative cells marked with white stars). In this immunofluorescence analysis, weak accumulations (see arrows) are present in vitamin D analog *#5* treated cells (see Figure 30).

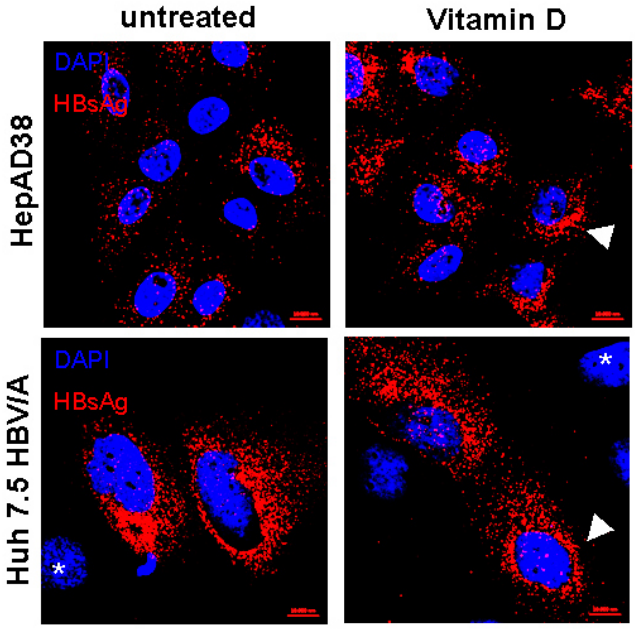

Figure 30: Distribution of HBsAg in vitamin D-treated cells.
HepAD38 cells and transiently HBV/A-expressing Huh 7.5 cells were treated with 10 nM vitamin D analog *#5*. The cells were stained with an HBsAg-specific antibody (Abcam, goat). Nuclei were visualized by DAPI-staining. Pictures are taken by CLSM with 100x magnification. Representative pictures are illustrated.

To analyze the co-localization of SHBs with different cell compartments, a co-transfection experiment was performed. The co-transfection of Huh 7.5 with pCEP-gtA-1.5 and plasmids encoding for molecules labeled GFP/YFP allowed the visualizing of SHBs and markers for ER, Golgi, MVB and the ESCRT-machinery (see 3.2.7). The analysis of the overlap coefficient of untreated and with vitamin D *#5*-treated cells showed no significant differences for all tested markers.

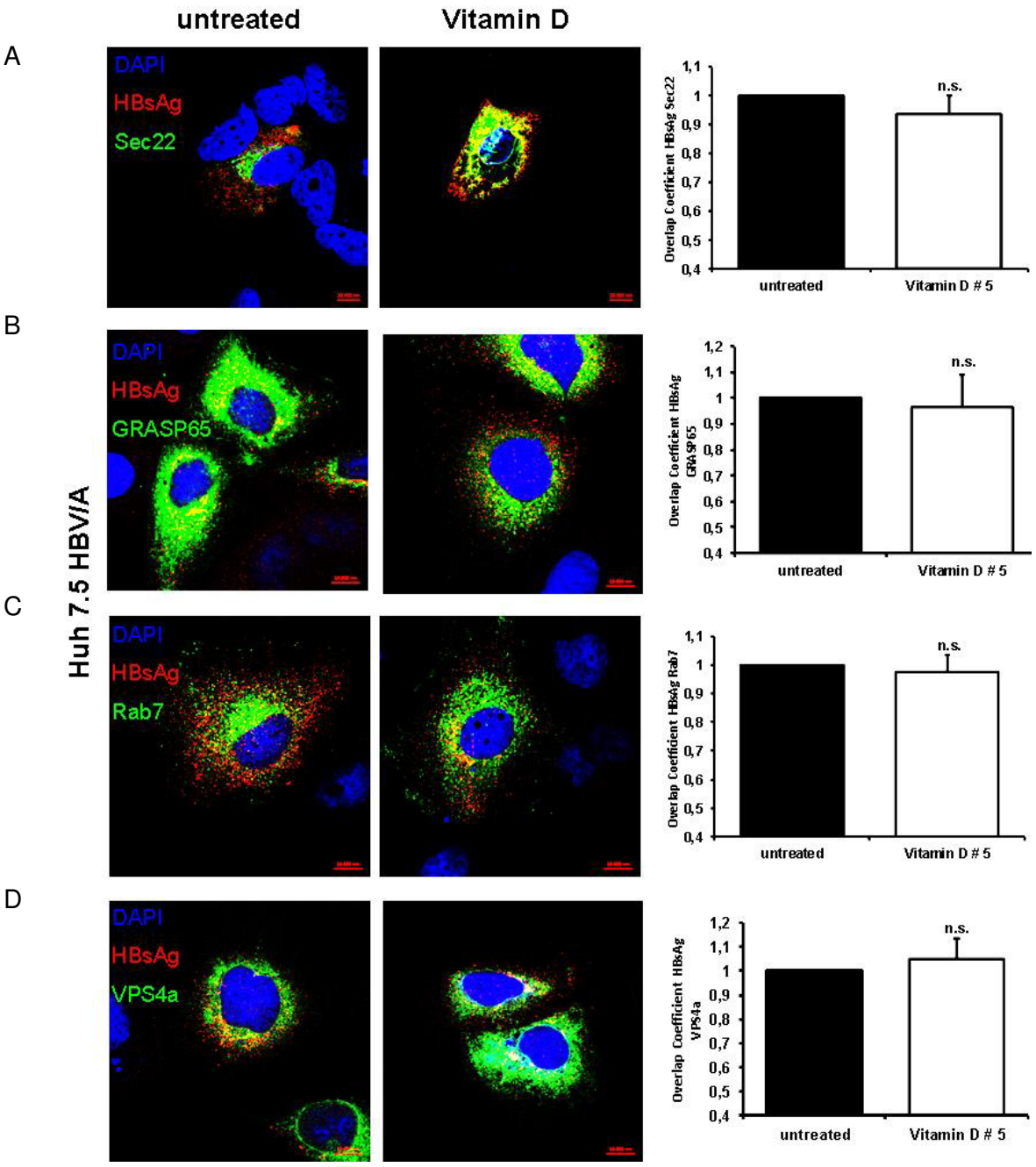

Figure 31: Distribution of HBsAg in vitamin D-treated cells with marker proteins.
Huh 7.5 cells were co-transfected with pCEP-gtA-1.5 and marker plasmids (peYFP-Rab7 and pEGFP-Vps4A.wt). The cells were treated with 10 nM vitamin D analog *#5* and stained with an HBsAg-specific antibody (Abcam, goat). Nuclei were visualized by DAPI staining. Pictures are taken by CLSM. Overlap coefficient was calculated for the whole cell with Zeiss Zen software. Values were normalized to untreated control. Sec22-YFP n= 10, p-value= 0.081; GRASP65-GFP n= 17, p-value= 0.440; peYFP-Rab7 n= 15, p-value= 0.338; PEGFP-VpsA.wt n= 15; p-value= 0.175. Representative pictures are illustrated.

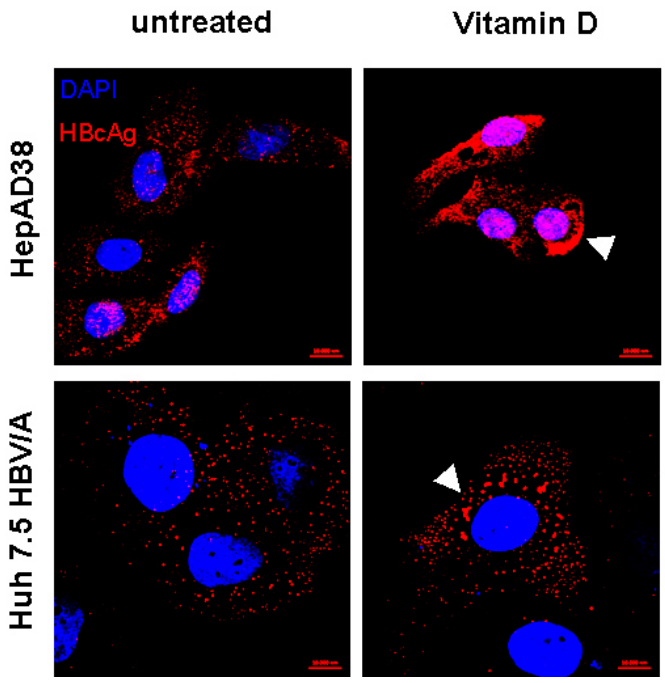

Figure 32: Distribution of HBcAg in vitamin D-treated cells.
HepAD38 cells and transiently HBV/A-expressing Huh 7.5 cells were treated with 10 nM vitamin D analog *#5*. The cells were stained by an HBcAg-specific antibody (Dako). Nuclei were visualized by DAPI staining. Pictures are taken by CLSM with 100x magnification. Representative pictures illustrated.

Moreover, the distribution of HBcAg was analyzed. It had to be considered that the staining with the used antibody was not optimal, as distribution of HBcAg is dot-like. Nevertheless, analysis gives evidence that vitamin D-treated cells showed aggregates for HBcAg (see Figure 32, arrows). Co-localizations studies with Rab7, VPS4A, and HBcAg showed no significant differences.

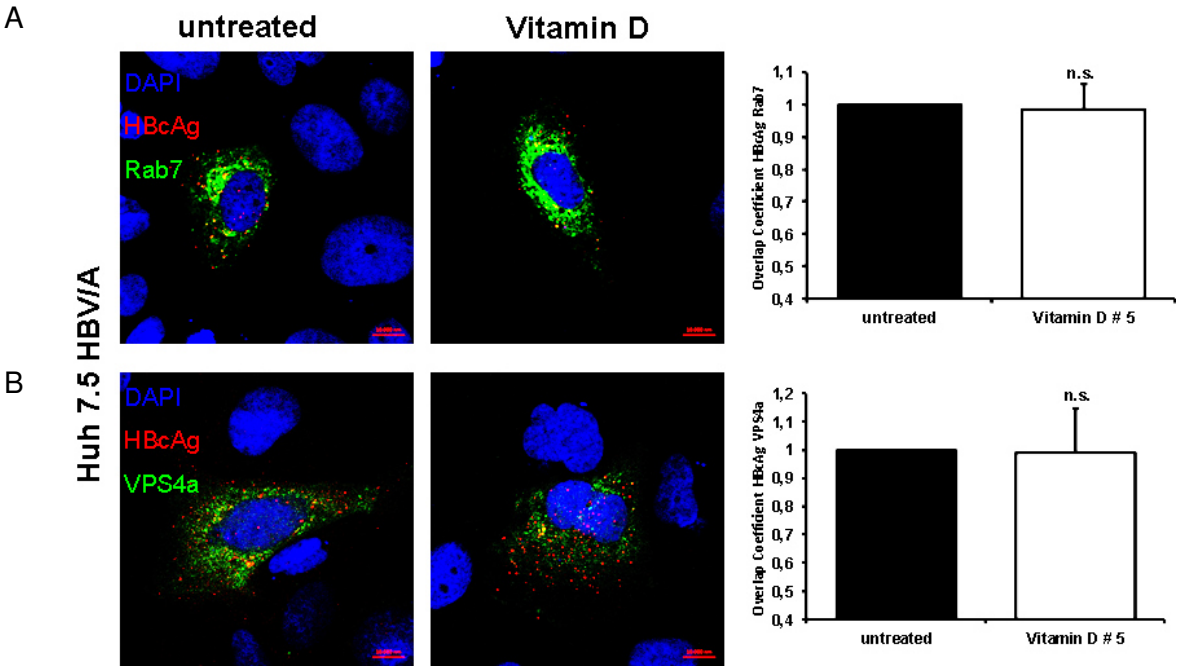

Figure 33: Distribution of HBcAg in vitamin D-treated cells with marker proteins. Huh 7.5 cells were co-transfected with pCEP-gtA-1.5 and marker plasmids (peYFP-Rab7 and pEGFP-Vps4A.wt). The cells were treated with 10 nM vitamin D analog *#5* and stained by an HBcAg-specific antibody (Dako). Nuclei were visualized by DAPI staining. Pictures were taken by CLSM. Overlap coefficient was calculated for the whole cell with the help of Zeiss Zen software. Values were normalized to untreated control., peYFP-Rab7 n= 12, p-value= 0.737; PEGFP-VpsA.wt n= 10, p-value= 0.896. Representative pictures are illustrated.

Taken together, the vitamin D analog *#5* treatment leads to an intracellularly accumulation, predominantly of LHBs, and a slight accumulation of SHBs. Furthermore, HBcAg formed aggregates upon vitamin D treatment.

To summarize the chapter 3.2, dealing with the influence of vitamin D on the life cycle of HBV, it can be concluded that the treatment with different vitamin D analogs leads to a reduction of secreted HBsAg in a dose-dependent manner. The infection experiments with PHHs could confirm these observations. The vitamin D treatment causes an altered ratio of the secretion of LHBs and SHBs. A stronger reduction of LHBs was observed in contrast to SHBs. Moreover, a reduction of the viral genomes and HBcAg were observed in the SN upon treatment.

The western blot analysis and immunofluorescence analysis revealed intracellularly elevated amounts of LHBs and HBcAg. The main compartments of VPs accumulated intracellularly, whereby the final localization of accumulation was not confirmed. Finally,

the vitamin D treatment had no effect on the secretion of HBeAg or the production of viral transcripts.

3.3 Influence of vitamin D on the viral factor TXLNA

Due to the collected data, it is obvious to focus in the following on a potential mechanism of vitamin D causative for the observed reduction on release of HBsAg and viral genomes. Therefore, the influence of vitamin D on the viral factor TXLNA was characterized. TXLNA is the adaptor protein of the virus with the ESCRT-machinery by binding on the one hand to LHBs and on the other hand to TSG101. Consequently, TXLNA is crucial for the release of HBV VPs (Hoffmann et al., 2013). Hitherto, its involvement in the release of filaments has not been further characterized.

3.3.1 Vitamin D treatment leads to diminished amounts of TXLNA

First, it should be clarified whether vitamin D influences TXLNA without the effect of HBV, hence HBV negative cell lines Huh 7.5, Hek 293-T and HepG2 were used for analysis. The cells were treated with 10 nM vitamin D analog *#5* and tested for the gene expression of *TXLNA* (Gen-Bank ID, NCBI: 200081) by RT-qPCR. The expected vitamin D response was verified by measurement of *CYP24A1* gene expression.

Huh 7.5 and HepG2 cells showed significantly decreased amounts of *TXLNA* expression upon vitamin D treatment. Huh 7.5 cells showed a reduction of *TXLNA* transcription of 57.79% (see Figure 34A) and HepG2 of 50.08% (see Figure 34B).

Further analysis should reveal whether protein amounts of TXLNA were also affected by treatment with vitamin D. The western blot analysis showed a clear signal for TXLNA with a defined band at an estimated size of 61.8 kDa. The analysis implicated decreasing amounts of TXLNA with vitamin D treatment in tested cell lines. These results agreed with the observations made on gene transcription level. It was concluded that vitamin D reduces the expression of TXLNA in HBV negative cell lines.

In previous studies, it was described that HBV leads to an induction of TXLNA in transiently HBV expressing cells, HBV-infected PHHs, and liver tissue of patients (Hoffmann et al., 2013). In the following, it was investigated whether vitamin D can lead to a downregulation of *TXLNA* in HBV positive cells. For this approach, HBV-stably expressing HepAD38 and Huh 7.5 cells transiently transfected with HBV/A were used.

The cells were treated with 10 nM vitamin D *#5* and the transcription of *TXLNA* was analyzed with RT-qPCR. The tested cell lines showed a significant reduction in expression of *TXLNA*. In transiently transfected Huh 7.5 HBV/A cells, a reduction of 26.29% (see Figure 35A) and in HepAD38 a reduction of 36.90% (see Figure 35B) was observed. Strikingly, the vitamin D-dependent relative reduction in HBV expressing cells was lower upon vitamin D treatment in contrast to HBV negative cells. This might be a consequence of the presence of HBV and induction of *TXLNA* by its regulatory proteins HBx and LHBs via c-Raf (Hoffmann et al., 2013).

Moreover, protein levels of TXLNA were analyzed by western blot analysis. A defined band at the correct size occurred (61.9 kDa). In both tested cell lines (Huh 7.5 HBV/A, HepAD38), decreased amounts of TXLNA were observed after treatment with 10 nM vitamin D analog *#5*. These data are in agreement with the previous observations.

A

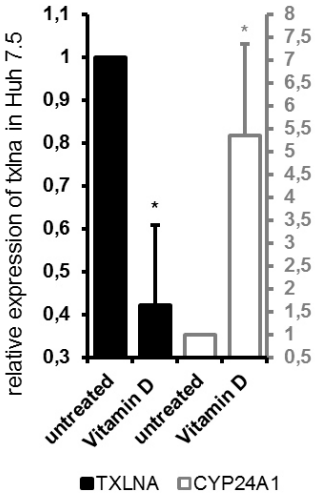

B

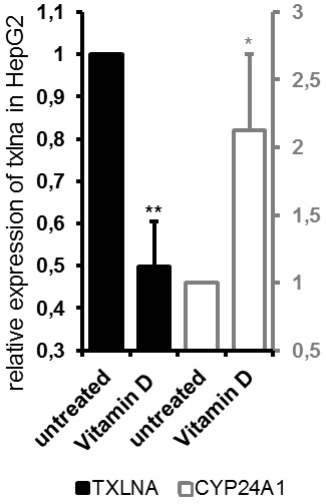

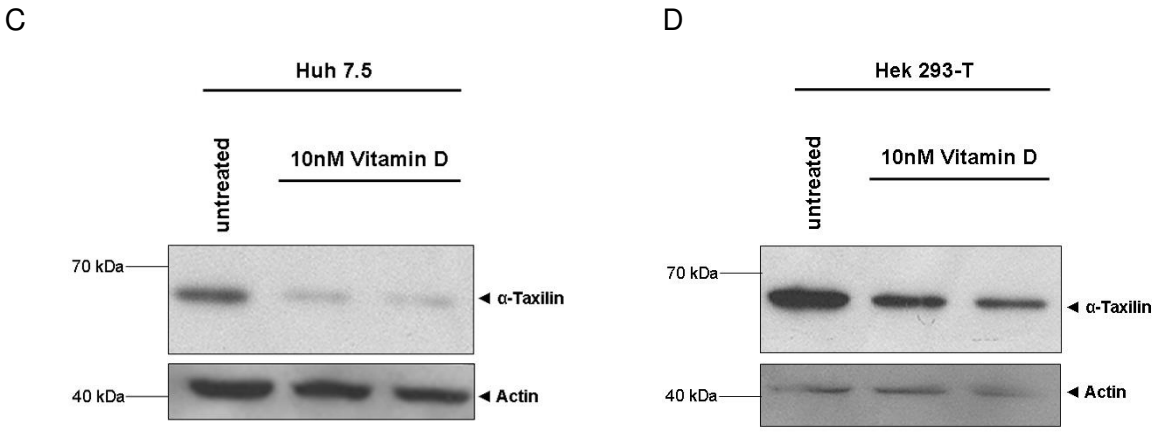

Figure 34: Influence of vitamin D on TXLNA in HBV negative cell lines.
A, B: Huh 7.5 and HepG2 cells were treated with 10 nM vitamin D analog *#5*. The gene expression was measured by RT-qPCR. The values were calculated with the ΔΔct method by referring CPs of *TXLNA* to CPs of *RPL27* as the housekeeping gene. n= 3.
C, D: Huh 7.5 and Hek 293-T cells were treated with 10 nM vitamin D analog *#3* (lane 2) and *#5* (lane 3). The cells were lysed and the proteins were separated on a 10% SDS-gel. The western blot analysis was carried out by a TXLNA-specific antibody (E2). The Actin-detection served as loading control. One representative blot is illustrated.

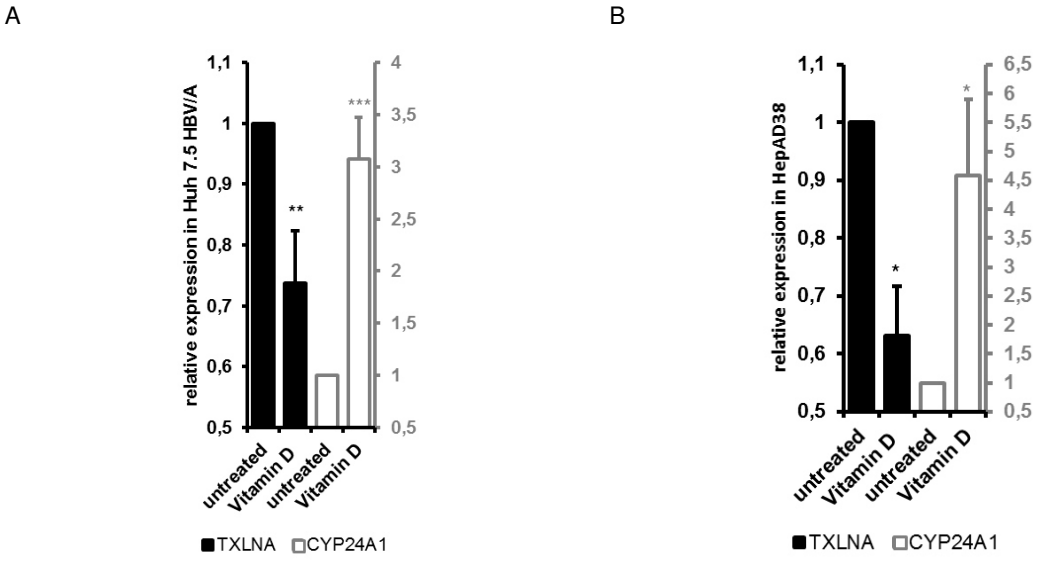

C

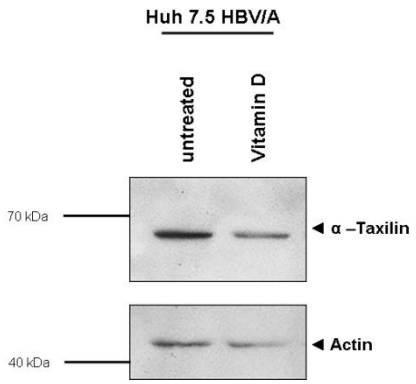

D

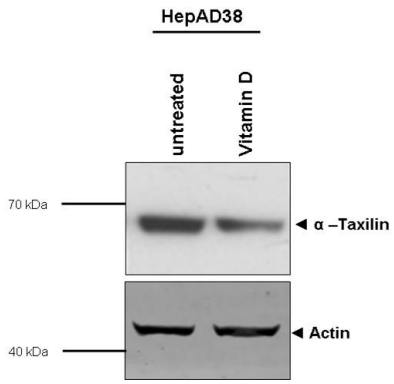

Figure 35: Expression of TXLNA in HBV expressing cells.
A: Huh 7.5 cells were transiently transfected with pCEP-gtA-1.5. Sixteen hours after transfection, vitamin D treatment was carried out as described before with 10 nM of substance *#5*. The RNA was isolated and transcribed into cDNA. The gene expression was measured by qPCR. Values were calculated with the ΔΔct method by referring CPs of *TXLNA* to CPs of *RPL27* as the housekeeping gene. n= 3.
B: HepAD38 cells were treated with vitamin D analog *#5* as described before. RNA was isolated and gene expression was measured by RT-qPCR. Values were calculated with the ΔΔct method by referring CPs of *TXLNA* to CPs of *RPL27* as the housekeeping gene. n= 3.
C: Huh 7.5 cells were transiently transfected with pCEP-gtA-1.5. Sixteen hours after the transfection, vitamin D treatment was carried out as described before with 10 nM of substance *#5*. The cells were lysed and separated on a 12% SDS-gel. The western blot analysis was conducted with a TXLNA-specific antibody (E2). Actin-detection served as loading control. One representative blot is illustrated.
D: HepAD38 cells were treated with vitamin D analog *#5* as described before. The cells were lysed and separated on a 12% SDS-gel. The western blot analysis was conducted with a TXLNA-specific antibody (E2). Actin-detection served as loading control. One representative blot is illustrated.

3.3.2 Vitamin D treatment leads to decreased overlap coefficient of TXLNA and LHBs

After the western blot analysis of the total protein levels of TXLNA, further investigations of TXLNA with its binding partner LHBs were carried out. Previous studies of the laboratory with coimmunopreciptations and CLSM revealed an interaction of the preS1-/preS2-domain with TXLNA mediated by its late domain (Hoffmann et al., 2013).
Accordingly, the overlap coefficient of LHBs and TXLNA upon vitamin D treatment was investigated by immunofluorescence analysis. HBV/A-expressing Huh 7.5 cells were stained with an anti-TXLNA-specific antibody (E2) and an anti-preS1-specific antibody (Ma18/7). The analysis by CLSM gave evidence to support the observations of a vitamin D-induced reduction of TXLNA in HBV positive and HBV negative cells (see Figure 36A). It is obvious that a reduction of TXLNA by vitamin D analog *#5* treatment goes hand-in-hand within a significantly decreased overlap coefficient with LHBs of

12.08% (see Figure 36B). These observations might be ensured by coimmunopreciptation in future analysis.

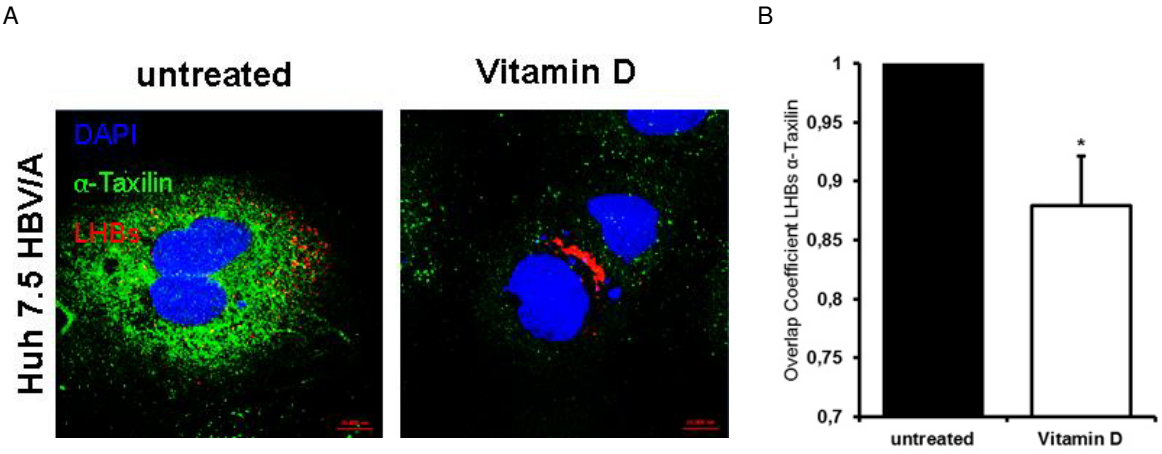

Figure 36: Influence on co-localization of LHBs and α-Taxilin.
Huh 7.5 cells were transiently transfected with pCEP-gtA-1.5 and treated with 10 nM vitamin D analog *#5*.The cells were stained with a TXLNA-specific (E2) and a LHBs-specific (Ma18/7)antibody. The nuclei were visualized by DAPI staining. Pictures were taken by CLSM and 100 x magnification. The overlap coefficient was calculated for the whole cell with Zeiss Zen software. The values were normalized to the untreated control. n= 9.

3.3.3 Vitamin D treatment has no influence on TXLNA localized on the cell surface

TXLNA is described as a potential HBV entry relevant molecule, as the blocking of TXLNA by the incubation with TXLNA-specific antibodies leads to a diminished uptake of the virus in susceptible cells (Hoffmann, 2013). Annexin A5 was identified as interaction partner of TXLNA which anchors TXLNA in the cell membrane (TXLNA has no transmembrane domain of its own) (Hoffmann, 2013; Röttger, 2011).
Since vitamin D induces a reduction of intracellular TXLNA, it was interesting to see whether vitamin D leads to decreased amounts of TXLNA located on the cell surface of HBV-susceptible cell lines.

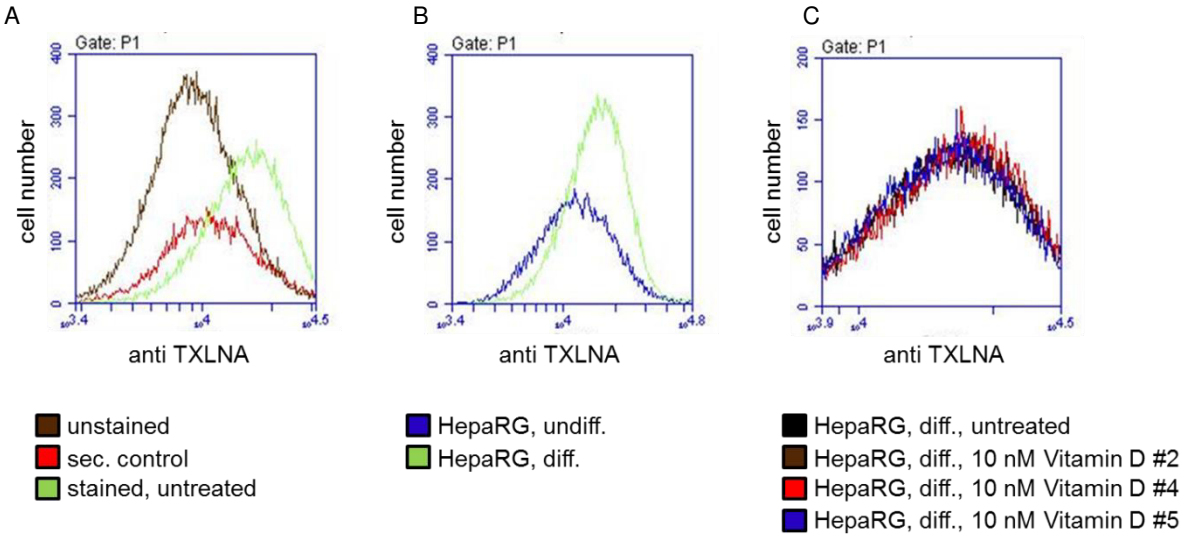

Figure 37: FACS analysis of TXLNA on the surface of HepaRG cells upon vitamin D treatment.
HepaRG cells were differentiated for fourteen days and treated with 10 nM vitamin D analogs. The cells were stained with a TXLNA-specific antibody (E2). > 10,000 living cells were recorded.
A: The cells were stained differently. Brown: unstained cells; Red: cells stained only with secondary antibody; Green: cells stained with standard protocol, untreated.
B: Blue: undifferentiated HepaRG cells, untreated; green: differentiated HepaRG cells, untreated.
C: The cells treated with: Black: untreated, grey: 10 nM vitamin D *#2*; red: 10 nM vitamin D *#4*; blue: 10 nM vitamin D *#5.*

For this approach, differentiated HepaRG cells were treated with different vitamin D analogs and tested by FACS analysis with a TXLNA-specific antibody (E2). FACS analysis showed a specific binding of the antibody (see Figure 37A). Moreover, differentiation of HepaRG lead to a localization of TXLNA on the cell surface (see Figure 37B) (Hoffmann et al., 2013). All tested vitamin D analogs showed no considerably differences in the amounts of TXLNA located on the cell surface of differentiated HepaRG cells.

In summary, the results reveal that hepatocytes, regardless whether HBV expressing or not, exhibit upon vitamin D treatment diminished transcriptional levels of *TXLNA,* resulting in impaired protein amounts intracellular (but not located on the cell surface) and a reduced interaction with the viral protein LHBs.

3.3.4 Vitamin D has no effect on the viral factors AP1G1 and TSG101

After successful analysis of the influence of vitamin D on the expression of *TXLNA,* further viral factors were considered for this study to ensure the specificity of the regulation. To address this issue, AP1G1 (adaptor-related protein complex 1 gamma 1 subunit) (also known as Adaptin-γ, ADTG, CLAPG1) and TSG101 (also known as TSG10; VPS23), which are important proteins for virus morphogenesis were chosen.

Adaptins are organized in heterotetramers, which are entitled AP-1, AP-2, AP-3 und AP-4 and involved in the trafficking of intracellular vesicles. γ2-Adaptin is a protein which belongs to the family of Clathrin-Adaptors. With the help of the yeast-two-hybrid system, it was discovered that γ 2-Adaptin is interacting with the preS1-domain of LHBs (Hartmann-Stuhler and Prange, 2001). A depletion of γ 2-Adaptin in cell culture systems lead to a decreased secretion of VPs in HBV expressing hepatocytes (Rost et al., 2006; Thomé, 2007). In a publication of Wood et al., published in 2004, microarray analysis showed a vitamin D-induced expression of 2.1.-fold of *AP1G1* in a human colon carcinoma cell line.

In the following, the expression of *AP1G1* (Gen-Bank ID, NCBI: 164) was tested with RT-qPCR in HBV negative HepG2 and HBV positive HepAD38 cells. *CYP24A1* expression verified a successful vitamin D treatment.

The expression of *AP1G1* was slightly, but not significantly increased in HepG2 (1.20-fold) (see Figure 38A) and HepAD38 (1.37-fold) (see Figure 38B). The conclusion of this experiment was that the tested cell lines showed no considerable difference in the transcriptional level of *AP1G1*. To obtain results that are more precise and to test whether slight differences of expression level exist, the number of measurements (n) has to be increased in future studies.

To investigate the influence of vitamin D on the protein level, western blot analyses were performed. The separated cell lysates of HepAD38 cells presented a clear signal of a band at a molecular weight of 90 kDa (estimated size 91 kDa) (see Figure 38C) on the western blot membrane. The quantification showed a slightly and significantly increased signal of AP1G1 (1.27-fold) in HBV expressing HepAD38 cells (see Figure 38D), corroborating the observations on a transcriptional level.

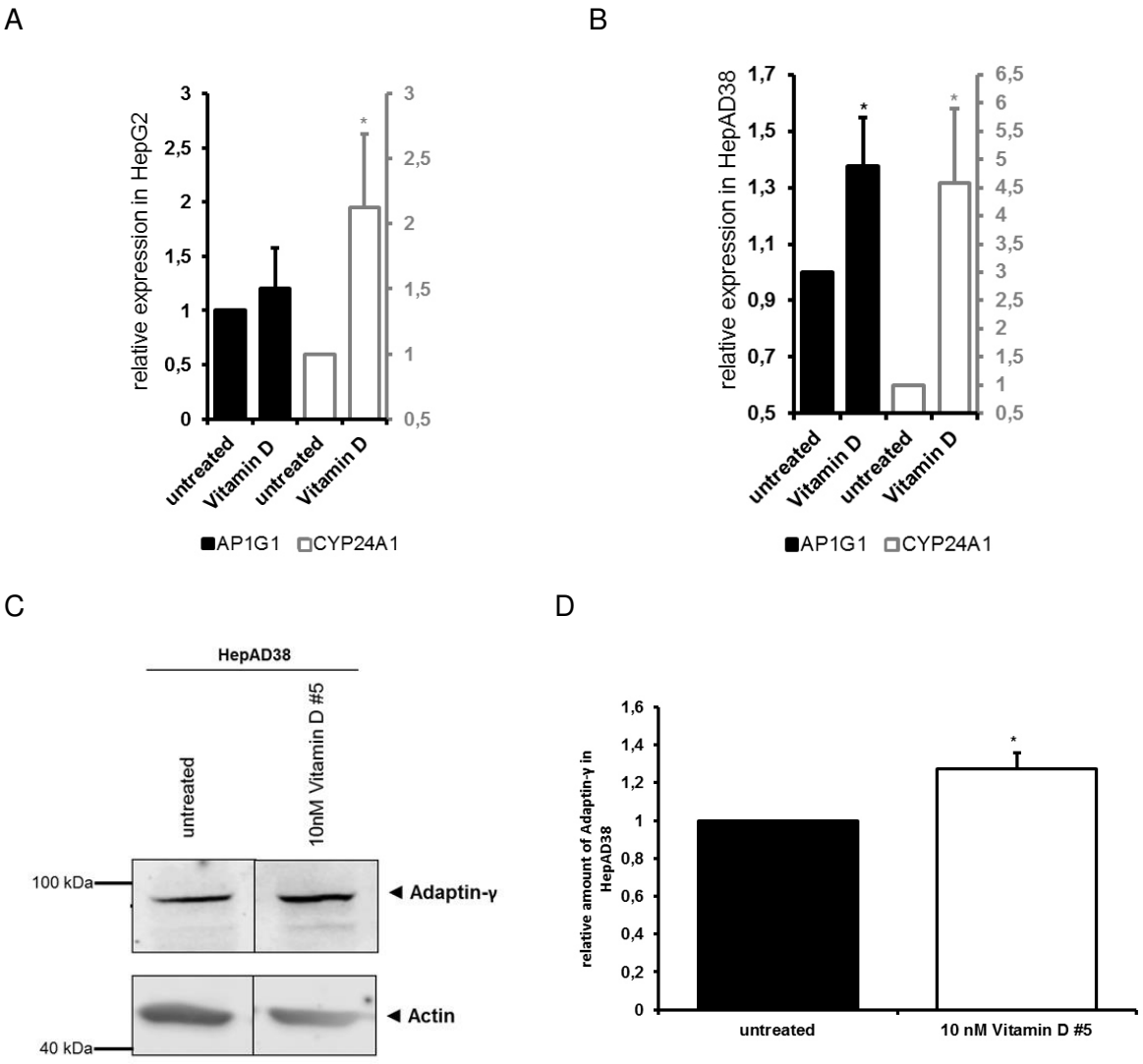

Figure 38: Influence of vitamin D on AP1G1.
A: HepG2 cells were treated with vitamin D analog *#5* as described before. RNA was isolated and transcribed into cDNA. The gene expression was measured by qPCR and values were calculated with the ΔΔct method by referring CPs of *AP1G1* to CPs of *RPL27* as housekeeping gene. n= 3, p-value= 0.261.
B: HepAD38 cells were treated with vitamin D analog *#5* as described before. RNA was isolated and gene expression was measured by RT-qPCR. Values were calculated with the ΔΔct method by referring CPs of *AP1G1* to CPs of *RPL27* as housekeeping gene. n= 3.
C: HepAD38 cells were treated with 10 nM vitamin D analog *#5*, as described before. The cells were lysed and separated on a 12% SDS-gel. Western blot analysis was conducted with an Adaptin-γ-specific antibody. Actin blot served as loading control. One representative blot is illustrated.
D: Western blot was quantified by referring to the Actin loading control. Values were normalized to the untreated control. n= 3.

TSG101 is a component of the ESCRT-machinery (ESCRT-I subunit) (Stieler and Prange, 2014). The involvement of TSG101 for the virus release is controversially discussed. A research group of the University Medical Center in Mainz claims that RNAi experiments

led to the conclusion that TSG101 is not an essential factor for the virus release (Stieler and Prange, 2014), whereas published data of our research division reveal that TXLNA mediates the interaction of HBV particles with the ESCRT-machinery by acting as an adaptor protein between on the one hand LHBs and TSG101 on the other (Hoffmann et al., 2013).

Therefore, the influence of vitamin D on TSG101 was investigated. Expression analyses of *TSG101* (Gen-Bank ID, NCBI: 7251) in HBV negative HepG2 cells and HBV positive HepAD38 cells were performed with RT-qPCR. The expected vitamin D response was verified with the measurement of *CYP24A1* expression.

The transcriptional levels of *TSG101* in HepG2 cells showed no considerable differences upon vitamin D treatment measured by this method (induction of 1.03-fold) (see Figure 39A). Treatment in HepAD38 cells lead to a significant increase of *TSG101* expression of 1.72-fold (see Figure 39B).

Furthermore, protein amounts of TSG101 were determined by western blot analysis in HepAD38 in the context of vitamin D treatment. The analysis indicated that protein levels of TSG101 are reduced (reduction of 12.35%), but not significantly (Figure 39C, D). The results were interpreted in the range of error fluctuation and that vitamin D had no considerable effect on TSG101 protein levels.

Taken together, the results demonstrate that the influence of treatment with vitamin D on other viral factors such as AP1G1 and TSG101 is only modest. It is concluded from these experiments that the reduction of TXLNA by vitamin D treatment is caused specifically.

In closing, chapter 3.3 can be summarized as follows: Analysis proves that vitamin D leads to a reduction of TXLNA in HBV negative and HBV positive cells, caused by reduced expression of *TXLNA*. The degree of reduction in HBV positive cells is diminished in contrast to HBV negative cells, reflecting an induction of TXLNA by HBV (Hoffmann et al., 2013). It is published that TXLNA is crucial for the interaction of HBV with the ESCRT-machinery and therefore responsible for the release of VPs (Hoffmann et al., 2013). With decreased amounts of TXLNA, the interaction of the protein with its binding partner LHBs might be diminished.

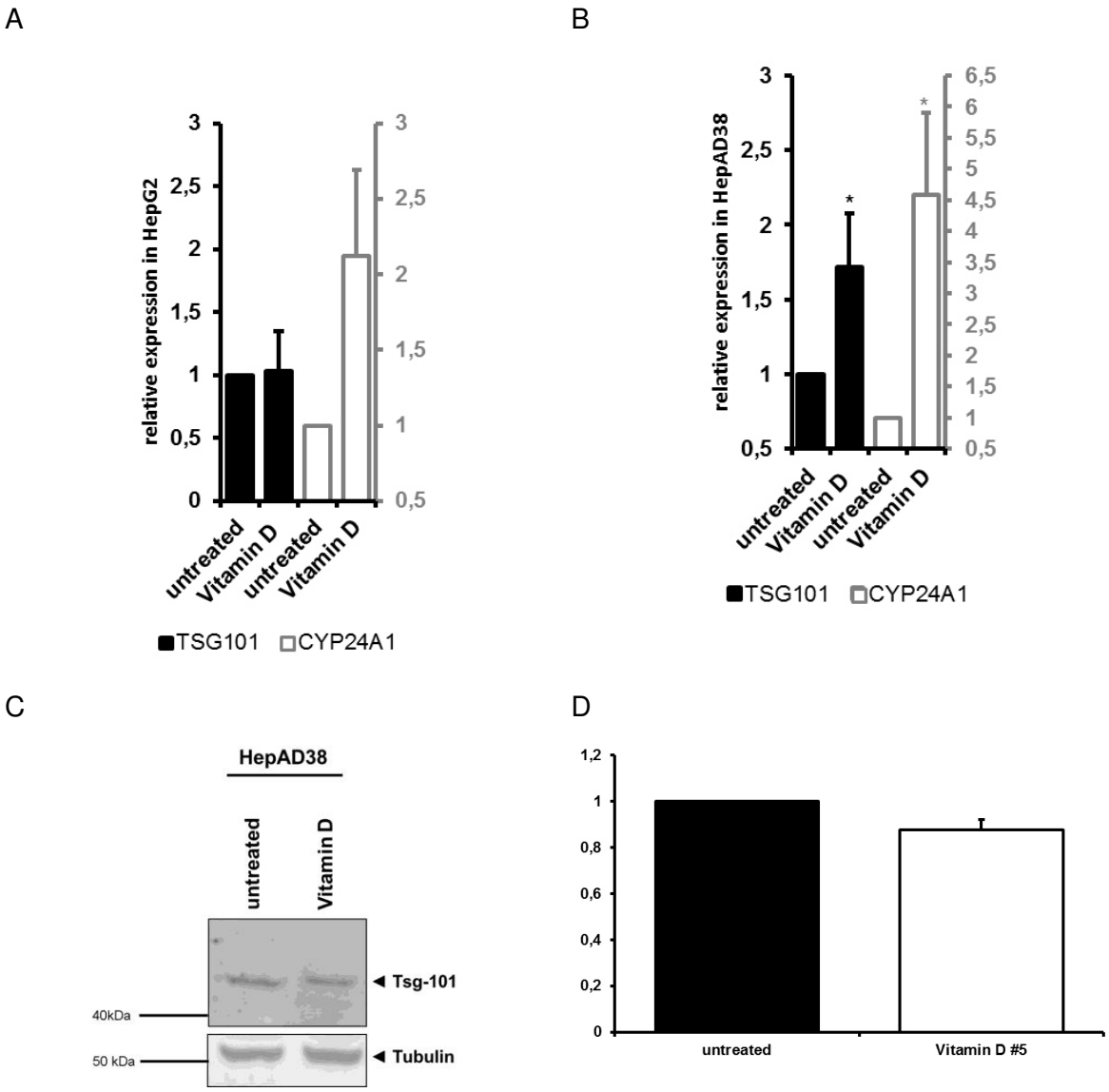

Figure 39: Influence of vitamin D on TSG101.
A: HepG2 cells were treated with vitamin D analog *#5* as described before. RNA was isolated and transcribed into cDNA. The gene expression was measured by qPCR and values were calculated with the ΔΔct method by referring CPs of target genes to CPs of *RPL27* as housekeeping gene. n= 3, p-value= 0,899.
B: HepAD38 cells were treated with vitamin D analog *#5* as described before. RNA was isolated and transcribed into cDNA. The gene expression was measured by qPCR and values were calculated with the ΔΔct method by referring CPs of target genes to CPs of *RPL27* as the housekeeping gene. n= 3.
C: HepAD38 cells were treated with 10 nM vitamin D analog *#5*, as described before. The cells were lysed and a sample was separated on a 12% SDS-gel. The western blot analysis was conducted with an TSG101-specific antibody. Tubulin-blot served as loading control. One representative blot is illustrated.
D: Western blot was quantified by referring to Tubulin loading control. The values were normalized to the untreated control. n= 3, p-value= 0.623.

3.4 Characterization of HBV genotypes

Over 7% of the genome sequence has to differ for the definition of a new HBV genotype. HBV genotypes reveal considerable differences with regard to clinical parameters (Kao, 2002). For analyzing HBV genotypes *in vitro* in more detail, constructs isolated from patient samples were cloned into a pCEP-Puro vector. This vector was cloned in 2011 by Dr. A. Geipel on base of the pCEP4 (Life Technologies (Darmstadt)) and the pPur (Clontech (Saint-Germain-en-Laye)) vector. The plasmid served as backbone for the 1.5-fold HBV constructs which are regulated by its autologous promotor. Cloning work was conducted by Dr. Hauke Niekamp in the laboratory of the cooperation partner PD Dr. Dieter Glebe in Gießen (Niekamp, 2013).

3.4.1 Secretion of HBsAg in different HBV genotypes

Comparative analysis of the secretion of SVPs and VPs of genotypes A and G lead to the conclusion that HBV/G is secretion-incompetent for HBsAg particles, not affecting the release of VPs and viral replication (Peiffer et al., 2014). In the following, also HBV/B, HBV/C, and HBV/D were analyzed regarding their secretion of HBsAg.

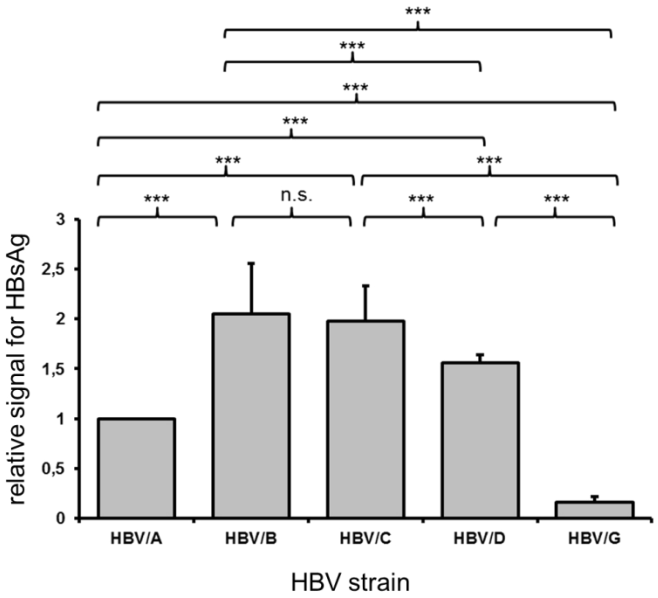

Figure 40: Release of HBsAg in different genotypes.
Huh 7.5 cells were transiently transfected with 1 µg plasmid per 250,000 Huh 7.5 cells (pCEP-gtA-1.5, pCEP-gtB-1.5, pCEP-gtC-1.5, pJo19, pCEP-gtG-1.5). The SN was harvested after 48 h and secretion of HBsAg was tested with HBsAg-ELISA. The values were normalized to HBV/A n= 6.

The comparative analysis of HBV genotypes resulted in a significant difference in the secretion of HBsAg. Previously described data of a secretion-incompetence for HBV/G were confirmed by HBsAg-ELISA (signal under detection limit). HBV/A significantly secreted the lowest amount of HBsAg in contrast to the tested genotypes (normalized to 1) (see Figure 40). HBV/D showed a 1.56-fold increased secretion of HBsAg compared to HBV/A. HBV/B and HBV/C significantly secreted the most HBsAg. Genotype B secreted 2.05-fold more HBsAg in contrast to genotype A, whereas HBV/C secreted 1.98-fold more. The differences of genotype B and C was not significant.

3.4.2 Influence of vitamin D on different genotypes

Since the vitamin D treatment in HBV expressing and replicating cells leads to an impaired secretion of HBsAg and viral genomes in HBV/A and HBV/D, it was tempting to analyze whether other genotypes can be influenced in the same quantity.

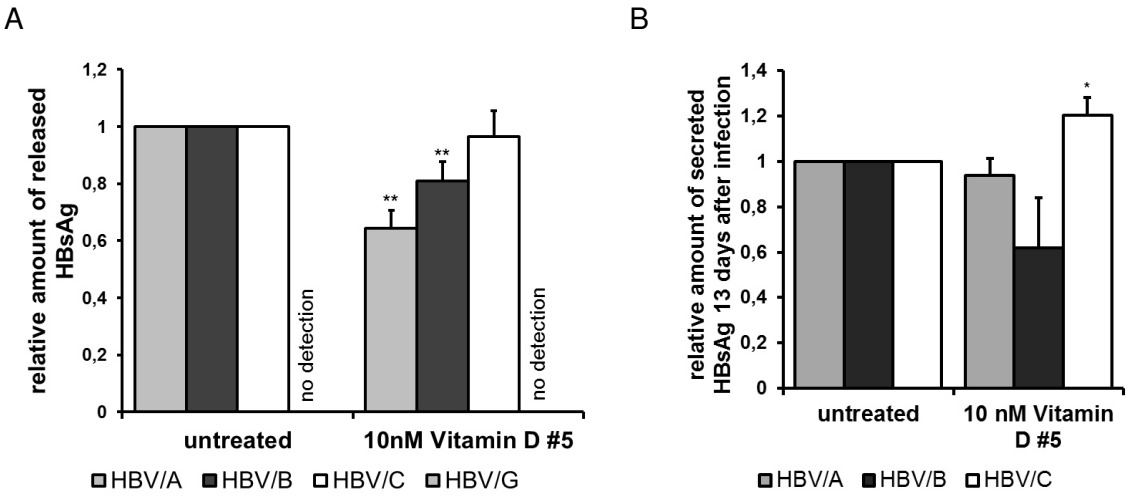

Figure 41: Release of HBsAg in different genotypes by vitamin D treatment.
A: Huh 7.5 cells were transiently transfected with pCEP-gtA-1.5, pCEP-gtB-1.5, pCEP-gtC-1.5, pCEP-gtG-1.5 and treated with 10 nM vitamin D analog *#5*. The SN was harvested and HBsAg measured by HBsAg-ELISA and the values were normalized to the untreated control. n= 3, HBV/C: p-value= 0.354.
B: PHHs were infected with genotype A, B and C (MOI 500). The infection was monitored as described before. HBsAg was detected by HBsAg-ELISA of the SN on day 13 after the infection and the values were normalized to the untreated control. HBV/A: p-value= 0.528; HBV/B: p-value= 0.407. The expected vitamin D response was verified by the measurement of the *CYP24A1* gene expression (data not shown).

For this purpose, Huh 7.5 cells were transiently transfected with the HBV genotypes A, B, C, and G and treated with vitamin D analog *#5*. Upon the vitamin D treatment, the release of HBsAg was measured by HBsAg-ELISA. HBV/A and HBV/B showed a significant reduction for the treatment with vitamin D (HBV/A: 39.81%; HBV/B: 21.41%), whereas for HBV/C no significant reduction was observed (HBV/C: 3.4%). As expected, for HBV/G no signal for HBsAg was measured in the SN.
A similar result was observed in infected PHH. For HBV/A, the reduction of HBsAg amounts to 6.12%, for HBV/B to 38.2%. For genotype C, no reduction was observed (+20.41%). Finally, it can be concluded that the release of HBsAg in HBV/C is not affected upon the treatment with vitamin D.

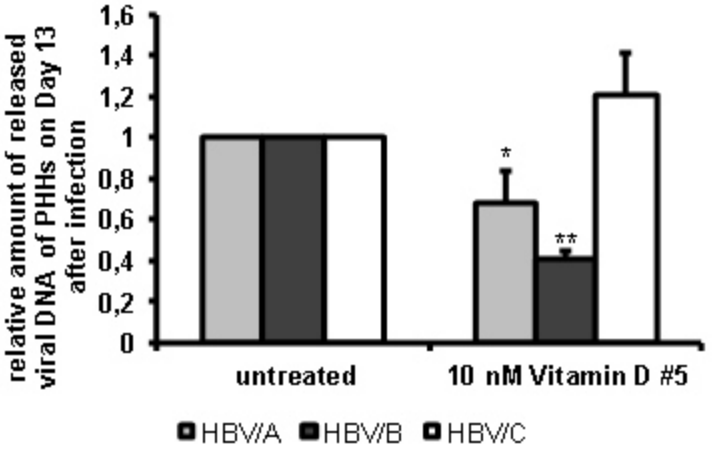

Figure 42: Release of viral genomes after vitamin D treatment in PHHs infection with different genotypes.
PHHs were infected with genotype A, B, and C (MOI 500). The infection was monitored as described before. The number of viral genomes was detected by qPCR of the SN on day 13 after the infection and the values were normalized to the untreated control. The expected vitamin D response was verified with the measurement of the *CYP24A1* gene expression (data not shown).

In further analysis, the release of viral genomes in the SN after vitamin D treatment was tested in different genotypes. PHHs were infected as described before and the viral genomes were quantified on day thirteen after the infection. For HBV/A, a significant reduction of viral genomes of 32.3% was observed. For HBV/B, the reduction of viral genomes is 59.77% and for HBV/C no reduction at all was observed (+21.08%). It can be deduced from the result that vitamin D treatment leads to no reduction of VPs in HBV/C.

In summary, the vitamin D treatment causes an intracellular accumulation of LHBs and HBcAg in HBV expressing cells (see 3.2.5). In further analysis, it was scrutinized whether this effect has been observed in all HBV genotypes. For the comparative analysis, Huh 7.5 cells were transiently transfected with the HBV genotypes A, B, C, and G. The cells were lysed and the samples were analyzed by western blot analysis with an HBcAg-specific antibody (K46). The western blot presents a specific signal for HBcAg for all tested genotypes (negative control see Figure 25). The analysis showed increased amounts of HBcAg upon vitamin D *#5* in HBV/A, B and G. For HBV/C, the result is not as particularly pronounced among for the other genotypes. This corroborates that vitamin D treatment results in an altered response in HBV/C in contrast to other genotypes.

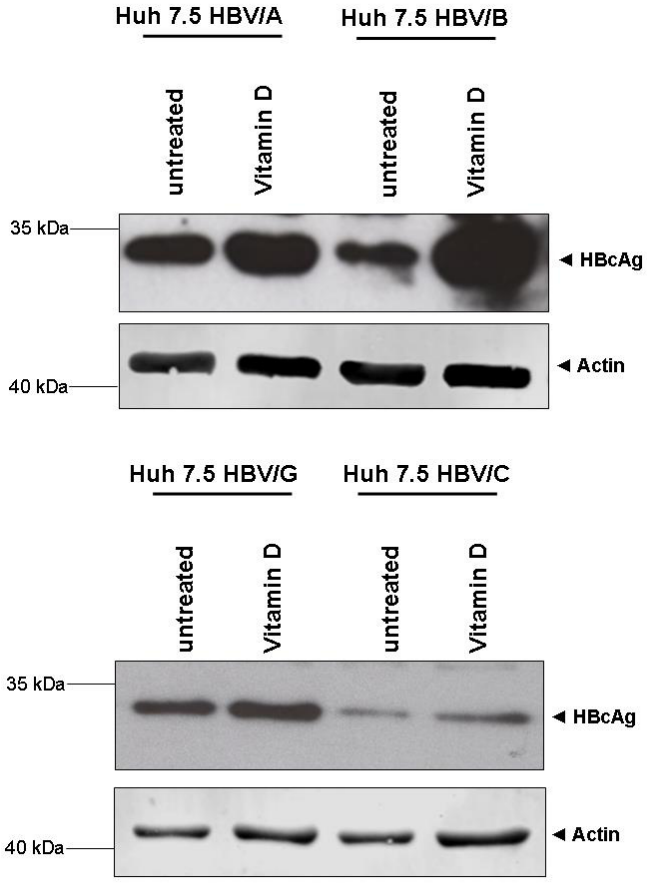

Figure 43: Intracellular amounts of HBcAg after vitamin D treatment in different genotypes.
Huh 7.5 cells were transiently transfected with pCEP-gtA-1.5, pCEP-gtB-1.5, pCEP-gtC-1.5, pCEP-gtG-1.5 and treated with 10 nM vitamin D analog *#5*. The cells were lysed and proteins separated on a 14% SDS-gel. Western blot analysis was performed with an HBcAg-specific antibody (K46). Actin blot served as loading control.

In further analysis, a closer look was taken on the distribution of LHBs in different genotypes upon vitamin D treatment. Conclusively, Huh 7.5 cells were transiently transfected with the HBV genotype constructs, treated with 10 nM vitamin D *#5,* and stained with a LHBs-specific antibody (Ma18/7). The immunofluorescence analysis of the distribution of LHBs shows an intracellularly accumulation in genotype A, B, D, and G. This effect was only modest in HBV/C. This result gives further evidence that vitamin D has only a weak influence on HBV/C.

In summary, published data give clear evidence for different molecular characteristics of the HBV genotypes and the detection efficiency for diagnostic testing systems (Peiffer et al., 2015; Hassemer et al., 2016). The HBV genotypes differ in their secretion of HBsAg and ratio of VPs and SVPs (Hassemer et al., 2016). The data illustrated in 3.4.2 reveal that vitamin D serves as a feasible tool for the further characterization of HBV genotypes, as not all genotypes show the same quantity in vitamin D induced reduction on the secretion of HBV. The tested genotypes are affected differently upon vitamin D treatment, and HBV/C is not affected at all.

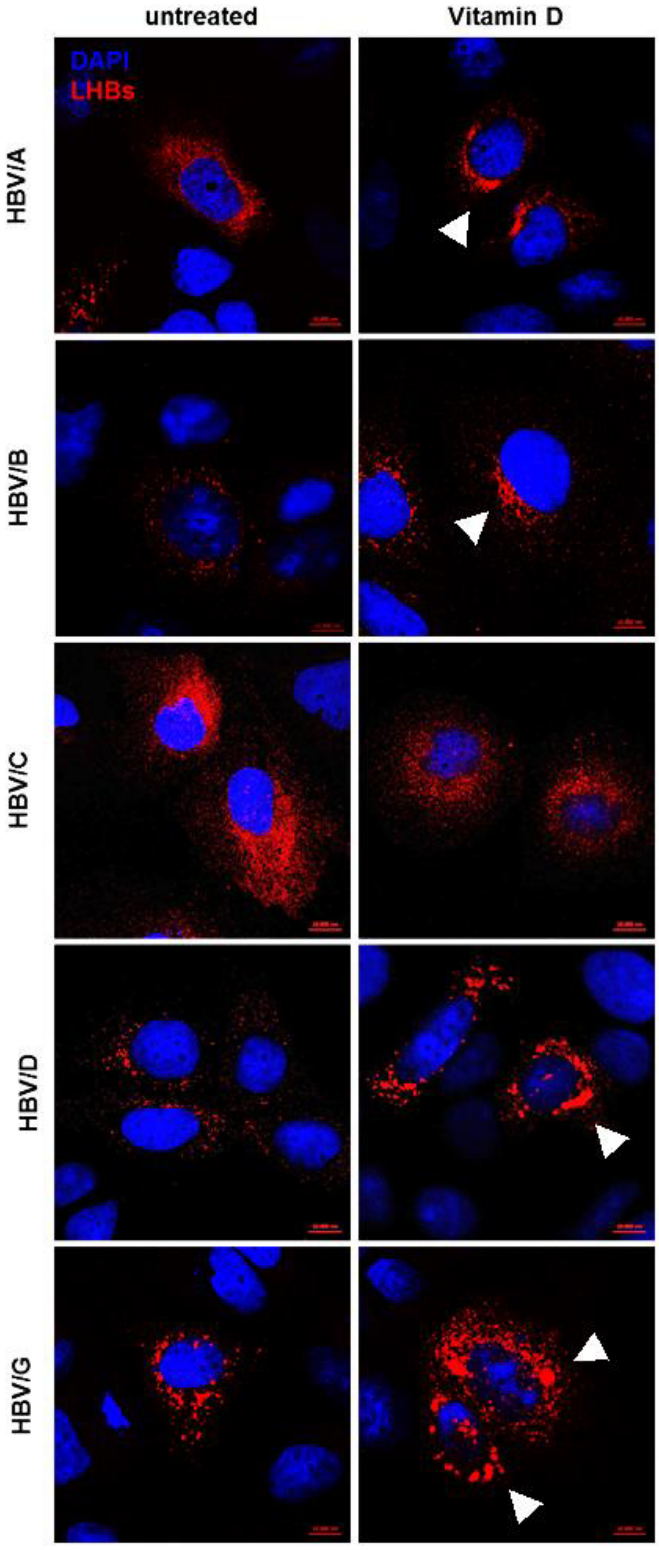

Figure 44: LHBs distribution in different genotypes after vitamin treatment.
Huh 7.5 cells were transiently transfected with pCEP-gtA-1.5, pCEP-gtB-1.5, pCEP-gtC-1.5, pJo19, pCEP-gtG-1.5 and treated with 10 nM vitamin D analog *#5*. The cells were stained with a LHBs-specific antibody (Ma18/7). Nuclei were visualized by DAPI staining. Pictures were taken by CLSM. Representative pictures are illustrated.

4. Discussion

In the following chapter, the obtained data will be discussed with regard to previously published studies.

4.1 Influence of vitamin D analogs on the HBV life cycle

Chronic HBV infection is characterized by the persistence of HBV in the liver for decades. Patients with chronic active hepatitis suffer from a severe disease and have a dire prognosis. In spite of the use of antivirals like nucleoside therapeutics (e.g. lamivudine, telbivudine, entecavire, adefovire or tenofovire) or IFN α, therapies cannot clear the infection all the time and may lead to a merely delayed progression of HCC. The lifelong clearance is rare and drug resistances are rising, which makes it important to further investigate molecular mechanisms of the infection and to search for new potential treatments (Lin and Kao, 2016; WHO, 2015).

In recent studies, it has been shown that low vitamin D serum levels in chronically infected patients are associated with high replication rates of HBV (Chen et al., 2015; Farnik et al., 2013; Mohamadkhani et al., 2015; Wong et al., 2015). This is in line with the analyses of gene variants of proteins involved in vitamin D metabolism. Polymorphisms of *VDR*, *CYP27B1,* and *DBP* genes have been observed in patients undergoing a chronic HBV infection (Huang et al., 2010; Peng et al., 2014; Yao et al., 2013; Zhu et al., 2012). This gives strong evidence for an involvement of vitamin D in the progression of HBV infection and chronicity. Hence, scientists of the Ziv Medical center in Israel are currently testing the beneficial effect of vitamin D supplementation to pegIFNα or telbivudine monotherapy in patients suffering from a chronic HBV infection in a clinical trial (ClinicalTrials.gov, 2010). Furthermore, researchers from Sun Yat-Sen University in Guangzhou, China designed a clinical trial to analyze whether vitamin D given orally can prevent HCC development in patients suffering from HBV (ClinicalTrials.gov, 2016). To this day, no data of these trials are available.

Besides, vitamin D is associated with other infectious diseases, and already in 1903, Niels Ryberg Finsen received the Nobel Prize for his findings of light therapy against TB (Moller et al., 2005). In viral infections, vitamin D might play a role in the course of diseases of HCV (Hepatitis C Virus), DENV (Dengue virus), EBV (Epstein-Barr virus), HIV (Human immunodeficiency virus), A/H1N1 and HBV as previously described (Alagarasu et al., 2012; Grant, 2010; Gutierrez et al., 2014; Nugmanova et al., 2015). Nevertheless, the

listed viruses differ completely in their structure and morphogenesis and no general mechanism of the influence of vitamin D on the virus life cycle is known so far. Thus, the aim of this project was to analyze the effect of vitamin D on the HBV life cycle.

HBV produces in addition to VPs, with 42 nM diameters in size, the so-called SVPs (filaments, and spheres), consisting of HBsAg (Bruns et al., 1998) only. The three types of particles differ in their release pathway (Lambert, Doring, and Prange, 2007; Patient et al., 2007). The spheres are built of approximately one hundred SHBs monomers, which are formed to dimers in the ER-lumen by the building of disulfide linkers due to the activity of the enzyme PDI (protein disulfide isomerase) (Huovila, Eder, and Fuller, 1992; Vyas, Rao, and Ibrahim, 1972). After their transport to the ERGIC, SHBs dimers form higher oligomers, assemble to spheres, and leave the cell via the Golgi by the constitutive secretory pathway (Patient, Hourioux, and Roingeard, 2009). On the contrary, VPs leave the cell MVB-dependently and hence need the recruitment of a network of cellular proteins involved in the budding. This network is the ESCRT-machinery composed of ESCRT-0, -I, -II -III -complexes that form the MVBs on the membrane of the late endosomes (Lambert, Doring, and Prange, 2007; Watanabe et al., 2007). The sorting is terminated by the ATPase Vps4, which leads to the disassembling of the ESCRT proteins from the membranes and results in the recycling of the ESCRT-machinery (Hill and Babst, 2012). By now, it has been described that ESCRT-II, -III and Vps4 complexes are required for the release of the HBV VPs (Hoffmann et al., 2013; Lambert, Doring, and Prange, 2007; Stieler and Prange, 2014). Moreover, the release mechanism of HBV filaments was identified in a recent study of our laboratory. HBV filaments leave the cell like VPs, due to MVBs and the recruitment of the ESCRT-machinery (Jiang, et al., 2015). Other enveloped viruses (e.g. HIV-1) use for their release the ESCRT-machinery as well (Chen and Lamb, 2008).

The presented data reveal that the vitamin D treatment significantly impairs the release of HBsAg for the tested vitamin D analogs (see 3.2.2). Strikingly, the effect on HBsAg secretion was only moderate for the natural form of the hormone calcitriol (*#1*) in low concentrations in contrast to the other tested analogs (see Figure 16 and Figure 17). This might be caused by analog selectivity and specificity of the molecular binding to VDR and the resulting formation of the heterodimer with RXR (Brown, 2001). Because SVPs are abundantly composed of SHBs, the HBsAg signal represents most dominantly this type of particles. However, due to an altered ratio of HBsAg in the SN (see Figure 20) and impaired amounts of HBcAg (see Figure 22) and viral DNA (see Figure 21), it is concluded that the release of SVPs and VPs is influenced upon vitamin D analogs. Data obtained from infection experiments confirmed the hypothesis observed in stably and transiently

HBV expressing hepatocytes (see Figure 18 and Figure 21). In PHHs, the effect on HBsAg was limited, whereas the reduction on the release of viral DNA was more pronounced (see Figure 21).

In order to clarify the mechanism of the effect, the intracellular amounts of viral proteins and transcripts were investigated. Vitamin D treatment leads to an impaired release of HBsAg, HBcAg, and viral genomes, whereas the synthesis of viral proteins is not eliminated in HBV expressing cells (see 3.2.5 and 3.2.6). An intracellular accumulation of HBV proteins, predominantly LHBs and HBcAg, the main components of VPs, has been observed (see Figure 24, Figure 25, and Figure 27). Furthermore, vitamin D had no influence on the ratio of the HBV transcripts. All in all, the effects of vitamin D on the HBV life cycle are only moderate. Newly clinical studies invalidate the observations of an association of viral replication and vitamin D deficiency. It is argued that the deficiency is only a consequence of liver dysfunction and lacking vitamin D metabolism (Yu et al., 2015; Zhao et al., 2016). Therefore, it is recommended to prove in further experiments the specificity of the observed effect of vitamin D on the HBV life cycle with a VDR-deficient cell line or a VDR antagonist.

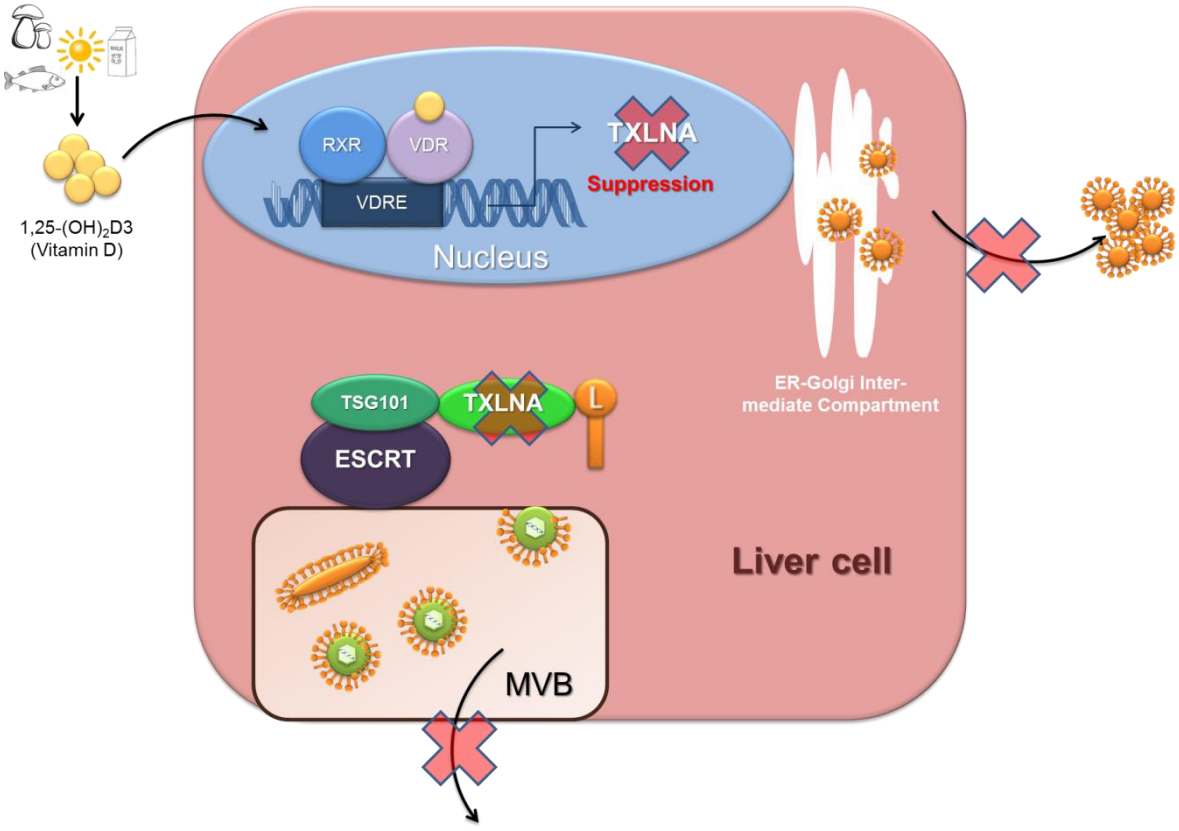

Figure 45: Illustration of potential mechanism of vitamin D influencing HBV life cycle.
Vitamin D leads to a suppression of *TXLNA*. Lacking TXLNA cannot act as an adaptor between TSG101 and LHBs (L), resulting in decreased amounts of MVB-mediated release of HBV. HBsAg particle release is decreased upon vitamin D treatment.

TXLNA is described as a binding partner of syntaxins, which belong to the SNARE-proteins and form complexes in vesicles of eukaryotic cells (Nogami et al., 2003). Recently, TXLNA was discovered as an adapter protein between on the one hand TSG101, a component of the ESCRT-machinery, and on the other the preS1-domain of LHBs (Hofmann et al., 2013). It enables the MVB-dependent release of HBV. Hitherto, the role of TXLNA for the release of filaments has not been described.

Moreover, TXLNA seems to play a crucial role in the life cycle of other viruses. The protein was identified as a novel factor controlling the release of HCV and is heavily deregulated in NS5A-transgenic mice (Elgner et al., 2016a; Kriegs et al., 2009). In the present study, it was demonstrated that the treatment of hepatocytes (HBV positive and negative) with vitamin D leads to a suppression of *TXLNA* transcription (see 3.3). Because HBV leads to an induction of the expression of *TXLNA* in HBV expressing cells, the effect was more prevalent in HBV negative cells. This leads to the hypothesis that the protein TXLNA might be the key molecule for the observed effects of an altered release of HBV. It is concluded that the effect of vitamin D on *TXLNA* is specific, as other components involved in viral life cycle such as TSG101 and AP1G1 are not affected by vitamin D treatment (see 3.3.4). Strikingly, the data on vitamin D-induced reduction of TXLNA are conflicting with previously observed results. It has been described that TXLNA silencing leads to an increase of HBsAg secretion (Hoffmann et al., 2013). This effect has not been observed for the vitamin D-induced repression of TXLNA (see 3.2.2). This is presenting evidence for a more complex mechanism of the suppression of TXLNA. The VDR has activating and suppressing functions by the recruitment of a variety of coregulatory complexes (Pike and Meyer, 2012). The analysis of potential VDR binding sites with ChIP-seq of the whole genome in lymphoblastoid cells, monocytes, colorectal cancer cells, and hepatic stellate cells presented no evidence for a binding site in the promotor region for TXLNA (Carlberg, 2014). However, the absence of a binding site in these cell lines does not exclude the possibility of its existence in others. It remains to be determined how exactly an intracellular decrease of *TXLNA* expression occurs in vitamin D-treated cells.

Taken together, calcitriol was identified, in addition to five vitamin D analogs, as potential inhibitor on the release of HBV. In spite of the strong evidence of *in vivo* data, the direct effects on the HBV life cycle are only modest. Nevertheless, the data might be relevant for

further clinical applications. It is hypothesized that the decreasing release of VPs might lead to a reduction of new infections of neighboring hepatocytes, but this has to be proven in further experiments. It is possible that − due to vitamin D treatment − the potential of clearance of infection by the immune system or in combination with a therapeutic vaccine with antibodies is strengthened. Conclusively, it has not been shown whether vitamin D might affect MHC class I presentation of HBV proteins and the recognition of immune cells. Further investigation is needed in this respect.

Ongoing clinical trials of vitamin D as potential drug for HBV substantiate the impact of vitamin D in HBV treatment. From a public health point, vitamin D usage is very convincing as it might be a cost-effective opportunity for areas with high prevalence of HBsAg and low financial resources for the health care sector. Notwithstanding potential side effects have to be discussed. Calcitriol treatment over a long time can induce hypercalcemia[2] and hyperphosphatemia[3] and associated diseases (Steddon, Schroeder, and Cunningham, 2001). Therefore, it makes sense to consider the vitamin D analogs for treatment to reduce these side effects, but keep the beneficial properties of treatment. In the presented study, the focus was on the vitamin D analogs oxacalcitriol (*#3*) and calcipotriol (*#5*). The treatment with these analogs resulted in the strongest effect on the release of HBsAg. Oxacalcitriol (*#3*) is modified by the replacement of an oxygen atom by carbon-22 on the side chain (see Table 30) (Steddon, Schroeder, and Cunningham, 2001). It suppresses PTH synthesis, leading to minimal effects on calcium homeostasis in contrast to calcitriol (Brown et al., 1989). Oxacalcitriol (*#3*) is available as a drug for the treatment of secondary hyperparathyroidism in Japan since 2000 and tested for direct injection into the parathyroid (Mizobuchi and Ogata, 2014). The other tested vitamin D derivate calcipotriol (*#5*) is characterized by rapid clearance and reduced occurrence of hypercalcemia (Knutson et al., 1997). However, calcipotriol can only be obtained as ointment in Germany (Daivonex®, Daivobet®), commonly used for treatment of Psoriasis[4] and therefore is currently not suitable for HBV treatment application (Leo-Pharma, 2016). Considering this, it seems to be a long way of clinical trials and licensing for potential use of vitamin D analogs, whereas vitamin D itself is already available on the market.

Vitamin D is famous for its involvement in the calcium homeostasis, which affects the cellular metabolism and neuromuscular functions (reviewed in Chung et al., 2009). The active transport of calcium is depending on vitamin D; thus, VDR leads to an activation of

[2] elevated Ca^{2+} levels in the blood
[3] elevated H_3PO_4 levels in the blood
[4] autoimmune diseases leading to abnormal skin

calcium transporting proteins in the epithelia cells and increase of the intestinal absorption. When the extracellular Ca^{2+} concentrations in the plasma are low, PTH is secreted. This leads to a bone demineralization by the export of Ca^{2+} and induces the conversion of cholecalciferol into calcitriol (reviewed in Chung et al., 2009) (see 1.2).
In addition to vitamin D, HBV activator proteins are also associated with Ca^{2+}. They lead to an increase of Ca^{2+} in the cytosol. HBx leads to increased intracellular calcium levels by targeting Bcl-2 (Bouchard et al., 2003; Bouchard, Wang, and Schneider, 2001; Geng et al., 2012a; Geng et al., 2012b; McClain et al., 2007; Yang and Bouchard, 2012). This finally leads to the activation of tyrosinkinases, such as Prk2 (prolin rich tyrosin kinase 2), FAK (focal adhesion kinase) and Src (sarcoma and cellular) -kinases, which induces the Ras-Raf-MEK-ERK signal cascade (Benn and Schneider, 1994; Bouchard et al., 2003). The cytosolic Ca^{2+} promotes the assembly of HBV core (Choi et al., 2005; Zhang et al., 2016) and preS2 leads to a Ca^{2+} release from the ER (Yen et al., 2016). Furthermore, HBV is predominantly replicating in resting cells. For resting within the G1-phase, the induction of HBx is crucial and depends on Ca^{2+} (Gearhart and Bouchard, 2010). Finally, it is also described, that TXLNA is involved in Ca^{2+}-dependent exocytose in neuroendocrine cells, and a potential link of vitamin D, HBV, TXLNA and Ca^{2+} cannot be excluded.

As mentioned above, the current clinical trials are dealing with the beneficial role of vitamin D on HBV chronicity. Vitamin D influences the expression of over 200 genes and hence, the influence of vitamin D on other cellular factors involved in the HBV chronicity might be an interesting research target (Smyk et al., 2013). For instance, vitamin D alters the activation of the insulin receptor (Maestro et al., 2000; Maestro et al., 2003), Nrf2 (reviewed in Berridge, 2015) and TXLNA (see 3.3) and further investigations should address the crosstalk of VDR in this context and the role of the anti-inflammatory capacity of the hormone for the formation of fibrosis, chronicity, and liver regeneration.

4.2 Comparative analysis of HBV genotypes

In total, eight HBV genotypes are known and designated as HBV/A to HBV/H (Glebe and Bremer 2013). Recently isolated viruses of patients from Asia suggest two additional strains, genotype I and J (Kim, Revill, and Ahn, 2011). The HBV genotypes differ by > 8% of their genome and are regionally distributed. They show different characteristics in clinical parameters and the progression of diseases (Tian and Jia, 2016). The carriers of distinct HBV genotypes have better clinical outcomes due to the better responses to antivirals and a lower risk of HCC development (see 1.1.5) (Kao, 2002).

Therefore, a comparative analysis of the HBV genotypes under standardized conditions is of great importance for a better understanding of the clinical appearance. For a long time, HBV/G infections were only detected as coinfections with other genotypes. Firstly, Chudy et al. described the existence of monoinfections of HBV/G (Chudy et al., 2006). Cell culture based analysis revealed that HBV/G is incompetent for the secretion of HBsAg particles and has a diminished activation of Nrf2 (Peiffer et al., 2015). Further analysis on the secretion of HBsAg is giving evidence for differences in the ratio of released SVPs and VPs in the HBV genotypes (see 3.4, and Hassemer et al., 2016). This provides important knowledge for assessing the limits in the detection with the available diagnostic kits (Hassemer et al. 2016). As HBV is diagnosed mostly by HBsAg/HBeAg, it is estimated that HBV/G, which has no secretion for HBeAg and only small amounts of HBsAg, is often failed to be diagnosed (Peiffer et al, 2015).

The presented work reveals that the vitamin D treatment is a feasible tool for the further analysis of the HBV genotypes (see 3.4.2). Experiments show that vitamin D treatment does not lead to an effective reduction of the HBV secretion in all HBV genotypes. It has been observed that the vitamin D treatment of HBV/A, B, and D results in a reduction of released HBsAg and viral DNA in transiently HBV expressing cells and PHHs (see Figure 41 and Figure 42). HBV/B showed the strongest effect. On the contrary, the effect is the absence in HBV/C. Hence, protein sequences of these HBV genotypes were compared in more detail (see Hassemer et al, 2016). Hofmann et al. published that for the binding of TXLNA and LHBs, the aa2–47 of preS1 are crucial (Hoffmann, 2013). The comparative analysis of the protein sequence of the HBV genotypes showed that in this region HBV/C has one amino acid variation. In position aa10, lysine is changed to glutamine, which is accompanied by a loading change. By now, there is no description available whether HBV genotypes leave the cell on different routes, but differences in amino acid sequences might lead to different binding affinities with proteins related to release pathways resulting in altered ratios of secreted VPs and SVPs (Hassemer et al., 2016).

Clinical observations revealed that patients infected with HBV/B had a higher prevalence of vitamin D deficiency than those infected with HBV/C (Yu et al., 2015). Other clinical studies, which observed an association of a vitamin D deficiency and high HBV replication rates, did not determine HBV genotypes.

The data emphasizes the relevance of further analyses of HBV genotypes for a better understanding of molecular interactions and an effective eradication of HBV.

In summary, for the investigation of the influence of vitamin D on the morphogenesis of HBV, six different vitamin D analogs were tested in stably and transiently HBV expressing

hepatoma cell lines and infected PHHs. All tested analogs lead to a reduction of secreted HBsAg. The strongest effects showed the substances oxacalcitriol (*#3*) and calcipotriol (*#5*). Selective analysis of the SN and cell lysates revealed that vitamin D leads to an altered ratio of LHBs/SHBs intra- and extracellularly. The extracellular amounts of HBcAg and viral DNA were diminished upon vitamin D treatment, and viral proteins accumulate intracellularly. The viral replication and the secretion of HBeAg was not affected due to vitamin D treatment and leads to the conclusion that the secretory pathway in general is not influenced and a specific effect was observed. Furthermore, it was investigated that vitamin D induces a repression of *TXLNA*, which gene product is crucial for the MVB-dependent release of VPs (Hoffmann et al., 2013).

Finally, it has been demonstrated that vitamin D treatment is a feasible tool for the further characterization of HBV genotypes. The genotypes are affected differently upon treatment with vitamin D, and HBV/C is not affected at all. Eventually, the thesis confirms the impact of the analysis of the influence of vitamin D on the HBV life cycle and the comparative analysis of HBV genotypes.

5. References

Adhikary, T., Kaddatz, K., Finkernagel, F., Schonbauer, A., Meissner, W., Scharfe, M., Jarek, M., Blocker, H., Muller-Brusselbach, S., and Muller, R. (2011). Genomewide analyses define different modes of transcriptional regulation by peroxisome proliferator-activated receptor-beta/delta (PPARbeta/delta). *PLoS One* 6(1), e16344.

Alagarasu, K., Honap, T., Mulay, A. P., Bachal, R. V., Shah, P. S., and Cecilia, D. (2012). Association of vitamin D receptor gene polymorphisms with clinical outcomes of dengue virus infection. *Hum Immunol* 73(11), 1194-9.

Aleksunes, L. M., and Manautou, J. E. (2007). Emerging role of Nrf2 in protecting against hepatic and gastrointestinal disease. *Toxicol Pathol* 35(4), 459-73.

Aranow, C. (2011). Vitamin D and the immune system. *J Investig Med* 59(6), 881-6.

Averhoff, F. (2016). Hepatitis B. *CDC Health Information for International Travel*, Chapter 3: Infectious Diseases Related to Travel.

Bardens, A., Doring, T., Stieler, J., and Prange, R. (2011). Alix regulates egress of hepatitis B virus naked capsid particles in an ESCRT-independent manner. *Cell Microbiol* 13(4), 602-19.

Bartenschlager, R., Junker-Niepmann, M., and Schaller, H. (1990). The P gene product of hepatitis B virus is required as a structural component for genomic RNA encapsidation. *J Virol* 64(11), 5324-32.

Bartenschlager, R., and Schaller, H. (1988). The amino-terminal domain of the hepadnaviral P-gene encodes the terminal protein (genome-linked protein) believed to prime reverse transcription. *EMBO J* 7(13), 4185-92.

Basaras, M., Arrese, E., Blanco, S., Sota, M., de las Heras, B., and Cisterna, R. (2007). Characterization of hepatitis B virus genotypes in chronically infected patients. *Rev Esp Quimioter* 20(4), 442-5.

Beck, J., and Nassal, M. (2007). Hepatitis B virus replication. *World J Gastroenterol* 13(1), 48-64.

Benn, J., and Schneider, R. J. (1994). Hepatitis B virus HBx protein activates Ras-GTP complex formation and establishes a Ras, Raf, MAP kinase signaling cascade. *Proc Natl Acad Sci U S A* 91(22), 10350-4.

Berridge, M. J. (2015). Vitamin D cell signalling in health and disease. *Biochem Biophys Res Commun* 460(1), 53-71.

Biosciences, B. (2016). BD FACSCanto II.

Birnboim, H. C., and Doly, J. (1979). A rapid alkaline extraction procedure for screening recombinant plasmid DNA. *Nucleic Acids Res* 7(6), 1513-23.

Blight, K. J., McKeating, J. A., and Rice, C. M. (2002). Highly permissive cell lines for subgenomic and genomic hepatitis C virus RNA replication. *J Virol* 76(24), 13001-14.

Block, T. M., Guo, H., and Guo, J. T. (2007). Molecular virology of hepatitis B virus for clinicians. *Clin Liver Dis* 11(4), 685-706, vii.

Blumberg, B. S., Alter, H. J., and Visnich, S. (1965). A "New" Antigen in Leukemia Sera. *JAMA* 191, 541-6.

Bobilev, I., Novik, V., Levi, I., Shpilberg, O., Levy, J., Sharoni, Y., Studzinski, G. P., and Danilenko, M. (2011). The Nrf2 transcription factor is a positive regulator of myeloid differentiation of acute myeloid leukemia cells. *Cancer Biol Ther* 11(3), 317-29.

Bock, C. T., Schwinn, S., Locarnini, S., Fyfe, J., Manns, M. P., Trautwein, C., and Zentgraf, H. (2001). Structural organization of the hepatitis B virus minichromosome. *J Mol Biol* 307(1), 183-96.

Bouchard, M. J., Puro, R. J., Wang, L., and Schneider, R. J. (2003). Activation and inhibition of cellular calcium and tyrosine kinase signaling pathways identify targets of the HBx protein involved in hepatitis B virus replication. *J Virol* 77(14), 7713-9.

Bouchard, M. J., Wang, L. H., and Schneider, R. J. (2001). Calcium signaling by HBx protein in hepatitis B virus DNA replication. *Science* 294(5550), 2376-8.

Bradford, M. M. (1976). A rapid and sensitive method for the quantitation of microgram quantities of protein utilizing the principle of protein-dye binding. *Anal Biochem* 72, 248-54.

Brandenburg, B., Stockl, L., Gutzeit, C., Roos, M., Lupberger, J., Schwartlander, R., Gelderblom, H., Sauer, I. M., Hofschneider, P. H., and Hildt, E. (2005). A novel system for efficient gene transfer into primary human hepatocytes via cell-permeable hepatitis B virus-like particle. *Hepatology* 42(6), 1300-9.

Brown, A. J. (2001). Therapeutic uses of vitamin D analogues. *Am J Kidney Dis* 38(5 Suppl 5), S3-S19.

Brown, A. J., Ritter, C. R., Finch, J. L., Morrissey, J., Martin, K. J., Murayama, E., Nishii, Y., and Slatopolsky, E. (1989). The noncalcemic analogue of vitamin D, 22-oxacalcitriol, suppresses parathyroid hormone synthesis and secretion. *J Clin Invest* 84(3), 728-32.

Bruns, M., Miska, S., Chassot, S., and Will, H. (1998). Enhancement of hepatitis B virus infection by noninfectious subviral particles. *J Virol* 72(2), 1462-8.

Bruss, V., Lu, X., Thomssen, R., and Gerlich, W. H. (1994). Post-translational alterations in transmembrane topology of the hepatitis B virus large envelope protein. *EMBO J* 13(10), 2273-9.

Burnette, W. N. (1981). "Western blotting": electrophoretic transfer of proteins from sodium dodecyl sulfate--polyacrylamide gels to unmodified nitrocellulose and radiographic detection with antibody and radioiodinated protein A. *Anal Biochem* 112(2), 195-203.

Carlberg, C. (2014). Genome-wide (over)view on the actions of vitamin D. *Front Physiol* 5, 167.

CDC (2015). Viral Hepatitis - Hepatitis B Information, http://www.cdc.gov/hepatitis/hbv/

Chai, N., Chang, H. E., Nicolas, E., Han, Z., Jarnik, M., and Taylor, J. (2008). Properties of subviral particles of hepatitis B virus. *J Virol* 82(16), 7812-7.

Chan, H. L., Wong, M. L., Hui, A. Y., Hung, L. C., Chan, F. K., and Sung, J. J. (2003). Hepatitis B virus genotype C takes a more aggressive disease course than hepatitis B virus genotype B in hepatitis B e antigen-positive patients. *J Clin Microbiol* 41(3), 1277-9.

Chang, J. J., and Lewin, S. R. (2007). Immunopathogenesis of hepatitis B virus infection. *Immunol Cell Biol* 85(1), 16-23.

Chen, B. J., and Lamb, R. A. (2008). Mechanisms for enveloped virus budding: can some viruses do without an ESCRT? *Virology* 372(2), 221-32.

Chen, E. Q., Bai, L., Zhou, T. Y., Fe, M., Zhang, D. M., and Tang, H. (2015). Sustained suppression of viral replication in improving vitamin D serum concentrations in patients with chronic hepatitis B. *Sci Rep* 5, 15441.

Chisari, F. V. (2000). Rous-Whipple Award Lecture. Viruses, immunity, and cancer: lessons from hepatitis B. *Am J Pathol* 156(4), 1117-32.

Chisari, F. V., Isogawa, M., and Wieland, S. F. (2010). Pathogenesis of hepatitis B virus infection. *Pathol Biol (Paris)* 58(4), 258-66.

Choi, Y., Gyoo Park, S., Yoo, J. H., and Jung, G. (2005). Calcium ions affect the hepatitis B virus core assembly. *Virology* 332(1), 454-63.

Chou, S. F., Tsai, M. L., Huang, J. Y., Chang, Y. S., and Shih, C. (2015). The Dual Role of an ESCRT-0 Component HGS in HBV Transcription and Naked Capsid Secretion. *PLoS Pathog* 11(10), e1005123.

Chudy, M., Hanschmann, K. M., Kress, J., Nick, S., Campos, R., Wend, U., Gerlich, W., and Nubling, C. M. (2012). First WHO International Reference Panel containing hepatitis B virus genotypes A-G for assays of the viral DNA. *J Clin Virol* 55(4), 303-9.

Chudy, M., Schmidt, M., Czudai, V., Scheiblauer, H., Nick, S., Mosebach, M., Hourfar, M. K., Seifried, E., Roth, W. K., Grunelt, E., and Nubling, C. M. (2006). Hepatitis B virus genotype G monoinfection and its transmission by blood components. *Hepatology* 44(1), 99-107.

Chung, M., Balk, E. M., Brendel, M., Ip, S., Lau, J., Lee, J., Lichtenstein, A., Patel, K., Raman, G., Tatsioni, A., Terasawa, T., and Trikalinos, T. A. (2009). Vitamin D and calcium: a systematic review of health outcomes. *Evid Rep Technol Assess (Full Rep)*(183), 1-420.

ClinicalTrials.gov (2010). The Beneficial Effect of Vitamin D Supplement to Peg Interferon Alpha 2a or to Telbivudine Monotherapy in Patients With Chronic Hepatitis B Virus (HBV) Infection. *U.S. National Institutes of Health* NCT01083251.

ClinicalTrials.gov (2016). Oral Vitamin D Treatment for the Prevention of Hepatocellular Carcinoma (VDHCC). *NCT02779465*.

Colgrove, R., Simon, G., and Ganem, D. (1989). Transcriptional activation of homologous and heterologous genes by the hepatitis B virus X gene product in cells permissive for viral replication. *J Virol* 63(9), 4019-26.

Cooksley, G. (2003). The treatment of hepatitis B e antigen-positive chronic hepatitis B with pegylated interferon. *J Hepatol* 39 Suppl 1, S143-5.

Croagh, C. M., Desmond, P. V., and Bell, S. J. (2015). Genotypes and viral variants in chronic hepatitis B: A review of epidemiology and clinical relevance. *World J Hepatol* 7(3), 289-303.

Dal Molin, G., Poli, A., Croce, L. S., D'Agaro, P., Biagi, C., Comar, M., Tiribelli, C., and Campello, C. (2006). Hepatitis B virus genotypes, core promoter variants, and precore stop codon variants in patients infected chronically in North-Eastern Italy. *J Med Virol* 78(6), 734-40.

Dane, D. S., Cameron, C. H., and Briggs, M. (1970). Virus-like particles in serum of patients with Australia-antigen-associated hepatitis. *Lancet* 1(7649), 695-8.

Datta, R. K., and Datta, B. (1977). Nobel Prize winners in medicine (1976). *J Indian Med Assoc* 68(10), 216-8.

Defresne, F., and Sokal, E. (2016). Chronic hepatitis B in children: therapeutic challenges and perspectives. *J Gastroenterol Hepatol*.

Deterding, K., Constantinescu, I., Nedelcu, F. D., Gervain, J., Nemecek, V., Srtunecky, O., Vince, A., Grgurevic, I., Bielawski, K. P., Zalewska, M., Bock, T., Ambrozaitis, A., Stanczak, J., Takacs, M., Chulanov, V., Slusarczyk, J., Drazd'akova, M., Wiegand, J., Cornberg, M., Manns, M. P., and Wedemeyer, H. (2008). Prevalence of HBV genotypes in Central and Eastern Europe. *J Med Virol* 80(10), 1707-11.

DGE, D. G. f. E. (2012). Neue Referenzwerte für Vitamin D. *Presseinformation*.

Di Rosa, M., Malaguarnera, M., Nicoletti, F., and Malaguarnera, L. (2011). Vitamin D3: a helpful immuno-modulator. *Immunology* 134(2), 123-39.

Dickie, L. J., Church, L. D., Coulthard, L. R., Mathews, R. J., Emery, P., and McDermott, M. F. (2010). Vitamin D3 down-regulates intracellular Toll-like receptor 9 expression and Toll-like receptor 9-induced IL-6 production in human monocytes. *Rheumatology (Oxford)* 49(8), 1466-71.

Ding, X., Mizokami, M., Yao, G., Xu, B., Orito, E., Ueda, R., and Nakanishi, M. (2001). Hepatitis B virus genotype distribution among chronic hepatitis B virus carriers in Shanghai, China. *Intervirology* 44(1), 43-7.

Doss, M., White, M. R., Tecle, T., and Hartshorn, K. L. (2010). Human defensins and LL-37 in mucosal immunity. *J Leukoc Biol* 87(1), 79-92.

Drexler, J. F., Geipel, A., König, A., Corman, V. M., van Riel, D., Leijten, L. M., Bremer, C. M., Rasche, A., Cottontail, V. M., Maganga, G. D., Schlegel, M., Muller, M. A., Adam, A., Klose, S. M., Carneiro, A. J., Stocker, A., Franke, C. R., Gloza-Rausch, F., Geyer, J., Annan, A., Adu-Sarkodie, Y., Oppong, S., Binger, T., Vallo, P., Tschapka, M., Ulrich, R. G., Gerlich, W. H., Leroy, E., Kuiken, T., Glebe, D., and Drosten, C. (2013). Bats carry pathogenic hepadnaviruses antigenically related to hepatitis B virus and capable of infecting human hepatocytes. *Proc Natl Acad Sci U S A* 110(40), 16151-6.

Eble, B. E., MacRae, D. R., Lingappa, V. R., and Ganem, D. (1987). Multiple topogenic sequences determine the transmembrane orientation of the hepatitis B surface antigen. *Mol Cell Biol* 7(10), 3591-601.

Edfeldt, K., Liu, P. T., Chun, R., Fabri, M., Schenk, M., Wheelwright, M., Keegan, C., Krutzik, S. R., Adams, J. S., Hewison, M., and Modlin, R. L. (2010). T-cell cytokines differentially control human monocyte antimicrobial responses by regulating vitamin D metabolism. *Proc Natl Acad Sci U S A* 107(52), 22593-8.

Elgner, F., Donnerhak, C., Ren, H., Medvedev, R., Schreiber, A., Weber, L., Heilmann, M., Ploen, D., Himmelsbach, K., Finkernagel, M., Klingel, K., and Hildt, E. (2016a). Characterization of alpha-taxilin as a novel factor controlling the release of hepatitis C virus. *Biochem J* 473(2), 145-55.

Elgner, F., Medvedev, R., Ren, H., Himmelsbach, K., Hildt, E., and (2016b). The intra-cellular cholesterol transport inhibitor U18666A blocks the release of HCV particles. *Manuscript*.

Farnik, H., Bojunga, J., Berger, A., Allwinn, R., Waidmann, O., Kronenberger, B., Keppler, O. T., Zeuzem, S., Sarrazin, C., and Lange, C. M. (2013). Low vitamin D serum concentration is associated with high levels of hepatitis B virus replication in chronically infected patients. *Hepatology* 58(4), 1270-6.

Finkernagel, M. (2012). Diplomarbeit „Einfluss des *Sheddings* von CD99 durch die Metalloprotease Meprin beta bei der Diapedese“Johannes Gutenberg-University, Mainz.

Fitch, N., Becker, A. B., and HayGlass, K. T. (2016). Vitamin D [1,25(OH)2D3] Differentially Regulates Human Innate Cytokine Responses to Bacterial versus Viral Pattern Recognition Receptor Stimuli. *J Immunol* 196(7), 2965-72.

Gannon, J. C. (2000). The Global Infectious Disease Threat and Its Implications for the United States.

Garcia, P. D., Ou, J. H., Rutter, W. J., and Walter, P. (1988). Targeting of the hepatitis B virus precore protein to the endoplasmic reticulum membrane: after signal peptide cleavage translocation can be aborted and the product released into the cytoplasm. *J Cell Biol* 106(4), 1093-104.

Gearhart, T. L., and Bouchard, M. J. (2010). Replication of the hepatitis B virus requires a calcium-dependent HBx-induced G1 phase arrest of hepatocytes. *Virology* 407(1), 14-25.

Geng, X., Harry, B. L., Zhou, Q., Skeen-Gaar, R. R., Ge, X., Lee, E. S., Mitani, S., and Xue, D. (2012a). Hepatitis B virus X protein targets the Bcl-2 protein CED-9 to induce intracellular Ca2+ increase and cell death in Caenorhabditis elegans. *Proc Natl Acad Sci U S A* 109(45), 18465-70.

Geng, X., Huang, C., Qin, Y., McCombs, J. E., Yuan, Q., Harry, B. L., Palmer, A. E., Xia, N. S., and Xue, D. (2012b). Hepatitis B virus X protein targets Bcl-2 proteins to increase intracellular calcium, required for virus replication and cell death induction. *Proc Natl Acad Sci U S A* 109(45), 18471-6.

Gerlich, W. H. (2013). Medical virology of hepatitis B: how it began and where we are now. *Virol J* 10, 239.

Gerlich, W. H., Bremer, C., Saniewski, M., Schuttler, C. G., Wend, U. C., Willems, W. R., and Glebe, D. (2010). Occult hepatitis B virus infection: detection and significance. *Dig Dis* 28(1), 116-25.

Glebe, D., and König, A. (2014). Molecular virology of hepatitis B virus and targets for antiviral intervention. *Intervirology* 57(3-4), 134-40.

Grant, W. B. (2010). Latitude and multiple sclerosis prevalence: vitamin D reduces risk of Epstein-Barr virus infection. *Mult Scler* 16(3), 373; author reply 374-5.

Gripon, P., Rumin, S., Urban, S., Le Seyec, J., Glaise, D., Cannie, I., Guyomard, C., Lucas, J., Trepo, C., and Guguen-Guillouzo, C. (2002). Infection of a human hepatoma cell line by hepatitis B virus. *Proc Natl Acad Sci U S A* 99(24), 15655-60.

Guidotti, L. G., Ishikawa, T., Hobbs, M. V., Matzke, B., Schreiber, R., and Chisari, F. V. (1996). Intracellular inactivation of the hepatitis B virus by cytotoxic T lymphocytes. *Immunity* 4(1), 25-36.

Guidotti, L. G., Rochford, R., Chung, J., Shapiro, M., Purcell, R., and Chisari, F. V. (1999). Viral clearance without destruction of infected cells during acute HBV infection. *Science* 284(5415), 825-9.

Gutierrez, J. A., Jones, K. A., Flores, R., Singhania, A., Woelk, C. H., Schooley, R. T., and Wyles, D. L. (2014). Vitamin D Metabolites Inhibit Hepatitis C Virus and Modulate Cellular Gene Expression. *J Virol Antivir Res* 3(3).

Hadziyannis, S. J. (2011). Natural history of chronic hepatitis B in Euro-Mediterranean and African countries. *J Hepatol* 55(1), 183-91.

Halegoua-De Marzio, D., and Hann, H. W. (2014). Then and now: the progress in hepatitis B treatment over the past 20 years. *World J Gastroenterol* 20(2), 401-13.

Hannoun, C., Norder, H., and Lindh, M. (2000). An aberrant genotype revealed in recombinant hepatitis B virus strains from Vietnam. *J Gen Virol* 81(Pt 9), 2267-72.

Hartmann-Stuhler, C., and Prange, R. (2001). Hepatitis B virus large envelope protein interacts with gamma2-adaptin, a clathrin adaptor-related protein. *J Virol* 75(11), 5343-51.

Hasegawa, I., Tanaka, Y., Kurbanov, F., Yoshihara, N., El-Gohary, A., Lyamuya, E., Matee, M., Magessa, P., Fujiwara, K., Ozasa, A., Sugauchi, F., Orito, E., Ueda, R., and Mizokami, M. (2006). Molecular epidemiology of hepatitis B virus in the United Republic of Tanzania. *J Med Virol* 78(8), 1035-42.

Hassemer, M., Finkernagel M., Peiffer KH., Glebe D., Akhras S., Reuter A., Scheiblauer H., Sommer L., Chudy M., Nübling M., Hildt H., (2016). Comparative characterization of HBsAg derived from different HBV genotypes, manuscript

He, B., Fan, Q., Yang, F., Hu, T., Qiu, W., Feng, Y., Li, Z., Li, Y., Zhang, F., Guo, H., Zou, X., and Tu, C. (2013). Hepatitis virus in long-fingered bats, Myanmar. *Emerg Infect Dis* 19(4), 638-40.

Heermann, K. H., Goldmann, U., Schwartz, W., Seyffarth, T., Baumgarten, H., and Gerlich, W. H. (1984). Large surface proteins of hepatitis B virus containing the pre-s sequence. *J Virol* 52(2), 396-402.

Hewison, M. (2012). An update on vitamin D and human immunity. *Clin Endocrinol (Oxf)* 76(3), 315-25.

Hildt, E., Munz, B., Saher, G., Reifenberg, K., and Hofschneider, P. H. (2002). The PreS2 activator MHBs(t) of hepatitis B virus activates c-raf-1/Erk2 signaling in transgenic mice. *EMBO J* 21(4), 525-35.

Hill, C. P., and Babst, M. (2012). Structure and function of the membrane deformation AAA ATPase Vps4. *Biochim Biophys Acta* 1823(1), 172-81.

Hoffmann-La Roche AG, F. (2016). https://www.roche.de/pharma/indikation/hepatitis/hepatitis_b/images/1000_2_6_1_folgeschaeden.jpg

Hoffmann, J. (2013). Dissertation: "Charakterisierung der Rolle von α-Taxilin [Alpha-Taxilin] für den Zelleintritt und die Morphogenese von Hepatitis B".

Hoffmann, J., Boehm, C., Himmelsbach, K., Donnerhak, C., Roettger, H., Weiss, T. S., Ploen, D., and Hildt, E. (2013). Identification of alpha-taxilin as an essential factor for the life cycle of hepatitis B virus. *J Hepatol*.

Huang, H. C., Chen, C. C., Chang, W. C., Tao, M. H., and Huang, C. (2012). Entry of hepatitis B virus into immortalized human primary hepatocytes by clathrin-dependent endocytosis. *J Virol* 86(17), 9443-53.

Huang, Y. W., Liao, Y. T., Chen, W., Chen, C. L., Hu, J. T., Liu, C. J., Lai, M. Y., Chen, P. J., Chen, D. S., Yang, S. S., and Kao, J. H. (2010). Vitamin D receptor gene polymorphisms and distinct clinical phenotypes of hepatitis B carriers in Taiwan. *Genes Immun* 11(1), 87-93.

Huovila, A. P., Eder, A. M., and Fuller, S. D. (1992). Hepatitis B surface antigen assembles in a post-ER, pre-Golgi compartment. *J Cell Biol* 118(6), 1305-20.

Huy, T. T., Ishikawa, K., Ampofo, W., Izumi, T., Nakajima, A., Ansah, J., Tetteh, J. O., Nii-Trebi, N., Aidoo, S., Ofori-Adjei, D., Sata, T., Ushijima, H., and Abe, K. (2006). Characteristics of hepatitis B virus in Ghana: full length genome sequences indicate the endemicity of genotype E in West Africa. *J Med Virol* 78(2), 178-84.

Itoh, K., Chiba, T., Takahashi, S., Ishii, T., Igarashi, K., Katoh, Y., Oyake, T., Hayashi, N., Satoh, K., Hatayama, I., Yamamoto, M., and Nabeshima, Y. (1997). An Nrf2/small Maf heterodimer mediates the induction of phase II detoxifying enzyme genes through antioxidant response elements. *Biochem Biophys Res Commun* 236(2), 313-22.

Janssen, H. L., van Zonneveld, M., Senturk, H., Zeuzem, S., Akarca, U. S., Cakaloglu, Y., Simon, C., So, T. M., Gerken, G., de Man, R. A., Niesters, H. G., Zondervan, P., Hansen, B., and Schalm, S. W. (2005). Pegylated interferon alfa-2b alone or in combination with lamivudine for HBeAg-positive chronic hepatitis B: a randomised trial. *Lancet* 365(9454), 123-9.

Jeffery, L. E., Burke, F., Mura, M., Zheng, Y., Qureshi, O. S., Hewison, M., Walker, L. S., Lammas, D. A., Raza, K., and Sansom, D. M. (2009). 1,25-Dihydroxyvitamin D3 and IL-2 combine to inhibit T cell production of inflammatory cytokines and promote development of regulatory T cells expressing CTLA-4 and FoxP3. *J Immunol* 183(9), 5458-67.

Jiang, B., Himmelsbach, K., Ren, H., Boller, K., and Hildt, E. (2015). Subviral Hepatitis B Virus Filaments, like Infectious Viral Particles, Are Released via Multivesicular Bodies. *J Virol* 90(7), 3330-41.

Kao, J. H. (2002). Hepatitis B viral genotypes: clinical relevance and molecular characteristics. *J Gastroenterol Hepatol* 17(6), 643-50.

Kao, J. H., Chen, P. J., Lai, M. Y., and Chen, D. S. (2000). Hepatitis B genotypes correlate with clinical outcomes in patients with chronic hepatitis B. *Gastroenterology* 118(3), 554-9.

Kao, J. H., Chen, P. J., Lai, M. Y., and Chen, D. S. (2002). Genotypes and clinical phenotypes of hepatitis B virus in patients with chronic hepatitis B virus infection. *J Clin Microbiol* 40(4), 1207-9.

Kato, H., Orito, E., Gish, R. G., Sugauchi, F., Suzuki, S., Ueda, R., Miyakawa, Y., and Mizokami, M. (2002). Characteristics of hepatitis B virus isolates of genotype G and their phylogenetic differences from the other six genotypes (A through F). *J Virol* 76(12), 6131-7.

Kim, B. K., Revill, P. A., and Ahn, S. H. (2011). HBV genotypes: relevance to natural history, pathogenesis and treatment of chronic hepatitis B. *Antivir Ther* 16(8), 1169-86.

Kimbi, G. C., Kramvis, A., and Kew, M. C. (2004). Distinctive sequence characteristics of subgenotype A1 isolates of hepatitis B virus from South Africa. *J Gen Virol* 85(Pt 5), 1211-20.

Kitson, M. T., and Roberts, S. K. (2012). D-livering the message: the importance of vitamin D status in chronic liver disease. *J Hepatol* 57(4), 897-909.

Kneser, J., and Wedemeyer, H. (2005). Die Bedeutung der HBV-Genotypen bei chronischer HBV- und HBV/HIV-Infektion. *Kompetenznetz Hepatitis, c/o Medizinische Hochschule Hannover, Abt. f. Gaastroenterologie, Hepatologie und Endokrinologie*.

Knowles, B. B., Howe, C. C., and Aden, D. P. (1980). Human hepatocellular carcinoma cell lines secrete the major plasma proteins and hepatitis B surface antigen. *Science* 209(4455), 497-9.

Knutson, J. C., LeVan, L. W., Valliere, C. R., and Bishop, C. W. (1997). Pharmacokinetics and systemic effect on calcium homeostasis of 1 alpha,24-dihydroxyvitamin D2 in rats. Comparison with 1 alpha,25-dihydroxyvitamin D2, calcitriol, and calcipotriol. *Biochem Pharmacol* 53(6), 829-37.

Kohler, U. A., Kurinna, S., Schwitter, D., Marti, A., Schafer, M., Hellerbrand, C., Speicher, T., and Werner, S. (2014). Activated Nrf2 impairs liver regeneration in mice by activation of genes involved in cell-cycle control and apoptosis. *Hepatology* 60(2), 670-8.

Königer, C., Wingert, I., Marsmann, M., Rosler, C., Beck, J., and Nassal, M. (2014). Involvement of the host DNA-repair enzyme TDP2 in formation of the covalently closed circular DNA persistence reservoir of hepatitis B viruses. *Proc Natl Acad Sci U S A* 111(40), E4244-53.

Kriegs, M., Burckstummer, T., Himmelsbach, K., Bruns, M., Frelin, L., Ahlen, G., Sallberg, M., and Hildt, E. (2009). The hepatitis C virus non-structural NS5A protein impairs both the innate and adaptive hepatic immune response in vivo. *J Biol Chem* 284(41), 28343-51.

Kumar, R., Perez-Del-Pulgar, S., Testoni, B., Lebosse, F., and Zoulim, F. (2016). Clinical relevance of the study of hepatitis B virus covalently closed circular DNA. *Liver Int* 36 Suppl 1, 72-7.

Kyhse-Andersen, J. (1984). Electroblotting of multiple gels: a simple apparatus without buffer tank for rapid transfer of proteins from polyacrylamide to nitrocellulose. *Journal of biochemical and biophysical methods* 10(3-4), 203-9.

Ladero, J. M., Torrejon, M. J., Sanchez-Pobre, P., Suarez, A., Cuenca, F., de la Orden, V., Devesa, M. J., Rodrigo, M., Estrada, V., Lopez-Alonso, G., and Agundez, J. A. (2013). Vitamin D deficiency and vitamin D therapy in chronic hepatitis C. *Ann Hepatol* 12(2), 199-204.

Ladner, S. K., Otto, M. J., Barker, C. S., Zaifert, K., Wang, G. H., Guo, J. T., Seeger, C., and King, R. W. (1997). Inducible expression of human hepatitis B virus (HBV) in stably transfected hepatoblastoma cells: a novel system for screening potential inhibitors of HBV replication. *Antimicrob Agents Chemother* 41(8), 1715-20.

Lambert, C., Doring, T., and Prange, R. (2007). Hepatitis B virus maturation is sensitive to functional inhibition of ESCRT-III, Vps4, and gamma 2-adaptin. *J Virol* 81(17), 9050-60.

Lambert, S. W., Beer, E., Cannon, A. B., Osgood, A. T., Parsons, W. B., Samuels, B., Wright, A. M., Aranow, H., Kessel, L., Hartwell, J. A., and Williams, L. R. (1931). Extract from Report of Committee on Professional Standards. *Bull N Y Acad Med* 7(1), 50-2.

Leo-Pharma (2016). http://www.leo-pharma.de, Neu-Isenburg.

Levrero, M., and Zucman-Rossi, J. (2016). Mechanisms of HBV-induced hepatocellular carcinoma. *J Hepatol* 64(1 Suppl), S84-S101.

Liang, T. J. (2009). Hepatitis B: the virus and disease. *Hepatology* 49(5 Suppl), S13-21.

Lin, C. L., and Kao, J. H. (2016). Review article: novel therapies for hepatitis B virus cure - advances and perspectives. *Aliment Pharmacol Ther*.

Lin, R., Nagai, Y., Sladek, R., Bastien, Y., Ho, J., Petrecca, K., Sotiropoulou, G., Diamandis, E. P., Hudson, T. J., and White, J. H. (2002). Expression profiling in squamous carcinoma cells reveals pleiotropic effects of vitamin D3 analog EB1089 signaling on cell proliferation, differentiation, and immune system regulation. *Mol Endocrinol* 16(6), 1243-56.

Lindh, M., Hannoun, C., Dhillon, A. P., Norkrans, G., and Horal, P. (1999). Core promoter mutations and genotypes in relation to viral replication and liver damage in East Asian hepatitis B virus carriers. *J Infect Dis* 179(4), 775-82.

Lindh, M., Horal, P., Dhillon, A. P., and Norkrans, G. (2000). Hepatitis B virus DNA levels, precore mutations, genotypes and histological activity in chronic hepatitis B. *J Viral Hepat* 7(4), 258-67.

Littlejohn, M., Locarnini, S., and Yuen, L. (2016). Origins and Evolution of Hepatitis B Virus and Hepatitis D Virus. *Cold Spring Harb Perspect Med* 6(1).

Liu, C. J., and Kao, J. H. (2013). Global perspective on the natural history of chronic hepatitis B: role of hepatitis B virus genotypes A to J. *Semin Liver Dis* 33(2), 97-102.

Livak, K. J., and Schmittgen, T. D. (2001). Analysis of relative gene expression data using real-time quantitative PCR and the 2(-Delta Delta C(T)) Method. *Methods* 25(4), 402-8.

Lozano, R., Naghavi, M., Foreman, K., Lim, S., Shibuya, K., Aboyans, V., Abraham, J., Adair, T., Aggarwal, R., Ahn, S. Y., Alvarado, M., Anderson, H. R., Anderson, L. M., Andrews, K. G., Atkinson, C., Baddour, L. M., Barker-Collo, S., Bartels, D. H., Bell, M. L., Benjamin, E. J., Bennett, D., Bhalla, K., Bikbov, B., Bin Abdulhak, A., Birbeck, G., Blyth, F., Bolliger, I., Boufous, S., Bucello, C., Burch, M., Burney, P., Carapetis, J., Chen, H., Chou, D., Chugh, S. S., Coffeng, L. E., Colan, S. D., Colquhoun, S., Colson, K. E., Condon, J., Connor, M. D., Cooper, L. T., Corriere, M., Cortinovis, M., de Vaccaro, K. C., Couser, W., Cowie, B. C., Criqui, M. H., Cross, M., Dabhadkar, K. C., Dahodwala, N., De Leo, D., Degenhardt, L., Delossantos, A., Denenberg, J., Des Jarlais, D. C., Dharmaratne, S. D., Dorsey, E. R., Driscoll, T., Duber, H., Ebel, B., Erwin, P. J., Espindola, P., Ezzati, M., Feigin, V., Flaxman, A. D., Forouzanfar, M. H., Fowkes, F. G., Franklin, R., Fransen, M., Freeman, M. K., Gabriel, S. E., Gakidou, E., Gaspari, F., Gillum, R. F., Gonzalez-Medina, D., Halasa, Y. A., Haring, D., Harrison, J. E., Havmoeller, R., Hay, R. J., Hoen, B., Hotez, P. J., Hoy, D., Jacobsen, K. H., James, S. L., Jasrasaria, R., Jayaraman, S., Johns, N., Karthikeyan, G., Kassebaum, N., Keren, A., Khoo, J. P., Knowlton, L. M., Kobusingye, O., Koranteng, A., Krishnamurthi, R., Lipnick, M., Lipshultz, S. E., Ohno, S. L., Mabweijano, J., MacIntyre, M. F., Mallinger, L., March, L., Marks, G. B., Marks, R., Matsumori, A., Matzopoulos, R., Mayosi, B. M., McAnulty, J. H., McDermott, M. M., McGrath, J.,

Mensah, G. A., Merriman, T. R., Michaud, C., Miller, M., Miller, T. R., Mock, C., Mocumbi, A. O., Mokdad, A. A., Moran, A., Mulholland, K., Nair, M. N., Naldi, L., Narayan, K. M., Nasseri, K., Norman, P., O'Donnell, M., Omer, S. B., Ortblad, K., Osborne, R., Ozgediz, D., Pahari, B., Pandian, J. D., Rivero, A. P., Padilla, R. P., Perez-Ruiz, F., Perico, N., Phillips, D., Pierce, K., Pope, C. A., 3rd, Porrini, E., Pourmalek, F., Raju, M., Ranganathan, D., Rehm, J. T., Rein, D. B., Remuzzi, G., Rivara, F. P., Roberts, T., De Leon, F. R., Rosenfeld, L. C., Rushton, L., Sacco, R. L., Salomon, J. A., Sampson, U., Sanman, E., Schwebel, D. C., Segui-Gomez, M., Shepard, D. S., Singh, D., Singleton, J., Sliwa, K., Smith, E., Steer, A., Taylor, J. A., Thomas, B., Tleyjeh, I. M., Towbin, J. A., Truelsen, T., Undurraga, E. A., Venketasubramanian, N., Vijayakumar, L., Vos, T., Wagner, G. R., Wang, M., Wang, W., Watt, K., Weinstock, M. A., Weintraub, R., Wilkinson, J. D., Woolf, A. D., Wulf, S., Yeh, P. H., Yip, P., Zabetian, A., Zheng, Z. J., Lopez, A. D., Murray, C. J., AlMazroa, M. A., and Memish, Z. A. (2012). Global and regional mortality from 235 causes of death for 20 age groups in 1990 and 2010: a systematic analysis for the Global Burden of Disease Study 2010. *Lancet* 380(9859), 2095-128.

Lucifora, J., Arzberger, S., Durantel, D., Belloni, L., Strubin, M., Levrero, M., Zoulim, F., Hantz, O., and Protzer, U. (2011). Hepatitis B virus X protein is essential to initiate and maintain virus replication after the infection. *J Hepatol* 55(5), 996-1003.

Lundqvist, J., Yde, C. W., and Lykkesfeldt, A. E. (2014). 1alpha,25-dihydroxyvitamin D3 inhibits cell growth and NFkappaB signaling in tamoxifen-resistant breast cancer cells. *Steroids* 85, 30-5.

Luong, K., and Nguyen, L. T. (2012). Theoretical basis of a beneficial role for vitamin D in viral hepatitis. *World J Gastroenterol* 18(38), 5338-50.

Lupberger, J., Schädler, S., Peiran, A., and Hildt, E. (2013). Identification and characterization of a novel bipartite nuclear localization signal in the hepatitis B virus polymerase. *World J Gastroenterol* 19(44), 8000-10.

Maestro, B., Campion, J., Davila, N., and Calle, C. (2000). Stimulation by 1,25-dihydroxyvitamin D3 of insulin receptor expression and insulin responsiveness for glucose transport in U-937 human promonocytic cells. *Endocr J* 47(4), 383-91.

Maestro, B., Davila, N., Carranza, M. C., and Calle, C. (2003). Identification of a Vitamin D response element in the human insulin receptor gene promoter. *J Steroid Biochem Mol Biol* 84(2-3), 223-30.

Mahon, B. D., Wittke, A., Weaver, V., and Cantorna, M. T. (2003). The targets of vitamin D depend on the differentiation and activation status of CD4 positive T cells. *J Cell Biochem* 89(5), 922-32.

Marinho, A., Carvalho, C., Boleixa, D., Bettencourt, A., Leal, B., Guimaraes, J., Neves, E., Oliveira, J. C., Almeida, I., Farinha, F., Costa, P. P., Vasconcelos, C., and Silva, B. M. (2016). Vitamin D supplementation effects on FoxP3 expression in T cells and FoxP3+/IL-17A ratio and clinical course in systemic lupus erythematosus patients: a study in a Portuguese cohort. *Immunol Res*.

Marion, P. L., Salazar, F. H., Alexander, J. J., and Robinson, W. S. (1979). Polypeptides of hepatitis B virus surface antigen produced by a hepatoma cell line. *J Virol* 32(3), 796-802.

Maxwell, J. D. (1994). Seasonal variation in vitamin D. *Proc Nutr Soc* 53(3), 533-43.

McClain, S. L., Clippinger, A. J., Lizzano, R., and Bouchard, M. J. (2007). Hepatitis B virus replication is associated with an HBx-dependent mitochondrion-regulated increase in cytosolic calcium levels. *J Virol* 81(21), 12061-5.

McGregor, R., Li, G., Penny, H., Lombardi, G., Afzali, B., and Goldsmith, D. J. (2014). Vitamin D in renal transplantation - from biological mechanisms to clinical benefits. *Am J Transplant* 14(6), 1259-70.

Meyers, M. L., Trepo, L. V., Nath, N., and Sninsky, J. J. (1986). Hepatitis B virus polypeptide X: expression in Escherichia coli and identification of specific antibodies in sera from hepatitis B virus-infected humans. *J Virol* 57(1), 101-9.

Micorbewiki (2016). Hepatitis B virus.

Mizobuchi, M., and Ogata, H. (2014). Clinical uses of 22-oxacalcitriol. *Curr Vasc Pharmacol* 12(2), 324-8.

Mohamadkhani, A., Bastani, F., Khorrami, S., Ghanbari, R., Eghtesad, S., Sharafkhah, M., Montazeri, G., and Poustchi, H. (2015). Negative Association of Plasma Levels of Vitamin D and miR-378 With Viral Load in Patients With Chronic Hepatitis B Infection. *Hepat Mon* 15(6), e28315.

Moller, K. I., Kongshoj, B., Philipsen, P. A., Thomsen, V. O., and Wulf, H. C. (2005). How Finsen's light cured lupus vulgaris. *Photodermatol Photoimmunol Photomed* 21(3), 118-24.

Mora, J. R., Iwata, M., and von Andrian, U. H. (2008). Vitamin effects on the immune system: vitamins A and D take centre stage. *Nat Rev Immunol* 8(9), 685-98.

Morikawa, K., Suda, G., and Sakamoto, N. (2016). Viral life cycle of hepatitis B virus : host factors and druggable targets. *Hepatol Res*.

Mortality and Causes of Death Collaborators (2015). Global, regional, and national age-sex specific all-cause and cause-specific mortality for 240 causes of death, 1990-2013: a systematic analysis for the Global Burden of Disease Study 2013. *Lancet* 385(9963), 117-71.

Mullis, K., Faloona, F., Scharf, S., Saiki, R., Horn, G., and Erlich, H. (1986). Specific enzymatic amplification of DNA in vitro: the polymerase chain reaction. *Cold Spring Harb Symp Quant Biol* 51 Pt 1, 263-73.

Nakai, K., Fujii, H., Kono, K., Goto, S., Kitazawa, R., Kitazawa, S., Hirata, M., Shinohara, M., Fukagawa, M., and Nishi, S. (2014). Vitamin D activates the Nrf2-Keap1 antioxidant pathway and ameliorates nephropathy in diabetic rats. *Am J Hypertens* 27(4), 586-95.

Nassal, M. (2008). Hepatitis B viruses: reverse transcription a different way. *Virus Res* 134(1-2), 235-49.

Niekamp, H. (2013). Dissertation “Charakterisierung der phänotypischen Resistenz von Hepatitis-B-Virus Mutanten gegenüber antiviralen Nukleosid- und Nukleotidanaloga “. Justus-Liebig-University, Gießen.

Nogami, S., Satoh, S., Nakano, M., Shimizu, H., Fukushima, H., Maruyama, A., Terano, A., and Shirataki, H. (2003). Taxilin; a novel syntaxin-binding protein that is involved in Ca2+-dependent exocytosis in neuroendocrine cells. *Genes Cells* 8(1), 17-28.

Nogami, S., Satoh, S., Tanaka-Nakadate, S., Yoshida, K., Nakano, M., Terano, A., and Shirataki, H. (2004). Identification and characterization of taxilin isoforms. *Biochem Biophys Res Commun* 319(3), 936-43.

Nugmanova, Z., Patel, N., Akhmetova, G. M., Kurmangalieva, G. S., Abdumananova, M. K., Akanov, A. A., Kovtunenko, N. G., and McNutt, L. A. (2015). Relationship between vitamin D and human immunodeficiency virus (HIV) viral load among HIV-infected patients in Kazakhstan. *J Infect Dev Ctries* 9(11), 1277-83.

Oess, S., and Hildt, E. (2000). Novel cell permeable motif derived from the PreS2-domain of hepatitis-B virus surface antigens. *Gene Ther* 7(9), 750-8.

Ohtomo, N., Tomiya, T., Tanoue, Y., Inoue, Y., Nishikawa, T., Ikeda, H., Seyama, Y., Kokudo, N., Shibahara, J., Fukayama, M., Koike, K., Shirataki, H., and Fujiwara, K. (2010). Expression of alpha-taxilin in hepatocellular carcinoma correlates with growth activity and malignant potential of the tumor. *Int J Oncol* 37(6), 1417-23.

Orito, E., Ichida, T., Sakugawa, H., Sata, M., Horiike, N., Hino, K., Okita, K., Okanoue, T., Iino, S., Tanaka, E., Suzuki, K., Watanabe, H., Hige, S., and Mizokami, M. (2001). Geographic distribution of hepatitis B virus (HBV) genotype in patients with chronic HBV infection in Japan. *Hepatology* 34(3), 590-4.

Orito, E., Mizokami, M., Ina, Y., Moriyama, E. N., Kameshima, N., Yamamoto, M., and Gojobori, T. (1989). Host-independent evolution and a genetic classification of the hepadnavirus family based on nucleotide sequences. *Proc Natl Acad Sci U S A* 86(18), 7059-62.

Ostapchuk, P., Hearing, P., and Ganem, D. (1994). A dramatic shift in the transmembrane topology of a viral envelope glycoprotein accompanies hepatitis B viral morphogenesis. *EMBO J* 13(5), 1048-57.

Ou, J. H., Laub, O., and Rutter, W. J. (1986). Hepatitis B virus gene function: the precore region targets the core antigen to cellular membranes and causes the secretion of the e antigen. *Proc Natl Acad Sci U S A* 83(6), 1578-82.

Patient, R., Hourioux, C., and Roingeard, P. (2009). Morphogenesis of hepatitis B virus and its subviral envelope particles. *Cell Microbiol* 11(11), 1561-70.

Patient, R., Hourioux, C., Sizaret, P. Y., Trassard, S., Sureau, C., and Roingeard, P. (2007). Hepatitis B virus subviral envelope particle morphogenesis and intracellular trafficking. *J Virol* 81(8), 3842-51.

Peiffer, K. H., Akhras, S., Himmelsbach, K., Hassemer, M., Finkernagel, M., Carra, G., Nuebling, M., Chudy, M., Niekamp, H., Glebe, D., Sarrazin, C., Zeuzem, S., and Hildt, E. (2015). Intracellular accumulation of subviral HBsAg particles and diminished Nrf2 activation in HBV genotype G expressing cells lead to an increased ROI level. *J Hepatol* 62(4), 791-8.

Peng, Q., Yang, S., Lao, X., Li, R., Chen, Z., Wang, J., Qin, X., and Li, S. (2014). Association of single nucleotide polymorphisms in VDR and DBP genes with HBV-related hepatocellular carcinoma risk in a Chinese population. *PLoS One* 9(12), e116026.

Petersen, J., Thompson, A. J., and Levrero, M. (2016). "Aiming for cure in HBV and HDV infection". *J Hepatol*.

Peterson, D. L., Roberts, I. M., and Vyas, G. N. (1977). Partial amino acid sequence of two major component polypeptides of hepatitis B surface antigen. *Proc Natl Acad Sci U S A* 74(4), 1530-4.

Pike, J. W., and Meyer, M. B. (2012). The vitamin D receptor: new paradigms for the regulation of gene expression by 1,25-dihydroxyvitamin D3. *Rheum Dis Clin North Am* 38(1), 13-27.

Polo Rodriguez, R., Lozano, F., Gonzalez de Castro, P., Jimenez, M. A., Miro, O., Ramon Blanco, J., Moreno, D., Duenas, C., Munoz Platon, E., Fernandez Escribano, M., Sanz Sanz, J., Fumaz, C., Santos, I., Garcia, F., Tellez, M. J., Gonzalez Montero, R., Vals Jimenez, M. V., Losa, J., Valle Robles, M. L., Iribarren, J., and Ortega, E. (2016). Executive summary of the consensus document on post-exposure prophylaxis against HIV, HBV and HCV in adults and children. *Enferm Infecc Microbiol Clin* 34(2), 122-31.

Prange, R. (2012). Host factors involved in hepatitis B virus maturation, assembly, and egress. *Med Microbiol Immunol* 201(4), 449-61.

Prange, R., and Streeck, R. E. (1995). Novel transmembrane topology of the hepatitis B virus envelope proteins. *EMBO J* 14(2), 247-56.

Prietl, B., Treiber, G., Pieber, T. R., and Amrein, K. (2013). Vitamin D and immune function. *Nutrients* 5(7), 2502-21.

PubChem, D. (2016). PubChem Compound.

Rabe, B., Glebe, D., and Kann, M. (2006). Lipid-mediated introduction of hepatitis B virus capsids into nonsusceptible cells allows highly efficient replication and facilitates the study of early infection events. *J Virol* 80(11), 5465-73.

Rahman, A. H., and Branch, A. D. (2013). Vitamin D for your patients with chronic hepatitis C? *J Hepatol* 58(1), 184-9.

Rasche, A., Souza, B. F., and Drexler, J. F. (2016). Bat hepadnaviruses and the origins of primate hepatitis B viruses. *Curr Opin Virol* 16, 86-94.

Reifenberg, K., Nusser, P., Lohler, J., Spindler, G., Kuhn, C., von Weizsacker, F., and Kock, J. (2002). Virus replication and virion export in X-deficient hepatitis B virus transgenic mice. *J Gen Virol* 83(Pt 5), 991-6.

Ren, H., Elgner, F., Jiang, B., Himmelsbach, K., Medvedev, R., Ploen, D., and Hildt, E. (2016). The autophagosomal SNARE protein syntaxin 17 is an essential factor for the hepatitis C virus life cycle. *J Virol*.

RKI (2014). Virushepatitis B und D im Jahr 2013. *In* "Epidemiologisches Bulletin, aktuelle daten und informationen zu infektionskrankheiten und public health, Nr. 30".

Rost, M., Mann, S., Lambert, C., Doring, T., Thomé, N., and Prange, R. (2006). Gamma-adaptin, a novel ubiquitin-interacting adaptor, and Nedd4 ubiquitin ligase control hepatitis B virus maturation. *J Biol Chem* 281(39), 29297-308.

Röttger, H. Masterarbeit “Etablierung eines Verfahrens zur Identifierzung aplha-Taxilin und IL-14 bindener Proteine“ Christian-Albrechts-University, Kiel(2011).

Sablon, E., and Shapiro, F. (2005). Advances in Molecular Diagnosis of HBV Infection and Drug Resistance. *Int J Med Sci* 2(1), 8-16.

Sakamoto, T., Tanaka, Y., Orito, E., Co, J., Clavio, J., Sugauchi, F., Ito, K., Ozasa, A., Quino, A., Ueda, R., Sollano, J., and Mizokami, M. (2006). Novel subtypes (subgenotypes) of hepatitis B virus genotypes B and C among chronic liver disease patients in the Philippines. *J Gen Virol* 87(Pt 7), 1873-82.

Sanchez, L. V., Maldonado, M., Bastidas-Ramirez, B. E., Norder, H., and Panduro, A. (2002). Genotypes and S-gene variability of Mexican hepatitis B virus strains. *J Med Virol* 68(1), 24-32.

Sanchez, L. V., Tanaka, Y., Maldonado, M., Mizokami, M., and Panduro, A. (2007). Difference of hepatitis B virus genotype distribution in two groups of mexican patients with different risk factors. High prevalence of genotype H and G. *Intervirology* 50(1), 9-15.

Saudy, N., Sugauchi, F., Tanaka, Y., Suzuki, S., Aal, A. A., Zaid, M. A., Agha, S., and Mizokami, M. (2003). Genotypes and phylogenetic characterization of hepatitis B and delta viruses in Egypt. *J Med Virol* 70(4), 529-36.

Schädler, S., and Hildt, E. (2009). HBV life cycle: entry and morphogenesis. *Viruses* 1(2), 185-209.

Schädler, S., Krause, J., Himmelsbach, K., Carvajal-Yepes, M., Lieder, F., Klingel, K., Nassal, M., Weiss, T. S., Werner, S., and Hildt, E. (2010). Hepatitis B virus induces expression of antioxidant response element-regulated genes by activation of Nrf2. *J Biol Chem* 285(52), 41074-86.

Schäfer, S. (2007a). Hepatitis B virus genotypes in Europe. *Hepatol Res* 37(s1), S20-6.

Schäfer, S. (2007b). Hepatitis B virus taxonomy and hepatitis B virus genotypes. *World J Gastroenterol* 13(1), 14-21.

Schmitt, S., Glebe, D., Tolle, T. K., Lochnit, G., Linder, D., Geyer, R., and Gerlich, W. H. (2004). Structure of pre-S2 N- and O-linked glycans in surface proteins from different genotypes of hepatitis B virus. *J Gen Virol* 85(Pt 7), 2045-53.

Schmitz, A., Schwarz, A., Foss, M., Zhou, L., Rabe, B., Hoellenriegel, J., Stoeber, M., Pante, N., and Kann, M. (2010). Nucleoporin 153 arrests the nuclear import of hepatitis B virus capsids in the nuclear basket. *PLoS Pathog* 6(1), e1000741.

Schuster, I., Egger, H., Herzig, G., Reddy, G. S., Schmid, J. A., Schussler, M., and Vorisek, G. (2006). Selective inhibitors of vitamin D metabolism--new concepts and perspectives. *Anticancer Res* 26(4A), 2653-68.

Sells, M. A., Chen, M. L., and Acs, G. (1987). Production of hepatitis B virus particles in Hep G2 cells transfected with cloned hepatitis B virus DNA. *Proc Natl Acad Sci U S A* 84(4), 1005-9.

Shen, T., Yan, X. M., Liu, H. X., Zhang, B. X., Li, L., Zhang, J. P., Wang, J. L., and Xiao, C. J. (2015). Genotype I of hepatitis B virus was found in east Xishuangbanna, China and molecular dynamics of HBV/I. *J Viral Hepat* 22(1), 37-45.

Shin, E. C., Sung, P. S., and Park, S. H. (2016). Immune responses and immunopathology in acute and chronic viral hepatitis. *Nat Rev Immunol*.

Short, J. M., Chen, S., Roseman, A. M., Butler, P. J., and Crowther, R. A. (2009). Structure of hepatitis B surface antigen from subviral tubes determined by electron cryomicroscopy. *J Mol Biol* 390(1), 135-41.

Siegler, V. D., and Bruss, V. (2013). Role of transmembrane domains of hepatitis B virus small surface proteins in subviral-particle biogenesis. *J Virol* 87(3), 1491-6.

Simmonds, P. (2001). Reconstructing the origins of human hepatitis viruses. *Philos Trans R Soc Lond B Biol Sci* 356(1411), 1013-26.

Smyk, D. S., Orfanidou, T., Invernizzi, P., Bogdanos, D. P., and Lenzi, M. (2013). Vitamin D in autoimmune liver disease. *Clin Res Hepatol Gastroenterol* 37(5), 535-45.

Southern, E. M. (1975). Detection of specific sequences among DNA fragments separated by gel electrophoresis. *J Mol Biol* 98(3), 503-17.

Speeckaert, M., Huang, G., Delanghe, J. R., and Taes, Y. E. (2006). Biological and clinical aspects of the vitamin D binding protein (Gc-globulin) and its polymorphism. *Clin Chim Acta* 372(1-2), 33-42.

Stannard, L. (2016). Hepatitis B, University of Cape Town. http://www.virology.uct.ac.za/vir/teaching/mbchb/hepatitis

Steddon, S. J., Schroeder, N. J., and Cunningham, J. (2001). Vitamin D analogues: how do they differ and what is their clinical role? *Nephrol Dial Transplant* 16(10), 1965-7.

Stieler, J. T., and Prange, R. (2014). Involvement of ESCRT-II in hepatitis B virus morphogenesis. *PLoS One* 9(3), e91279.

Stoeckl, L., Funk, A., Kopitzki, A., Brandenburg, B., Oess, S., Will, H., Sirma, H., and Hildt, E. (2006). Identification of a structural motif crucial for infectivity of hepatitis B viruses. *Proc Natl Acad Sci U S A* 103(17), 6730-4.

Strom, S. C., Jirtle, R. L., Jones, R. S., Novicki, D. L., Rosenberg, M. R., Novotny, A., Irons, G., McLain, J. R., and Michalopoulos, G. (1982). Isolation, culture, and transplantation of human hepatocytes. *J Natl Cancer Inst* 68(5), 771-8.

Sugauchi, F., Chutaputti, A., Orito, E., Kato, H., Suzuki, S., Ueda, R., and Mizokami, M. (2002). Hepatitis B virus genotypes and clinical manifestation among hepatitis B carriers in Thailand. *J Gastroenterol Hepatol* 17(6), 671-6.

Sun, J. (2010). Vitamin D and mucosal immune function. *Curr Opin Gastroenterol* 26(6), 591-5.

Sutnick, A. I., London, W. T., Blumberg, B. S., Yankee, R. A., Gerstley, B. J., and Millman, I. (1970). Australia antigen (a hepatitis-associated antigen) in leukemia. *J Natl Cancer Inst* 44(6), 1241-9.

Szymczak, I., and Pawliczak, R. (2016). The Active Metabolite of Vitamin D3 as a Potential Immunomodulator. *Scand J Immunol* 83(2), 83-91.

Takeuchi, A., Reddy, G. S., Kobayashi, T., Okano, T., Park, J., and Sharma, S. (1998). Nuclear factor of activated T cells (NFAT) as a molecular target for 1alpha,25-dihydroxyvitamin D3-mediated effects. *J Immunol* 160(1), 209-18.

Tang, H., and McLachlan, A. (2001). Transcriptional regulation of hepatitis B virus by nuclear hormone receptors is a critical determinant of viral tropism. *Proc Natl Acad Sci U S A* 98(4), 1841-6.

Tatematsu, K., Tanaka, Y., Kurbanov, F., Sugauchi, F., Mano, S., Maeshiro, T., Nakayoshi, T., Wakuta, M., Miyakawa, Y., and Mizokami, M. (2009). A genetic variant of hepatitis B virus divergent from known human and ape genotypes isolated from a Japanese patient and provisionally assigned to new genotype J. *J Virol* 83(20), 10538-47.

Tedder, R. S., Bissett, S. L., Myers, R., and Ijaz, S. (2013). The 'Red Queen' dilemma--running to stay in the same place: reflections on the evolutionary vector of HBV in humans. *Antivir Ther* 18(3 Pt B), 489-96.

Thermofisher (2016). PrestoBlue ® Cell Viability Reagent Frequently Asked Questions.

Thimme, R., Wieland, S., Steiger, C., Ghrayeb, J., Reimann, K. A., Purcell, R. H., and Chisari, F. V. (2003). CD8(+) T cells mediate viral clearance and disease pathogenesis during acute hepatitis B virus infection. *J Virol* 77(1), 68-76.

Thomé, N. (2007). Dissertation “Virus/Wirt-Interaktionen bei Hepatitis-B-Virus Infektionen: Die Rolle von γ2-Adaptin.” Johannes Gutenberg University Mainz.

Tian, Q., and Jia, J. (2016). Hepatitis B virus genotypes: epidemiological and clinical relevance in Asia. *Hepatol Int*.

Tong, S., and Li, J. (2014). Identification of NTCP as an HBV receptor: the beginning of the end or the end of the beginning? *Gastroenterology* 146(4), 902-5.

Towbin, H., Staehelin, T., and Gordon, J. (1992). Electrophoretic transfer of proteins from polyacrylamide gels to nitrocellulose sheets: procedure and some applications. 1979. *Biotechnology* 24, 145-9.

Trautwein, C., Possienke, M., Schlitt, H. J., Boker, K. H., Horn, R., Raab, R., Manns, M. P., and Brabant, G. (2000). Bone density and metabolism in patients with viral hepatitis and cholestatic liver diseases before and after liver transplantation. *Am J Gastroenterol* 95(9), 2343-51.

Tugendheim, S. (2016). Hepatitis B Virus http://www.tugendheim.de/impfen/impfungen/hep_b/hepatitis_b.html.

Urashima, M., Segawa, T., Okazaki, M., Kurihara, M., Wada, Y., and Ida, H. (2010). Randomized trial of vitamin D supplementation to prevent seasonal influenza A in schoolchildren. *Am J Clin Nutr* 91(5), 1255-60.

Urban, S., Schulze, A., Dandri, M., and Petersen, J. (2010). The replication cycle of hepatitis B virus. *J Hepatol* 52(2), 282-4.

Vieth, S., Manegold, C., Drosten, C., Nippraschk, T., and Gunther, S. (2002). Sequence and phylogenetic analysis of hepatitis B virus genotype G isolated in Germany. *Virus Genes* 24(2), 153-6.

Vyas, G. N., Rao, K. R., and Ibrahim, A. B. (1972). Australia antigen (hepatitis B antigen): a conformational antigen dependent on disulfide bonds. *Science* 178(4067), 1300-1.

Watanabe, T., Sorensen, E. M., Naito, A., Schott, M., Kim, S., and Ahlquist, P. (2007). Involvement of host cellular multivesicular body functions in hepatitis B virus budding. *Proc Natl Acad Sci U S A* 104(24), 10205-10.

Watkins, R. R., Lemonovich, T. L., and Salata, R. A. (2015). An update on the association of vitamin D deficiency with common infectious diseases. *Can J Physiol Pharmacol* 93(5), 363-8.

Westland, C., Delaney, W. t., Yang, H., Chen, S. S., Marcellin, P., Hadziyannis, S., Gish, R., Fry, J., Brosgart, C., Gibbs, C., Miller, M., and Xiong, S. (2003). Hepatitis B virus genotypes and virologic response in 694 patients in phase III studies of adefovir dipivoxil1. *Gastroenterology* 125(1), 107-16.

White, J. H. (2012). Vitamin D metabolism and signaling in the immune system. *Rev Endocr Metab Disord* 13(1), 21-9.

WHO (2010). WHA63.18 "SIXTY-THIRD WORLD HEALTH ASSEMBLY, Agenda item 11.12, Viral hepatitis ".

WHO (2015). Hepatitis B Fact sheet N°204

WHO (2016). Global Health Sector Strategy on Viral Hepatitis, 2016-2021.

Wieland, S., Thimme, R., Purcell, R. H., and Chisari, F. V. (2004). Genomic analysis of the host response to hepatitis B virus infection. *Proc Natl Acad Sci U S A* 101(17), 6669-74.

Wong, G. L., Chan, H. L., Chan, H. Y., Tse, C. H., Chim, A. M., Lo, A. O., and Wong, V. W. (2015). Adverse effects of vitamin D deficiency on outcomes of patients with chronic hepatitis B. *Clin Gastroenterol Hepatol* 13(4), 783-90 e1.

Wood, R. J., Tchack, L., Angelo, G., Pratt, R. E., and Sonna, L. A. (2004). DNA microarray analysis of vitamin D-induced gene expression in a human colon carcinoma cell line. *Physiol Genomics* 17(2), 122-9.

Yachimski, P., and Chung, R. T. (2005). Hepatitis B virus infection in liver transplant candidates and recipients. *MedGenMed* 7(2), 20.

Yan, H., Zhong, G., Xu, G., He, W., Jing, Z., Gao, Z., Huang, Y., Qi, Y., Peng, B., Wang, H., Fu, L., Song, M., Chen, P., Gao, W., Ren, B., Sun, Y., Cai, T., Feng, X., Sui, J., and Li, W. (2014). Sodium taurocholate cotransporting polypeptide is a functional receptor for human hepatitis B and D virus. *elife* 3.

Yang, B., and Bouchard, M. J. (2012). The hepatitis B virus X protein elevates cytosolic calcium signals by modulating mitochondrial calcium uptake. *J Virol* 86(1), 313-27.

Yao, X., Zeng, H., Zhang, G., Zhou, W., Yan, Q., Dai, L., and Wang, X. (2013). The associated ion between the VDR gene polymorphisms and susceptibility to hepatocellular carcinoma and the clinicopathological features in subjects infected with HBV. *Biomed Res Int* 2013, 953974.

Yen, T. T., Yang, A., Chiu, W. T., Li, T. N., Wang, L. H., Wu, Y. H., Wang, H. C., Chen, L., Wang, W. C., Huang, W., Chang, C. W., Chang, M. D., Shen, M. R., and Su, I. J. (2016). Hepatitis B virus PreS2-mutant large surface antigen activates store-operated calcium entry and promotes chromosome instability. *Oncotarget*.

Yu, R., Sun, J., Zheng, Z., Chen, J., Fan, R., Liang, X., Zhu, Y., Liu, Y., Shen, S., and Hou, J. (2015). Association between vitamin D level and viral load or fibrosis stage in chronic hepatitis B patients from Southern China. *J Gastroenterol Hepatol* 30(3), 566-74.

Yuen, M. F., Sablon, E., Yuan, H. J., Wong, D. K., Hui, C. K., Wong, B. C., Chan, A. O., and Lai, C. L. (2003). Significance of hepatitis B genotype in acute exacerbation, HBeAg seroconversion, cirrhosis-related complications, and hepatocellular carcinoma. *Hepatology* 37(3), 562-7.

Zhang, L., Liu, C., Xiao, Y., and Chen, X. (2016). Oxethazaine inhibits hepatitis B virus capsid assembly by blocking the cytosolic calcium-signalling pathway. *J Gen Virol* 97(5), 1198-209.

Zhang, S. J., Chen, Z. X., Jiang, K. P., Wu, W. K., Zhang, C. Y., and Gu, Y. L. (2006). Effect of seasonal variation on the clinical course of chronic hepatitis B. *J Gastroenterol* 41(11), 1107-15.

Zhao, X. Y., Li, J., Wang, J. H., Habib, S., Wei, W., Sun, S. J., Strobel, H. W., and Jia, J. D. (2016). Vitamin D serum level is associated with Child-Pugh score and metabolic enzyme imbalances, but not viral load in chronic hepatitis B patients. *Medicine (Baltimore)* 95(27), e3926.

Zhou, S., and Standring, D. N. (1992). Hepatitis B virus capsid particles are assembled from core-protein dimer precursors. *Proc Natl Acad Sci U S A* 89(21), 10046-50.

Zhou, S. L., and Standring, D. N. (1991). Production of hepatitis B virus nucleocapsidlike core particles in Xenopus oocytes: assembly occurs mainly in the cytoplasm and does not require the nucleus. *J Virol* 65(10), 5457-64.

Zhu, Q., Li, N., Han, Q., Li, Z., Zhang, G., Li, F., Zhang, P., Chen, J., Lv, Y., and Liu, Z. (2012). Single-nucleotide polymorphism at CYP27B1-1260, but not VDR Taq I, is possibly associated with persistent hepatitis B virus infection. *Genet Test Mol Biomarkers* 16(9), 1115-21.

6. Appendix

6.1 Amino acid sequence of HBV genotypes A, B, and C

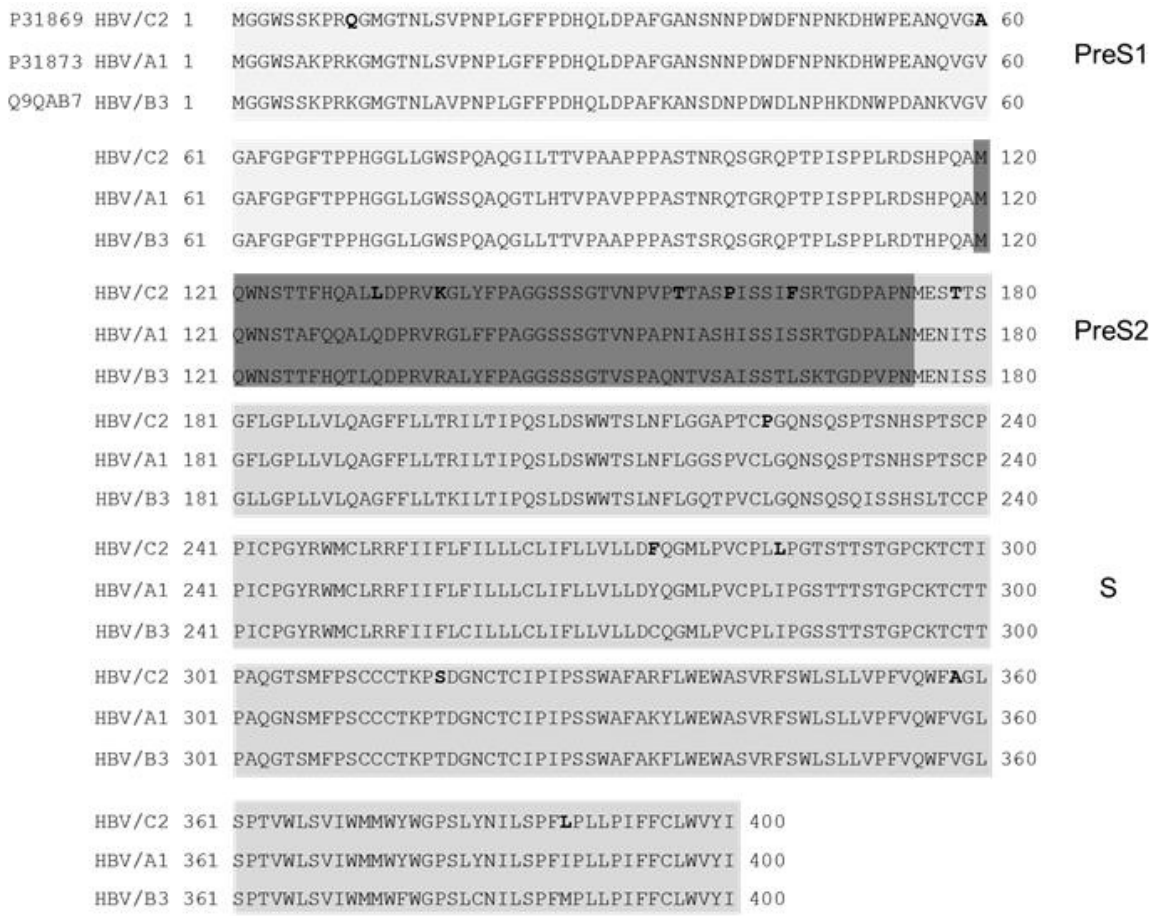

7. Curriculum Vitae

PERSONAL INFORMATION

Name	Malin Finkernagel
Nationality	German
Date of birth	20. April 1988
Place of birth	Gießen (Germany)

EDUCATION AND TRAINING

05/2013 –12/2016 PhD

Johannes Gutenberg-University, Mainz (Germany)

Degree: *doctor rerum naturalium*

Thesis title: *"INFLUENCE OF VITAMIN D ON THE HEPATITIS B VIRUS LIFE CYCLE IN DIFFERENT GENOTYPES"* conducted at the Paul-Ehrlich-Institut, Federal Institute for Vaccines and Biomedicines, Division of Virology, Langen (Germany)

10/2007 –12/2012 Diploma, Biology

Johannes Gutenberg-University, Mainz (Germany)

Degree: Diploma

Thesis title: „EINFLUSS DES *SHEDDINGS* VON CD99 DURCH DIE METALLOPROTEASE MEPRIN β BEI DER DIAPEDESE" conducted at the Christian-Albrechts-University, Institute of Biochemistry, Unit for Degradomics of the Protease Web, Kiel (Germany)

07/2005 –06/2007 Grammar School

Laubach-Kolleg, Laubach (Germany)

Grammar school of the Protestant Church of Hesse-Nassau

FURTHER PUBLICATIONS

ECTODOMAIN SHEDDING OF CD99 WITHIN HIGHLY CONSERVED REGIONS IS MEDIATED BY THE METALLOPROTEASE MEPRIN BETA AND PROMOTES TRANSENDOTHELIAL CELL MIGRATION

THE FASEB JOURNAL

Tillmann Bedau, Johannes Prox, Florian Peters, Philipp Arnold, Frederike Schmidt, **Malin Finkernagel**, Sandra Köllmann, Rielana Wichert, Anna Otte, Anke Ohler, Marit Stirnberg, Ralph Lucius, Tomas Koudelka, Andreas Tholey, Valentina Biasin, Claus Pietrzik, Grazyna Kwapiszewska, and Christoph Becker-Pauly

8. Acknowledgment

9. Eidesstattliche Versicherung

Hiermit versichere ich gemäß § 11, Abs. 3d der Promotionsordnung vom 22.12.2003 des Fachbereichs Biologie der Johannes Gutenberg-Universität in Mainz:

Ich habe die heute als Dissertation vorgelegte Arbeit selbst angefertigt und alle benutzten Hilfsmittel (Literatur, Apparaturen, Material) in der Arbeit angegeben.

Ich habe oder hatte die jetzt als Dissertation vorgelegte Arbeit nicht als Prüfungsarbeit für eine staatliche oder andere wissenschaftliche Prüfung eingereicht.

Ich hatte weder die jetzt als Dissertation vorgelegte Arbeit noch Teile einer Abhandlung bei einer anderen Fakultät bzw. einem anderen Fachbereich als Dissertation eingereicht.

Kigali, den 29.08.2016

Malin Finkernagel